7 Mechanisms of Drug Metabolism

ROBERT S. FOTI, DAN A. ROCK, LARRY C. WIENKERS, and JAN L. WAHLSTROM

Department of Pharmacokinetics and Drug Metabolism, Amgen Inc., Seattle, WA, USA

7.1 INTRODUCTION

Drug metabolism represents an integral contributor to the many physiological processes that govern the pharmacokinetic/dispositional fate of most therapeutic agents [1]. For the most part, drugs are taken orally and in order to be absorbed through the stomach and intestine, they need to possess a high degree of lipid solubility [2,3]. The requirement for drug lipid solubility is a physicochemical consequence to the fact that lipid-soluble (nonionized) molecules are able to pass through biological membranes by simple diffusion, while water-soluble (ionized) molecules cannot [4,5]. In this light, drug metabolism can be broadly described as the biological transformation of lipophilic, nonpolar molecules (drugs) to more hydrophilic, polar molecules (metabolites), which are in turn readily eliminated from the body. Restated, drug metabolism controls the systemic exposure of many drugs and without a metabolic pathway associated with drug clearance, these molecules would remain in the body for an extended period and possibly accumulate to toxic levels on repeated administration. In response to the role drug metabolism has in drug safety, regulatory agencies place a premium on gleaning information around the metabolic pathways and products associated for all new drug applications (NDAs) (e.g., Guidance for Industry: Safety Testing of Drug Metabolites).

In order to appreciate the role of drug metabolism in drug safety, it is important to consider how molecules are actually eliminated from the body. For the most part, molecules are removed from the body through two primary routes of elimination: the urinary and gastrointestinal systems [6]. The primary function of the kidney is the excretion of body wastes, and for the purpose of this chapter, drug metabolites. Renal elimination of drug metabolites is primarily dependent on the fraction of molecules that are susceptible to reabsorption in the distal renal tubule. In this region of the kidney,

Encyclopedia of Drug Metabolism and Interactions, 6-Volume Set, First Edition.
Edited by Alexander V. Lyubimov.

nonionic diffusion is responsible for the reabsorption [7]. Reabsorption occurs primarily by passive transfer and is mediated by a large hydrogen ion gradient between plasma and acidic urine. In this environment, metabolites, which are typically ionized, remain in the urine and are excreted, while drugs that are generally present as nonionized molecules, readily diffuse from the urine back into circulation [8].

Extraction via biliary and intestinal excretion of drug metabolites is important for the elimination of many therapeutic classes of drugs and corresponding metabolites [9]. Typically, biliary excretion is usually the primary route of elimination for compounds with a molecular weight of more than 400 Da and generally involves active secretion rather than passive diffusion [10]. Specific transport systems appear to exist for certain classes of molecules (e.g., organic bases, organic acids, and neutral substances) [11]. However, given that the molecules most likely to be excreted via biliary elimination are large, ionized molecules, once a molecule has been excreted into the bile (and subsequently delivered into the intestinal tract), it is not likely to be reabsorbed by passive diffusion.

If we disregard the role of small molecule transporters in drug metabolite elimination, it is clear that the biliary elimination of drug metabolites, similar to renal excretion, is primarily mediated by the physical properties of the molecule. Those substances that are ionized typically leave the body, while lipid-soluble molecules can be reabsorbed and reenter the blood circulation, which lengthens their half-life in the body and potential for toxicity [12,13].

The process of drug reabsorption is conceptually similar to the manner in which any molecule distributes between the two phases of water and a lipid-like solvent. With respect to the drug metabolites, the two phases are fatty tissue (cell membrane) and water (plasma). In organic chemistry, this concept is described in terms of a quantitative feature, the partition coefficient P, or as it is usually expressed, log P [14]. Factors that influence log P can be further distilled into descriptors such as size and polarity or hydrogen bonding capability of a molecule [15]. Therefore, it is important to understand the chemical features that can influence the partition ratio of a molecule as these concepts are the primary areas of chemical modifications associated with drug metabolism and safety [16].

Generally, polar solute molecules will dissolve in polar solvents and nonpolar solute molecules will dissolve in nonpolar solvents. Polarity in organic chemistry refers to a separation of charge and can describe a bond or an entire molecule [17,18]. The polarity of the molecule is the sum of all the bond polarities in the molecule [19]. Since the dipole moment is a vector (a quantity with both magnitude and direction), the molecular dipole moment is the vector sum of the individual dipole moments [20]. Restated, polar solute molecules have a positive and a negative end to the molecule. If the solvent molecule (water in the case of biological systems) is also polar then positive ends of solvent molecules will attract negative ends of solute molecules (Fig. 7.1).

As described above, drug metabolites are typically described as either being weak acids (a substance that gives up a proton) or weak bases (a substance that accepts a proton) and because of this, the disposition of most drug metabolites are governed by passive diffusion [21]. The extent to which a given drug metabolite exists in an ionized and nonionized species varies at different pH values. Therefore, the pH, or more specifically the hydrogen ion concentration, influences the ratio of ionized to nonionized species for a particular drug metabolite (Fig. 7.2). This concept is expanded

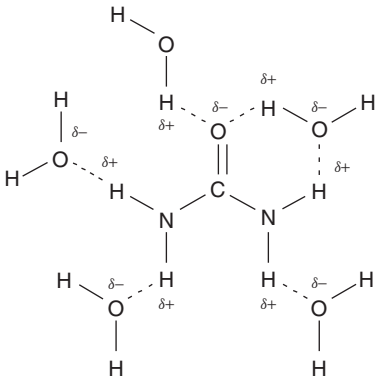

Figure 7.1 Hydrogen bonding of urea in water.

using the Brønsted–Lowry definition of acids and bases. The thermodynamic character that relates the charge in a molecule to the pH is the ionization constant, pK_a [22].

With respect to the elimination of drug metabolites, an understanding of the degree of ionization of a given molecule under physiological conditions is helpful to predict whether a metabolite will be long lived. At a particular pH, the relative concentration of the ionic and the molecular moieties of a given drug metabolite can be described by the Henderson–Hasselbach equation:

$$\text{pH} = pK_a + \log \frac{[\text{conjugate acid}]}{[\text{conjugate base}]}$$

Therefore, it follows, from the Henderson–Hasselbach equation, that when a substance is half ionized and half nonionized at a certain pH, its pK_a is equal to this pH. In other words, when the pH is equal to the pK_a value of the molecule, half of the molecules of a drug are in ionized and half are in nonionized form. It is important to consider that the relation between ionization and pH is not linear, but sigmoidal. Thus, small changes in pH will result in great changes in ionization, particularly if pH and pK_a values are close together.

With an appreciation of the physical chemical requirements that are required for the elimination of the drug metabolite, the next obvious question is what types of chemical modifications are biologically available to support drug metabolism enzyme reactions? The chemical routes by which drugs are susceptible to drug-metabolizing enzymes are large and varied. In fact, one particular feature that distinguishes drug-metabolizing enzymes from other "classical" enzymes is the wide variety of reactions that these enzymes can carry out. In 1959, Williams classified the drug metabolic reactions that are catalyzed by this group of enzymes into two general phases: phase I and II reactions [23]. Phase I reactions include oxidation [24], reduction [25], and hydrolysis [26], whereas phase II reactions are broadly defined as conjugation reactions and include glucuronidation [27], sulfation [28], acylation [29], methylation [30], and conjugation with glutathione (GSH) [31].

As with all enzyme-mediated reactions, drug-metabolizing enzymes are capable of accelerating a chemical reaction faster than reactions carried out on a laboratory bench top under the mild conditions of aqueous solution, room temperature, and neutral pH.

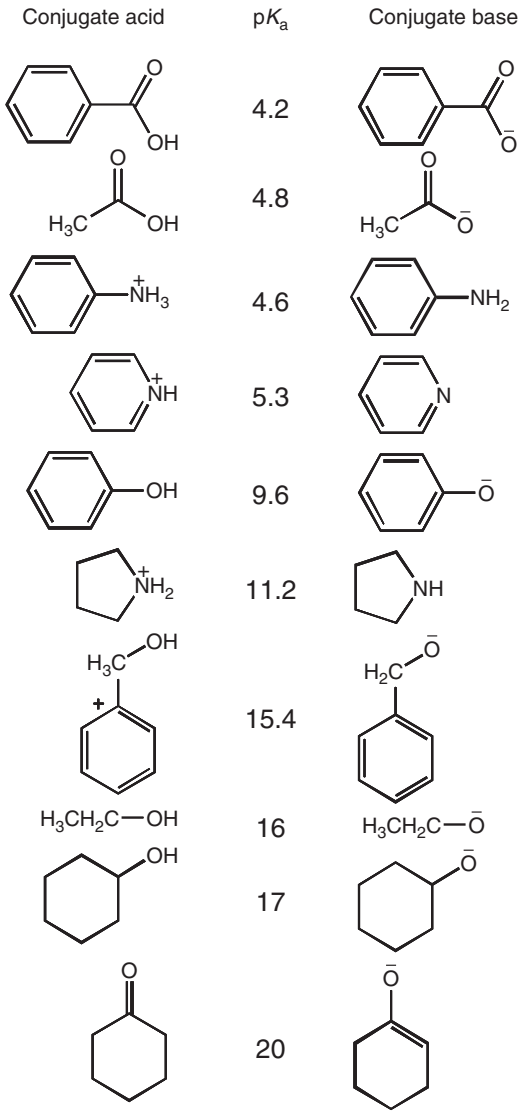

Figure 7.2 Examples of acids and acidity scale.

In terms of the concepts describing chemical thermodynamics, enzyme catalysis is essentially a lowering of the free energy function (G) associated with a given chemical reaction [32]. A change in free energy for a reaction, ΔG, determines if a reaction is spontaneous or not. Equilibrium conditions are governed by the standard free energy change ΔG°, and there are several means by which enzymes are able to decrease activation energy. The catalytic power and specificity of an enzyme is a reflection of the steric and electrostatic features associated with the enzyme's active site [33]. The most important of these involves the enzyme initially binding the substrate allows the molecule to exist in close proximity to the catalytic groups found within the active enzyme

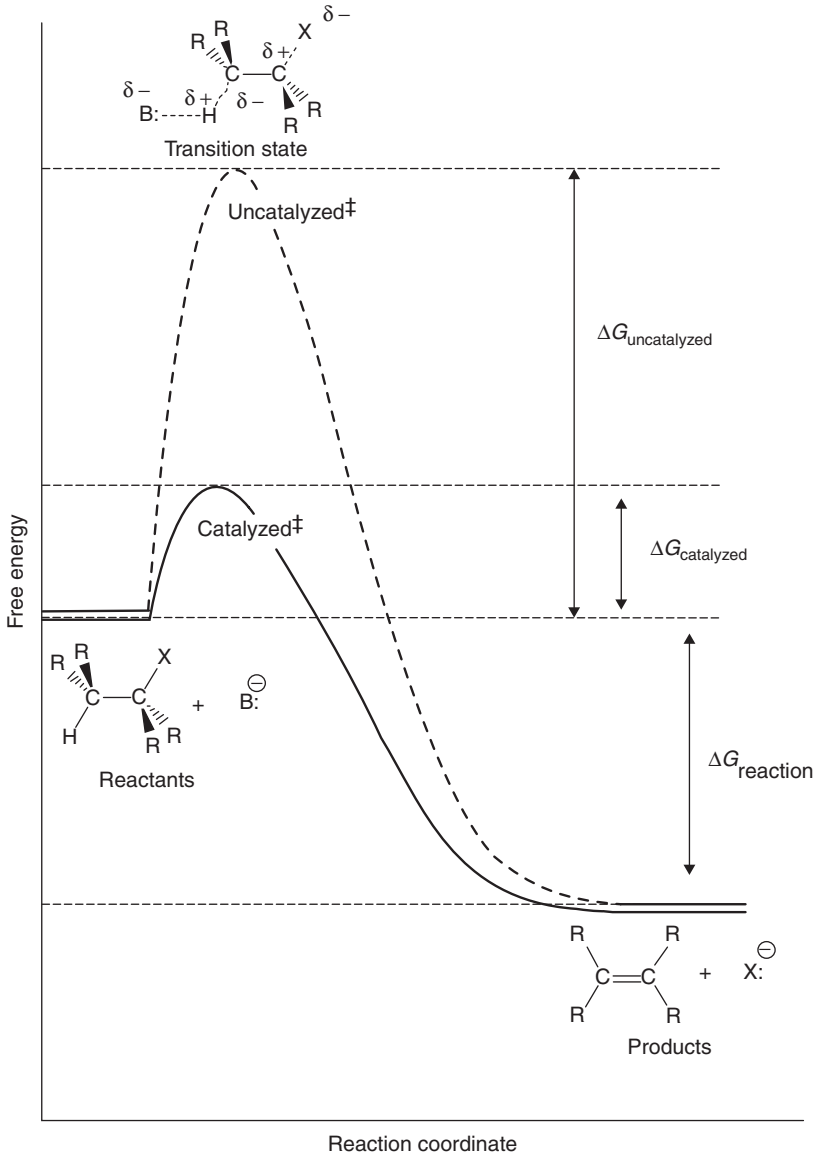

Figure 7.3 Free energy or potential energy diagram of a simple E2 elimination reaction of an alkyl halide to yield an alkene.

complex [34,35]. When the substrate is bound to the enzyme, the enzyme changes conformation and forces the substrate into a strained or distorted structure that mimics the reaction transition state [36], thus reducing the energy of activation (Fig. 7.3). In this conformation, the substrate is forced into a reactive state, due to the loss of the substrate's translational and rotational entropy, toward the total activation energy [37].

Although small in relative numbers, drug-metabolizing enzymes are able to catalyze a large variety of reactions because of their structural and chemical diversity. Some drug metabolism enzymatic reactions mimic organic chemistry reactions and proceed

via nucleophilic attack [38]. In this instance, enzyme's active residues can act as nucleophiles such as the sulfhydryl group of cysteine or the phenolic group of tyrosine. Alternatively, groups such as aspartic acid, glutamic acid, and histidine (as its conjugate acid) can act as general acids [39], while groups such as histidine, lysine, and arginine can act as general bases [40] in catalytic mechanisms. In contrast, while some drug-metabolizing enzymes can carry out their catalytic activity themselves, most others (phase I oxidative enzymes) require presence of cofactors and coenzymes to carry out reactions.

Coenzymes are organic molecules (often vitamins or vitamin derivatives) that are required by certain enzymes to carry out catalysis (Fig. 7.4). They bind to the active site of the enzyme and participate in catalysis but are not considered substrates of the reaction. Generally, coenzymes function as intermediate carriers of electrons, specific atoms, or functional groups that are transferred in the overall reaction [41]. An example of this would be the role of nicotinamide adenine dinucleotide phosphate (NADPH) in the transfer of electrons in certain coupled oxidation reactions [42]. In contrast, the term *cofactor* often refers to *inorganic substances* such as "metals" that are required for enzyme catalysis. In many instances, these metals are bound tightly by the enzyme or are complexed within prosthetic groups to form a permanent part of the protein structure. For example, cytochrome P450 enzymes derive catalytic function through a heme-complexed metal species (Fig. 7.4), through the formation of a reactive oxoiron(IV)-porphyrin π-radical cation, and are able to facilitate a wide range of reactions most notably the insertion of an oxygen atom between a carbon hydrogen bond [43].

While the notion of drug metabolism was appreciated before the 1950s, little was known about the oxidative source involved in these enzymatic reactions. However, in 1950s, several laboratories demonstrated the direct incorporation of molecular oxygen into small molecules [44–46]. In addition, during the same time period, other groups determined that the microsomal deamination of amphetamine [47] and dealkylation of aminopyrine [48] also required the presence of both the reduced form of NADPH and molecular oxygen (O_2) [24].

As illustrated in Fig. 7.5, the biological conversion of molecular oxygen to water involves four sequential one-electron reductions. The sequential nature of the reduction is necessitated by the fact that in the ground state, oxygen contains two unpaired electrons. Each stage of oxygen reduction generates a reactive intermediate, which can exist in a number of different energy levels or spin states and can generate new species, generally by the addition of a proton. This has special significance with regard to phase I drug-metabolizing enzymes that use oxene and hydrogen peroxide as the major oxygen species involved in oxidative drug metabolism reactions [49,50].

With respect to phase II drug-metabolizing enzymes, the chemistry that supports metabolite formation requires the presence of a cosubstrate. In these reactions, a foreign compound is covalently linked with a small endogenous molecule, derived from carbohydrate or amino acid sources, to yield a characteristic product known as a *conjugate* [23]. There are five major conjugation reactions that primarily make up phase II drug metabolism: glucuronidation, sulfation, acylation, methylation, and GSH conjugation. The corresponding cosubstrates involved in the listed reactions are listed in Fig. 7.6. Interestingly, while phase II reactions are collectively described as conjugation reactions, they differ greatly in terms of the nature of the substrates involved, their distribution through the body, and reaction mechanisms [51,52].

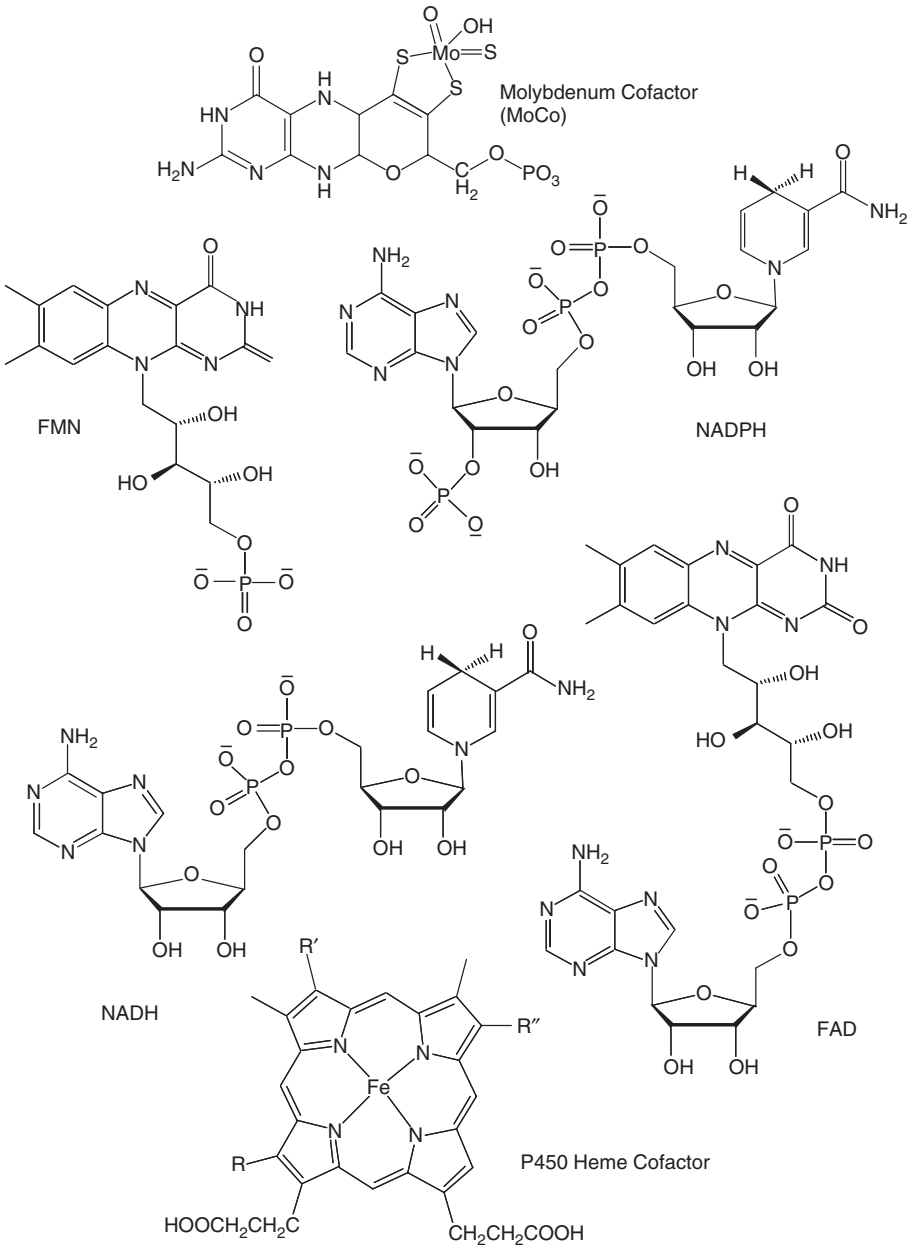

Figure 7.4 Structures of common phase I coenzymes and cofactors.

The biochemical tools used to understand the various mechanism of drug metabolism can be categorized into three primary groups: (i) experiments that are aimed to elucidate the factors that can affect the metabolite transition state; (ii) studies that characterize reaction pathways associated with product formation; and (iii) determinations of enzyme's active topography and influence on rates of metabolite formation.

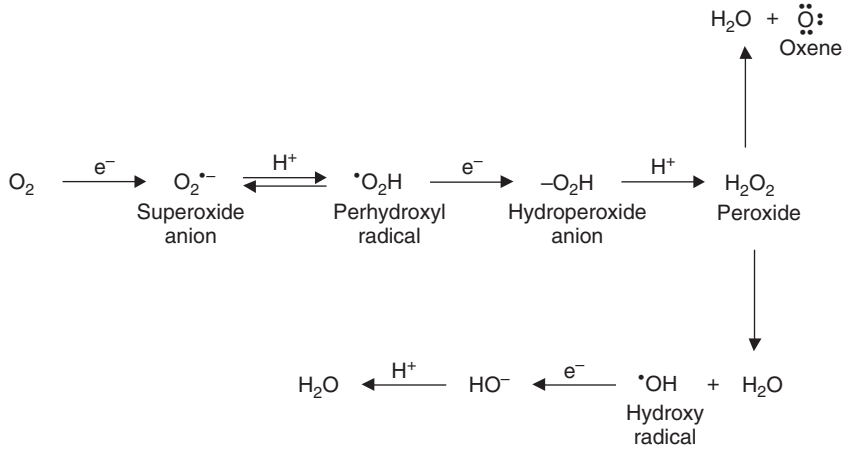

Figure 7.5 Reduced states of oxygen.

Kinetic deuterium isotope effect studies have been used extensively to understand the mechanism of drug metabolism reactions [53]. Primary kinetic isotope effects refer to processes in which the bond to deuterium (usually a C–D bond) is broken during the reaction and are expressed as the ratio of the specific rate constants, k_H/k_D, for the initial reaction of the protium- and deuterium-labeled compounds, respectively. The thermodynamic basis for the primary deuterium isotope effect lies in the large relative mass difference between H and D, which results in a difference (1.2–1.5 kcal mole) between the zero-point energy of a bond to deuterium versus hydrogen [54]. This difference results in a greater energy requirement for cleavage of a bond to deuterium and as a consequence, isotope effects on the rates of metabolic processes where rupture of a C–D bond is rate determining.

In addition to helping define the thermodynamics of an associated drug metabolism reaction transition state, selective use of isotopes (in particular, D and ^{18}O) has also been applied to dissect the nature of drug-metabolizing reactions [55]. For example, the mechanism by which most aromatic hydroxylations occur is via epoxidation of electron-rich π-bonds in the ring [56]. The resulting arene oxide is highly reactive for two main reasons: (i) three-membered rings are highly strained and open up readily and (ii) the ring on which the arene oxide forms is no longer aromatic (one double bond was used to make the epoxide). As a consequence, arene oxides can undergo two main types of reactions: rearrangement to yield a phenol or epoxide opening by reaction with a nucleophile. One of the first applications of selective deuterium labeling in drug metabolism was toward understanding the mechanism of reaction for the enzymatic conversion of naphthalene to 1-naphthol in rat microsomes [57]. The results of this experiment suggested that on enzyme-mediated oxidation of the aromatic ring to the corresponding *para*-phenolic metabolite, the deuterium was retained on the molecule (NIH shift), a result of rearrangement via a ring-opened intermediate [58].

In view of the widespread occurrence of oxidative transformations in drug metabolism, experiments with isotopically labeled oxygen ($^{18}O_2$ or $H_2{}^{18}O$) have been used extensively to characterize many drug metabolism reaction mechanisms [59,60]. A good example of the application of heavy oxygen to determine the mechanism of drug metabolism is through a series of *in vitro* experiments that were carried

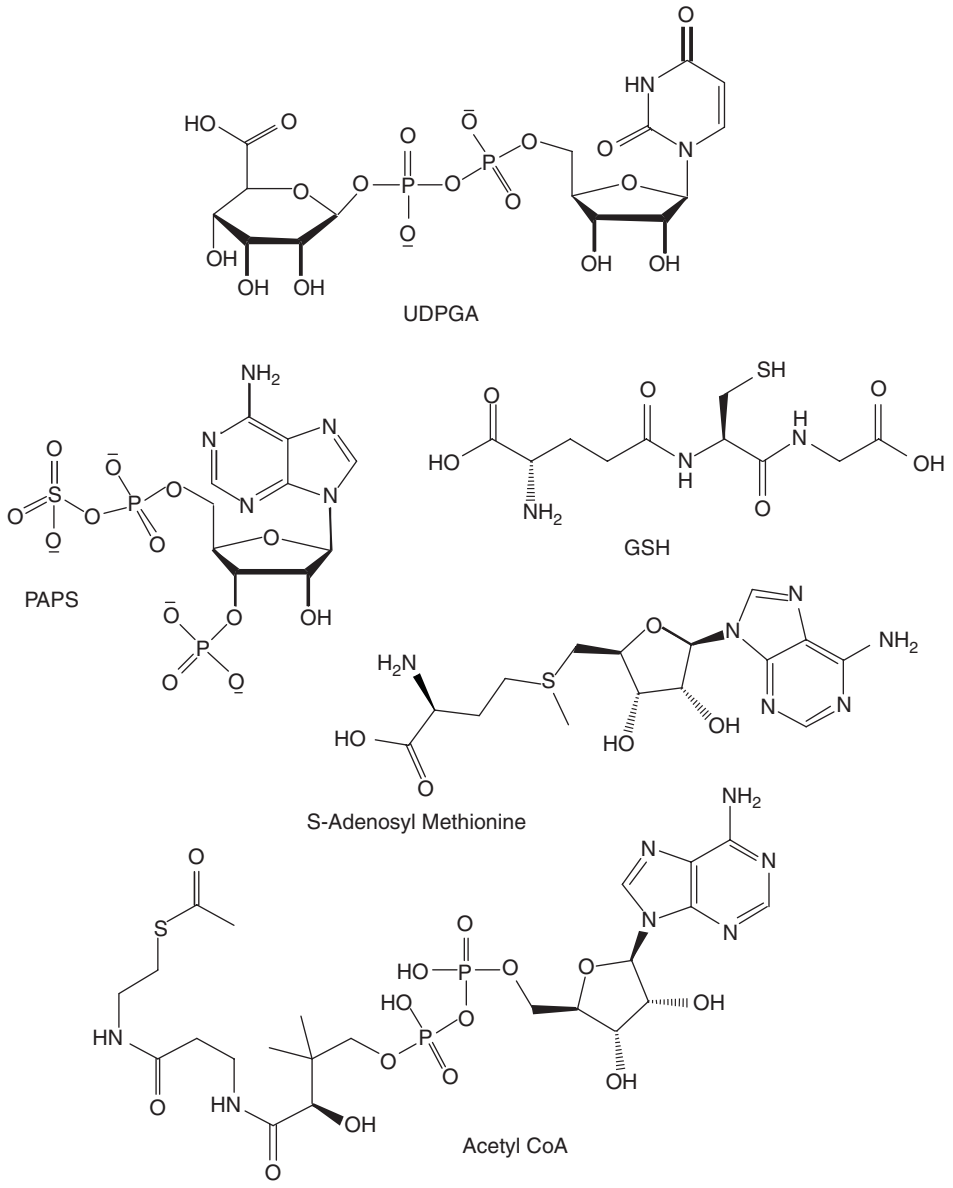

Figure 7.6 Structures of common phase II cosubstrates.

out under atmospheres enriched in $^{18}O_2$ and showed, by GC-MS analysis, that the dihydrodiol metabolite, 1,2-dihydro-1,2-dihydroxynaphthalene, contained only one atom of ^{18}O and that this labeled oxygen occupied the 1-position. In this study, the authors further inferred that the second oxygen atom was derived from water [61]. Subsequent experiments conducted by Jerina and others [62] verified this hypothesis by incubating the molecule in $H_2{}^{18}O$ fortified rat liver microsomal preparations.

Site-directed mutagenesis of proteins has developed into a powerful tool for studies of structure–function relationships for many drug-metabolizing enzyme systems. The strategy of these types of studies is to alter enzyme's amino acid residues that affect reaction features such as substrate specificity [63], catalytic competence [64,65], cooperativity [66], and product specificity [67]. In the past few years, advances in X-ray crystallography, homology modeling, and substrate docking techniques have allowed for more precise functions for drug-metabolizing enzyme residues, making it possible to utilize site-directed mutagenesis designed to test these predictions [68]. The primary aim of site-directed mutagenesis to investigate the catalytic mechanisms behind drug metabolism reactions is to replace essential residues (ionizable or nucleophilic amino acids) with unreactive ones [69,70]. In this fashion, general acids, general bases, and catalytic nucleophiles arguably represent the most "essential" residues in an active site as they directly participate in the formation and rupture of covalent bonds. For example, it has been proposed that the catalytic mechanism for uridine diphosphate glucuronosyltransferase (UGT) enzyme glucuronidation employs a serine proteaselike catalytic mechanism in which an Asp-His pair in the active-site deprotonates the hydroxyl on the substrate, which allows for nucleophilic attack on the sugar donor [71,72]. In an experiment carried out by Patana *et al*. [73], when the His37 residue of UGT1A9 was replaced with an alanine, drug metabolism studies conducted with the mutant enzyme revealed that His37 was not critical in UGT1A9 N-glucuronidation reactions, but was in O-glucuronidation reactions. The authors were able to conclude that for UGT1A9 reactions, *O*-nucleophiles require the active-site histidine residue to deprotonate them so that they become effective nucleophiles, while *N*-nucleophiles develop a formal positive charge during the reaction and thus requires a negatively charged active-site residue to stabilize the reaction transition state.

As described earlier, unlike most "traditional" enzyme systems, the group of enzymes that are loosely termed as *drug-metabolizing enzymes* exhibit considerable structural and catalytic diversity. For the most part, drug-metabolizing enzymes are capable of carrying out specific reactions. The multiplicity of various drug-metabolizing families was recognized more than 30 years ago [74,75]. Because most drug-metabolizing enzyme systems are actually a collection of isozymes, they have been broadly classified into families and subfamilies on a genetic basis [76,77]. For most drug metabolism enzyme families, there is some degree of substrate structural class preference within families and subfamilies, although some overlap in substrate recognition is observed [78,79]. However, independent of which isozyme is actually responsible for a drug metabolism reaction, it should be remembered that enzymes that make up a particular family, share the same chemical mechanism of catalysis. To this end, the scope of this chapter avoids any detailed description of any drug-metabolizing isozymes and will rather focus on the different reactions catalyzed within each family of drug-metabolizing enzymes and the chemistry involved in phase I (Section 7.2) and phase II (Section 7.3) reactions.

7.2 PHASE I DRUG METABOLISM REACTIONS

7.2.1 Cytochrome P450

Mammalian cytochrome P450 monooxygenases are heme-containing, membrane-bound enzymes that catalyze the oxidation and reduction of a variety of xenobiotics

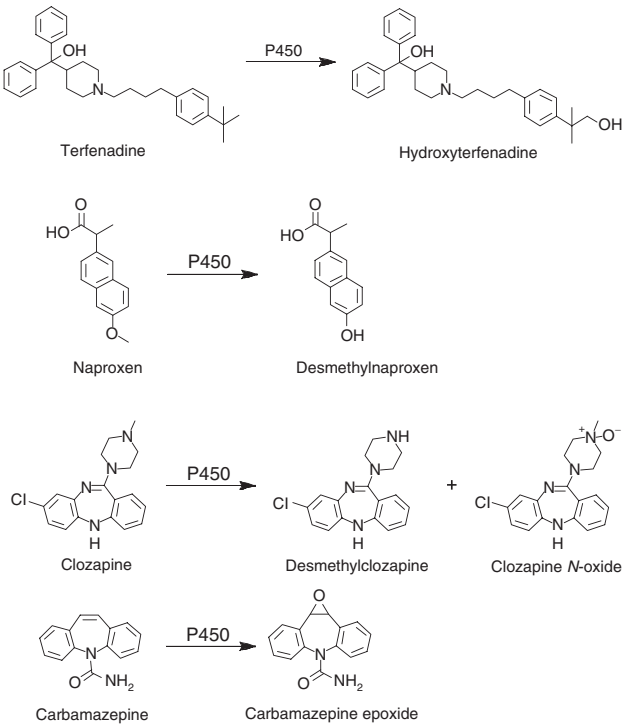

Figure 7.7 Examples of P450 metabolism reactions.

and endobiotics (Fig. 7.7) [80]. P450s require a redox partner protein to transfer electrons from NADPH for catalytic activity. Cytochrome P450 reductase serves as the redox partner for mammalian P450s; it accepts electrons from NADPH through its flavin adenine dinucleotide (FAD) moiety and donates electrons to P450 through its flavin mononucleotide (FMN) moiety [81–83]. Another redox partner protein, cytochrome *b*5, may enhance catalytic activity for certain mammalian P450s [84]. P450s frequently involved in human drug metabolism include CYP1A1, CYP1A2, CYP2B6, CYP2C8, CYP2C9, CYP2C19, CYP2D6, CYP2E1, CYP3A4, and CYP3A5, which differ in tissue localization and substrate selectivity [85]. P450s are expressed in many mammalian tissues, with the highest expression in the liver, gastrointestinal, and respiratory tracts [86]. Major biological roles for the P450s include xenobiotic metabolism, steroid biosynthesis, vitamin metabolism, eicosanoid metabolism, and fatty acid oxidation [87].

The P450 catalytic cycle is a multistep process shown in Fig. 7.8 [80,88,89]. The cycle is initiated by substrate binding to the P450. Substrate binding displaces water as a heme ligand, changing the spin state of the heme iron, thereby allowing for easier reduction of the heme for many P450s [90,91]. An electron from NADPH is then introduced to the P450 through transfer via P450 reductase. Binding of molecular oxygen to the P450 heme is followed by introduction of a second electron to form a nucleophilic ferric peroxo intermediate [92]. This intermediate may continue through the catalytic cycle or lose superoxide in a shunt (nonproductive) pathway. Subsequent protonation of

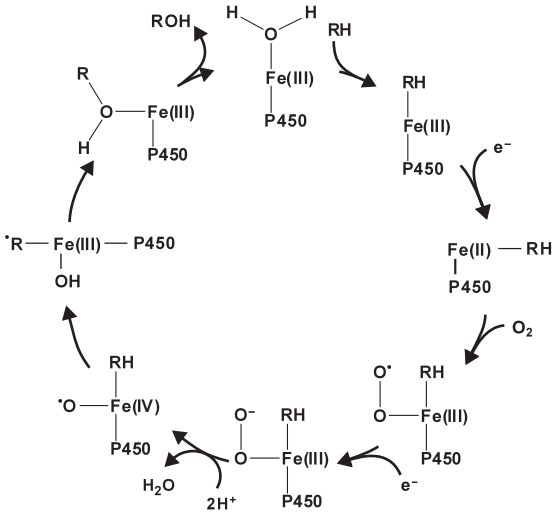

Figure 7.8 P450 catalytic cycle.

the distal oxygen results in an electrophilic ferric hydroperoxide intermediate [93–95]. The ferric hydroperoxide intermediate may continue through the catalytic cycle or lose hydrogen peroxide in a shunt pathway if the proximal oxygen is protonated. Protonation of the distal oxygen results in a species that rapidly undergoes heterolytic cleavage of the oxygen–oxygen bond to form a reactive iron–oxygen species, compound I [96]. Compound I may then react with substrate to form product or produce water via a shunt pathway through the introduction of two additional electrons and protons. While the general catalytic cycle applies to all P450-mediated reactions, specific reaction mechanisms are dependent on the functional groups present within the substrate.

7.2.1.1 Aliphatic Oxidation. P450s catalyze a variety of biotransformations (Fig. 7.9); common types of P450-mediated oxidations include hydrocarbon oxidation [97], olefin oxidation [98], aromatic hydroxylation [99], and heteroatom oxidation and dealkylation [100]. P450-mediated hydrocarbon oxidation is believed to proceed through a hydrogen atom abstraction (HAT) mechanism, where a hydrogen atom is abstracted from the substrate, followed by oxygen rebound to form a hydroxylation product (Fig. 7.10) [97]. Evidence for a HAT mechanism include a large isotope effect (typically >10) [101], partial stereochemical scrambling [102], and observed allylic rearrangement products [103].

Radical clocks have been used to assess the lifetime of radical intermediates and the rate of the oxygen rebound step [104]. Cyclopropyl groups are often used as radical clocks; radicals formed next to cyclopropyl rings may rearrange to homoallyic radicals that produce ring-opened products if the rate of rearrangement is faster than oxygen rebound or produce cyclopropyl carbinyl products if radical recombination is faster than rearrangement (Fig. 7.11). Adding ring strain to the cyclopropyl group increases the speed of rearrangement [105]. On the basis of experiments using radical clocks, rates for radical recombination during the oxygen rebound step of P450-mediated catalysis

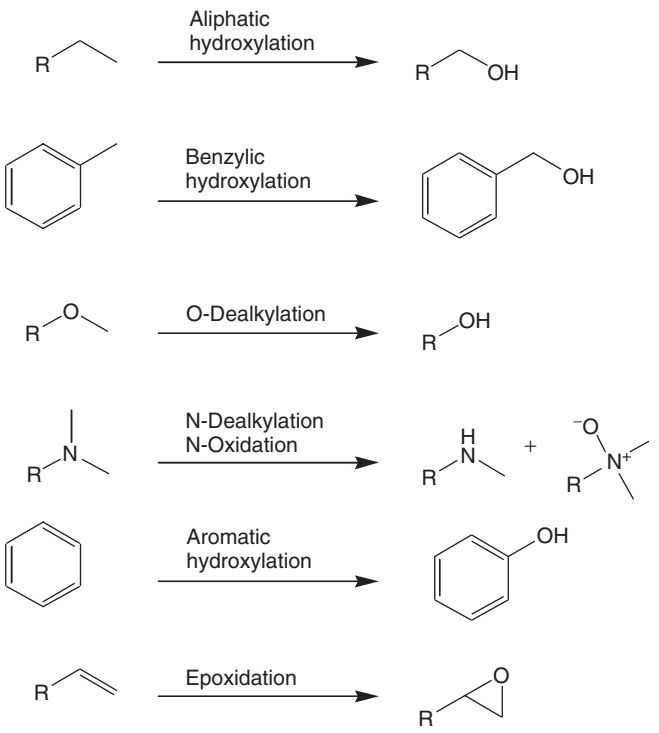

Figure 7.9 Generic examples of P450-mediated biotransformations.

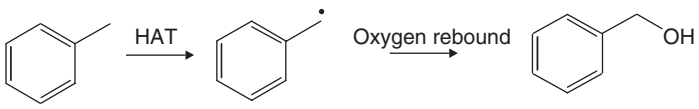

Figure 7.10 Example of the proposed hydrogen atom transfer mechanism.

vary from 1×10^{10} s^{-1} to those exceeding the theoretical rate constant of 2×10^{12} s^{-1} for highly strained radical clocks [106]. While higher ratios of rearranged products to carbonyl-derived products were expected from experiments using highly strained radical clocks, product formation ratios indicated that the rate of radical recombination generally increased in a compensatory fashion with radical rearrangement [107]. This finding suggests that P450-mediated hydrocarbon oxidation may proceed by a more complex mechanism than a simple radical recombination. Results observed from the radical clock experiments may be explained by a two-state reactivity model, with a low spin pathway that resembles concerted oxygen insertion and a high spin pathway that resembles radical recombination [108]. The influence of both substrate and enzyme environment influences which pathway predominates.

7.2.1.2 Olefin Oxidation. Olefins undergo oxidation by P450s to form epoxides, which may hydrolyze to form a diol product (Fig. 7.12). The olefin epoxidation mechanism may proceed through either a concerted or a nonconcerted mechanism. The

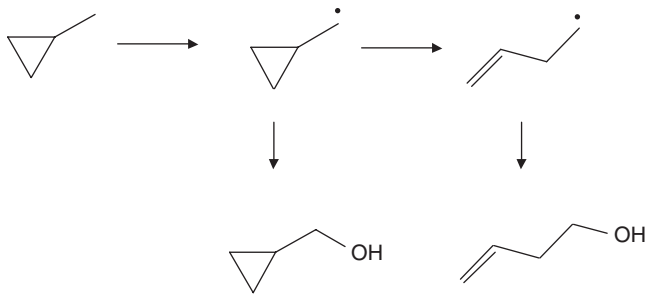

Figure 7.11 Example of a cyclopropyl radical clock.

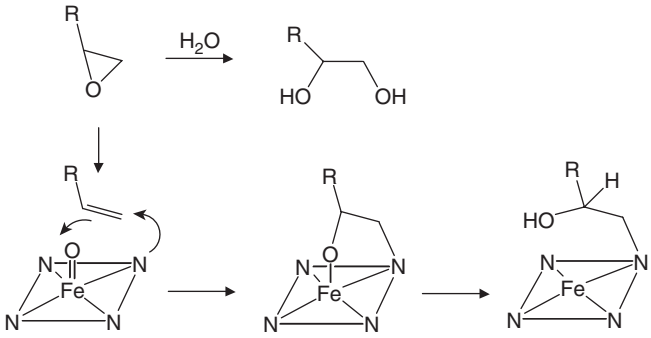

Figure 7.12 Proposed mechanism of P450-mediated olefin metabolism.

retention of stereochemistry on P450-mediated epoxidation suggests a concerted mechanism [109]. However, two pieces of evidence argue against a concerted mechanism. P450-mediated reactions with olefins form heme adducts in addition to epoxide products [110]. Direct addition of epoxides to the P450 did not alkylate the P450 prosthetic heme, suggesting that heme alkylation occurs before epoxidation [111]. Some olefins, such as trichloroethylene, form carbonyl compounds as a result of P450-mediated epoxidation [112]. The epoxides produced from these reactions do not form carbonyl products, suggesting that more than one oxidation pathway is needed to account for product formation. As with hydrocarbon oxidation, the observed results may be described using a two-state model, where closure of the epoxide ring in the low spin state proceeds with a small energy barrier such that the reaction is nearly concerted, while closure of the epoxide in the high spin state occurs with a larger energy barrier that allows for other mechanisms to compete with epoxidation [113].

Oxidation of acetylenes is believed to proceed through an oxirane intermediate (Fig. 7.13), which rearranges through shift of a terminal hydrogen to a ketene intermediate [114]. Evidence for this mechanism comes from the observed isotope effect, which suggests that deuterium migration occurs in the rate-limiting step as oxygen is transferred to the acetylene [115].

7.2.1.3 Aromatic Oxidation. Hydroxylation of aromatic rings proceeds through an arene oxide intermediate (Fig. 7.14) [99]. Formation of the arene oxide intermediate is

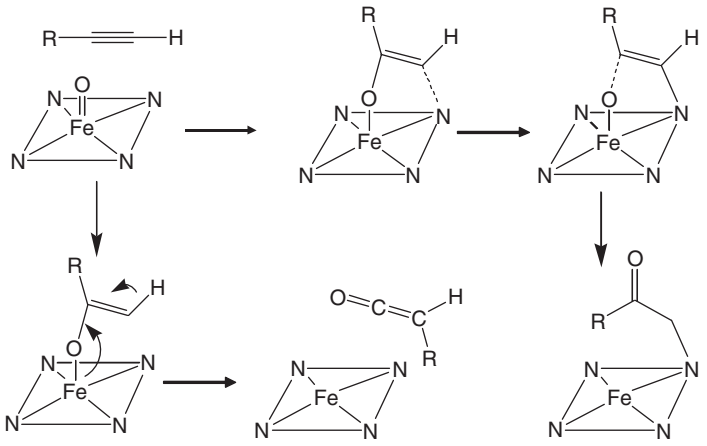

Figure 7.13 Proposed mechanism of P450-mediated acetylene metabolism.

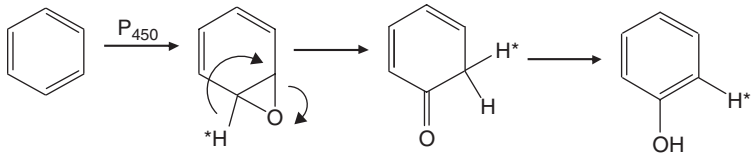

Figure 7.14 Proposed mechanism of P450-mediated aromatic oxidation.

followed by hydrogen migration in a process called an *NIH shift* [116]. Alkyl or halogen groups may also migrate, depending on the substrate [117]. The phenol product results from tautomerization. Evidence to support this mechanism includes partial retention of the shifted hydrogen and a small inverse secondary isotope effect for the reaction [118]. Since the NIH shift is not the rate-limiting step, the reaction is not sensitive to primary isotope effects. Hydroxylation of phenyl rings with adjacent cyclopropyl groups proceeds without ring opening, suggesting that a discrete radical mechanism is not favored for arene oxidation [119].

7.2.1.4 Heteroatom Dealkylation and Oxidation.

7.2.1.4.1 N-Dealkylation. Tertiary amines are metabolized predominantly through dealkylation, which can occur through various peroxidases, but the most common pathway for dealkylation is by the cytochrome P450 superfamily (Fig. 7.7). As such, a significant effort has been put forth to understand the mechanism of cytochrome P450 N-dealkylation reactions. The two predominant mechanisms in the literature are illustrated in Fig. 7.15. Mechanism A is that of single-electron transfer (SET) and mechanism B is that of HAT. For SET, the initial step is envisioned to occur by electron transfer from the amine nitrogen to the high valent iron oxene species forming a cation radical intermediate, which is then capable of catalyzing deprotonation of the ammonium radical followed by oxygen rebound to form the hydroxylamine [120]. Decomposition of the carbinolamine intermediate yields the N-dealkylated product.

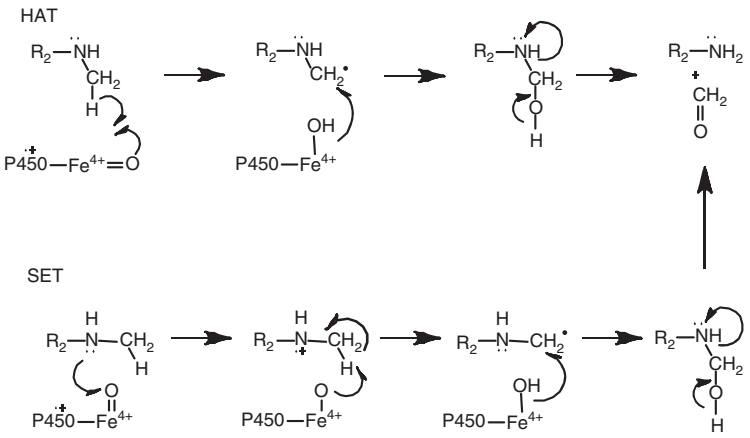

Figure 7.15 Proposed mechanisms for P450-mediated N-dealkylation: (i) single-electron transfer (SET) and (ii) hydrogen atom abstraction (HAT).

Alternatively, for HAT, a hydrogen atom is abstracted directly from the α-carbon followed directly by radical recombination to form the α-hydroxylamine. Differentiating between the two mechanisms has been explored extensively.

Kinetic isotope effects have been employed to differentiate between the two mechanisms. Initial interrogation of P450 N-dealkylation with selectively deuterated analogs such para-substituted *N*,*N*-dimethylanalines produces small kinetic isotope effects ($k_H/k_D < 4$). In contrast, alternate enzyme systems such as horseradish peroxidase (HRP) where SET is considered the mechanism of oxidation result in isotope effects that approximate the theoretical maximum. By comparison, HAT is the accepted mechanism for alkane hydroxylation which produces maximal kinetic deuterium isotope effect values ($k_H/k_D > 7$). The small isotope effects observed with *N*,*N*-dimethylaniline are consistent with hemeprotein catalyzed demethylation reactions that involve a deprotonation step [120]. However, small isotope effects have been demonstrated for demethylation of trimethylamine by *tert*-butoxy radical [121]. Dinnocenzo *et al*. [122] also observed a small isotope effect for hydrogen atom abstraction from *N*,*N*-dimethylaniline by *tert*-butoxy radical. The smaller observed isotope effects have been rationalized by the proposed weakening of the α-C–H bonds present in amines which facilitate a relatively early transition state. Nonsymmetrical transition states as described by the Westheimer kinetic postulate would produce an isotope effect below the theoretical maximum (Fig. 7.16). These contradicting results indicate isotope effect data alone may not be sufficient to distinguish the mechanism of P450 N-demethylation [123].

Synthetic heme mimetics and chemically designed metabolic probes have been employed to examine HAT (*tert*-butoxy radical) and SET (cation radical deprotonation) mechanisms in comparison to metabolites obtained directly from NADPH-supported P450 reactions. The combination of isotope effects with substituent effects has been used to generate isotope effect profiles for exploring reaction mechanisms. The increased number of compounds allows for trends to be explored in the resultant data to provide increased confidence in interpretation of reaction mechanism across different reaction systems. For example, P450 reactions revealed most similarity to *tert*-butoxy radical model supporting HAT as the mechanism for N-dealkylation (Fig. 7.17). The

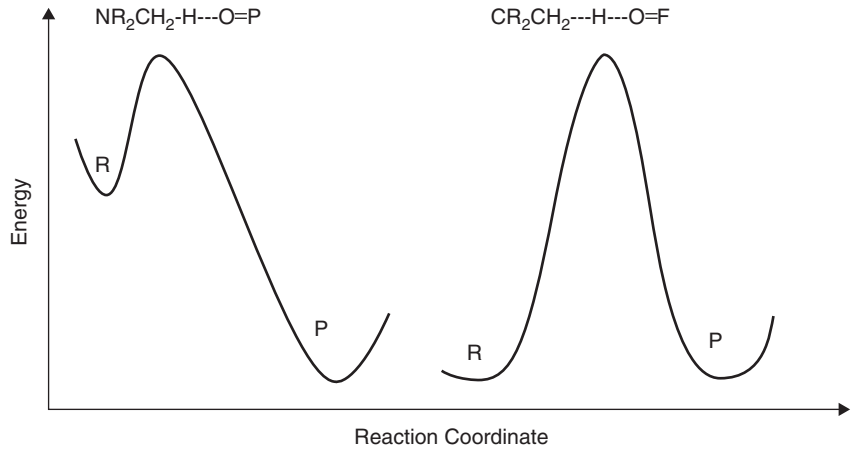

Figure 7.16 Example of asymmetrical and symmetrical transition state corresponding to theoretical difference in kinetic isotope effects: (a) early transition state $k_H/k_D > 4$ and (b) symmetrical transition state $k_H/k_D \sim 8$.

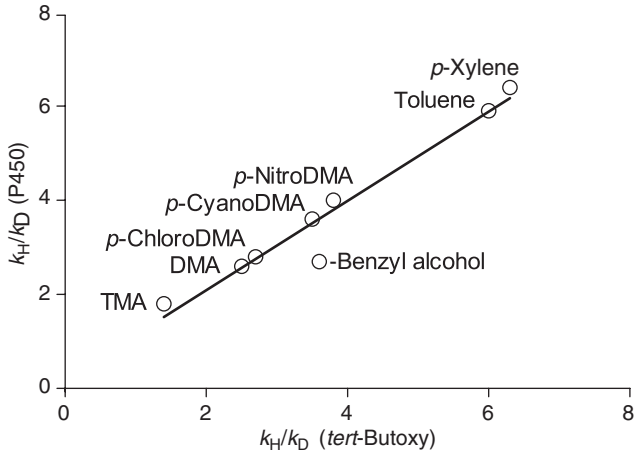

Figure 7.17 Isotope effects by *tert*-butoxy radical (HAT mediated) compared to P450-supported reactions. Plot includes accepted HAT pathways (xylene, toluene, and benzyl alcohol) in addition to several substituted *N*, *N*-dimethylanilines.

concordance between *tert*-butoxy radical and P450-supported reactions further support HAT mechanism for P450 reactions.

Chemical probes have been designed and synthesized to interrogate the mechanism of N-dealkylation. As described earlier in this section, radical clocks can differentiate oxidative mechanisms based on product ratios. A series of *N*-cyclopropyl anilines have been designed to evaluate different product ratios as a tool to rationalize HAT versus SET [105,124–126]. In principal, the rapid ring opening associated with *N*-cyclopropyl ring of the nitrogen cation radical would favor the N-decyclopropylation. However, the major pathway favored N-demethylation in support of HAT as the mechanism for oxidation (Fig. 7.18) [124]. Alternatively, Atkinson *et al*. [105] utilized a similar probe but in contrast yielded results supportive of the SET mechanism.

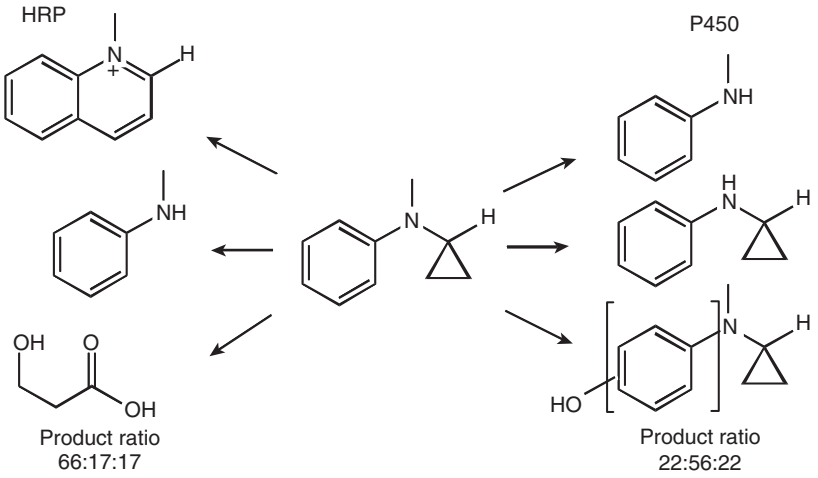

Figure 7.18 Example of product ratios from radical clock experiments with HRP and P450.

N-Oxides or *N*-hydroxyl products can also be catalyzed by P450s. The reaction is generally thought to proceed through the formation of a radical cation. The mechanism of partitioning between *N*-oxide and N-dealkylation remains unclear. Instability and potential for reduction of *N*-oxide may limit the extent of P450 *N*-oxide formation. The ability for *N*-oxides to back donate the oxygen to P450 was exploited in the form of synthesis of various deuterated *N*-oxide probes in order to specifically investigate the potential for high valent iron oxene to catalyze N-dealkylation reactions [127]. Specifically, the *N*-oxides for a series of para-substituted $^{13}C_2H_2$-labeled *N*,*N*-dimethylanilines were synthesized with the intent to function as both substrates and surrogate oxygen atom donors. This particular substrate probe isolates the high valent iron oxene in the P450 catalytic cycle on reduction of the *N*-oxide to the iron–porphyrin complex. Coupled with deuterium isotope effect profiles obtained using the *N*-oxide system were found to closely match the profiles produced using NAD(P)H/NAD(P)-P450 reductase/O_2 system.

7.2.1.4.2 O-Dealkylation. Oxidative O-dealkylation represents significant phase I oxidation pathway. O-Dealkylation reactions catalyzed by P450 enzymes have been studied using primary deuterium and tritium isotope effects to estimate the intrinsic isotope effect for this reaction using the technique of Northrop [128]. The large intrinsic isotope effect ($k_H/k_D > 7$) is consistent with a linear transition state on hemiacetal formation in which little to no bonding exists between the α-carbon and the hydrogen atom (Fig. 7.16) [128]. These results are consistent with hydrogen abstraction mechanism put forth by Groves and McClusky [97] for aliphatic oxidation. In addition, ^{18}O experiments illustrate that heavy water is incorporated into the metabolite byproduct [97]. Evidence for O-dealkylation to proceed through HAT is also provided by Dowers and Jones [129], wherein they designed and utilized quinoline analogs as evidence for HAT.

P450-mediated reactions follow the general reactivity pattern of N-dealkylation > benzylic hydroxylation > O-dealkylation > aliphatic hydroxylation >ω-hydroxylation [130]. These results correlate well with quantum mechanics-based AM1 calculations

of the stability and ionization potential of the radical resulting from HAT. These efforts have been extended to include aromatic oxidations through parameterization of the HAT and aromatic oxidation pathways based on experimentally determined regioselectivity data [131].

7.2.2 Flavin Monooxygenase

Mammalian flavin-containing monooxygenases (FMOs) are able to metabolize a variety of structurally diverse xenobiotics [132]. The structural requirements for FMO oxidation reactions (Fig. 7.19) are relatively straightforward as the substrate requires a soft nucleophile, usually a nitrogen or sulfur heteroatom but in rare cases may also include carbon, phosphorus, or selenium [133–138]. Interestingly, while nucleophilicity is the principal driver for FMO oxidations, structure–activity studies suggest that size and charge of potential substrates are important factors that mediate access to the enzyme's active site [139,140]. As a consequence, the mechanism of FMO oxidation reactions are all similar and observed differences in the substrate specificities across the family of enzymes are all nearly due to differences in the active-site topography and access to the oxygenating species [141,142]. The influence of active-site topography on substrate oxidation is particularly evident in terms of the stereoselectivity observed with many

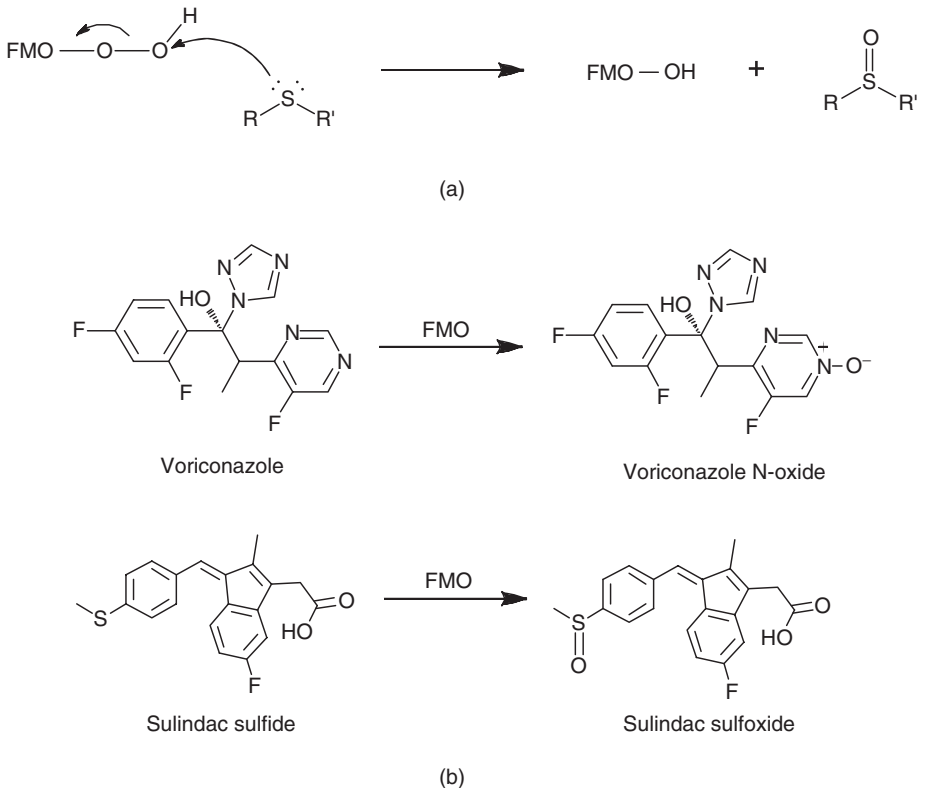

Figure 7.19 (a) Generic mechanism of FMO oxidation reaction. (b) Examples of FMO metabolism reactions with voriconazole and sulindac.

FMO oxidation reactions [143,144]. In the 1980s, Walsh and coworkers examined the stereochemistry of sulfoxidation of ethyl *p*-tolyl sulfide by hepatic microsomal FMO and found that the enzyme-catalyzed formation of the (R)-enantiomer of ethyl *p*-tolyl sulfoxide in great enantiomeric excess [145,146]. In this fashion, topography of the enzyme's active site not the substrate dictates the final chirality of the product as the enantiotopic electron pairs on the sulfur atom of an asymmetrically substituted sulfide are equivalent. Restated, chemical reactions that utilize peroxides or peracids as oxidants in solution proceed with no stereochemical preference and thus generate racemic sulfoxides [147]. However, in the chiral environment of the enzyme's active site, the electron pairs are not equivalent and stereoselective sulfoxidation can, and often times does, occur.

As with many biological oxidation reactions, the catalytic cycle for FMO enzymes is complex and involves several steps (Fig. 7.20). The underlying catalytic feature of this class of enzyme is their ability to stabilize a flavin-hydroperoxide intermediate [148,149]. Unlike the cytochromes P450 [150], the FMO peroxy intermediate has been found to be stable for minutes to hours at 4°C and can be observed spectrally [151].

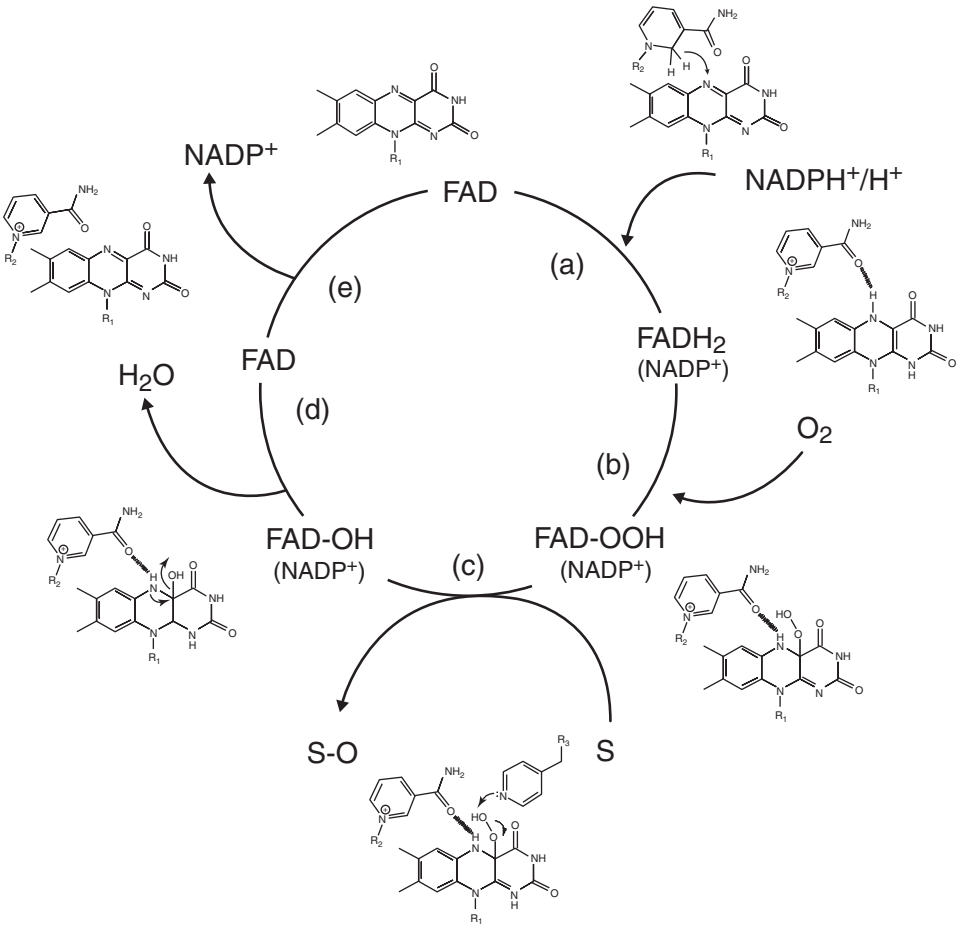

Figure 7.20 Proposed FMO catalytic cycle.

In the first step of the FMO catalytic cycle, FAD undergoes two-electron reduction by NADPH [152,153]. Chemistry of NADPH requires that reduction of the flavin cofactor is facilitated through a hydride transfer from the C4 atom of the nicotinamide ring to the flavin N5 atom (Fig. 7.20a) [154,155]. The reduced flavin reacts rapidly with molecular oxygen to form the stable peroxyflavin intermediate that is able to wait for a suitable nucleophile with which to react [156,157]. Stabilization of the intermediate requires the presence of $NADP^+$ [158], which remains tightly bound to the enzyme throughout the catalytic cycle [159]. It has been proposed through computer simulation of FMO active that $NADP^+$ is able to shield the enzyme's active site (Fig. 7.20b), and thus provide proper H-bonding environment, which in turn promotes a prolonged half-life to the peroxyflavin intermediate [160]. The binding of oxygen is followed by the nucleophilic attack by the substrate on the peroxyflavin, which results in one atom of molecular oxygen being transferred to the substrate (Fig. 7.20c). Following metabolite release, the resulting flavin hydroxy psuedobase is converted to FAD via the loss of water (Fig. 7.20d). It should be noted that the release of water and subsequent regeneration of FAD is a rate-limiting step in the FMO cycle [141]; thus, unlike the cytochrome P450 cycle [161], substrate binding has little influence on the rate of catalysis. The final step in the FMO catalytic cycle is the release of $NADP^+$, which regenerates the FMO FAD moiety (Fig. 7.20e).

7.2.3 Aldehyde Oxidase

Aldehyde oxidase (AO) and xanthine oxidase (XO) are cytosolic members of the molybdenum hydrolase family. Both enzymes are capable of oxidizing aldehydes and nitrogen-containing aromatic compounds. While the scope of AO/XO involvement in xenobiotics remains somewhat limited relative to P450s, their role in the clearance of new drugs is likely to see an increase based on several factors [162,163]. The desire to reduce P450 clearance leads to increase number of heteroaromatic rings, a primary pharmacophore feature of AO/XO substrates. The awareness of AO/XO in drug metabolism has increased the availability of recombinant enzymes and selective chemical inhibitors for characterization of AO/XO metabolism. For example, planar nitrogen-containing heteroaromatic systems serve as the primary pharmacophore associated with competitive inhibitors of ATP-binding site for kinases that may coincide with AO/XO contributing to the clearance of these xenobiotics [164].

In accord with attempts to reduce P450 metabolism, the addition of nitrogens into aromatic ring systems is often attempted. The added nitrogens decrease the electron density of the carbon atoms in the heterocycle and tend to reduce P450 metabolism [127]. However, the reduced electron density of the carbon atoms in the heterocycle increases the potential for nucleophilic oxidation by AO/XO [165]. Both XO and AO enzymes contain molybdenum pyranopterin cofactors (MoCo) that facilitate nucleophilic oxidation of electron deficient substrates [166]. Most commonly, the oxidation occurs adjacent to the nitrogen in a heterocycle. The active sites are speculated to have similar structure capable of oxidizing a variety of dissimilar structures possessing significant overlap of substrates between AO/XO [165]. Catalysis involves cleavage of C–H bond and the oxygen incorporated into product arises from water and the byproduct of the oxidative step are superoxide and hydrogen peroxide [167]. A depiction of the catalytic mechanism for AO/XO metabolism is shown in Fig. 7.21. The oxidation has been demonstrated to occur through the formation of a tetrahedral transition state [168].

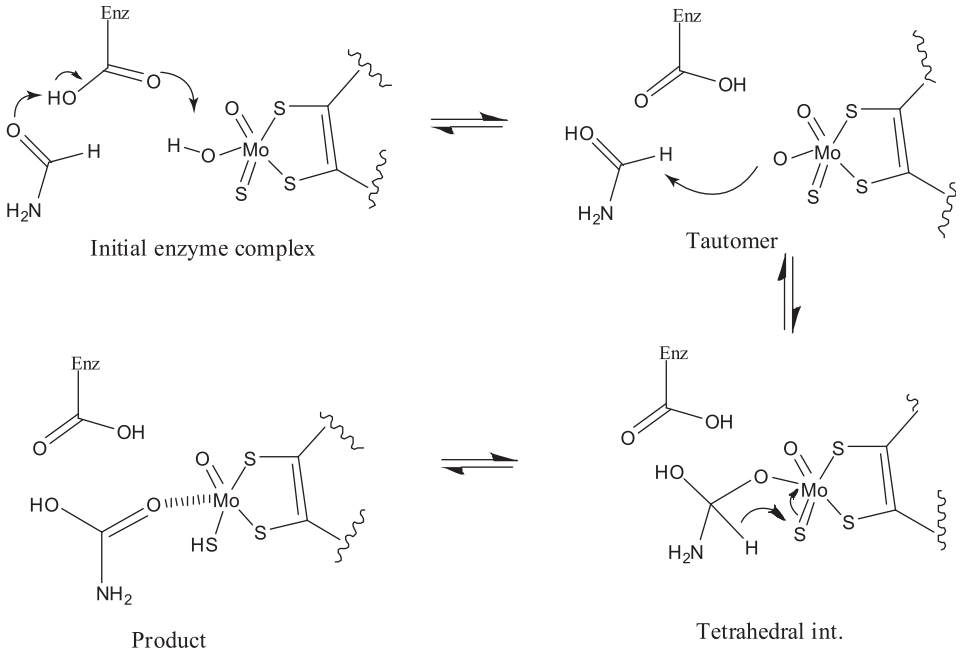

Figure 7.21 Proposed mechanism for AOX-mediated metabolism.

Several substrates and inhibitors exist for AO/XO, which can be helpful in distinguishing the enzymes involved in metabolism. XO is specific for the conversion of 1-methylxanthine to 1-methyluric acid, which are secondary metabolites of caffeine [169] (Fig. 7.22). Allopurinol is metabolized by XO to oxypurinol, which forms an inhibitory complex with the reduced form of the enzyme (Fig. 7.22) [170]. On reoxidation, the inhibition of oxypurinol is diminished [171]. FYX-051 also forms a tetrahedral complex and functions as structure-based inhibitor of XO [172]. In contrast, febuxostat does not complex to the molybdenum center but blocks substrate access directly [173,174]. Several compounds including hydralazine, chlorpromazine, and isovanillin were identified as reasonably selective inhibitors of AO after screening a panel of 239 drugs for AO inhibition [162].

AO/XO have also been exploited for the purpose of converting prodrugs to active drug species in order to overcome ADME-related issues. For example, 5-fluorouracil (5-FU) is a generic antineoplastic, which is rapidly metabolized in the gastrointestinal tract limiting the bioavailability of 5-FU [175]. In order to overcome this obstacle, a prodrug form, 5-fluoro-pyrimidinone, was employed, whereby the keto group is introduced by hepatic AO after absorption [176]. Another example is that of the antiviral penciclovir, which displays poor oral absorption [177]. The diacetyl 6-deoxy prodrug derivative of penciclovir, famciclovir, displays improved absorption and systemic availability [178].

Predictions of AO metabolism have been studied using density functional theory to qualitatively determine the site(s) of oxidation based on the analysis of the energetics of the proposed tetrahedral intermediate with the oxidized carbon [165]. In general, it has been suggested the AO metabolism will occur at the most electropositive carbon in a molecule with some influence on regioselectivity determined by steric bulk

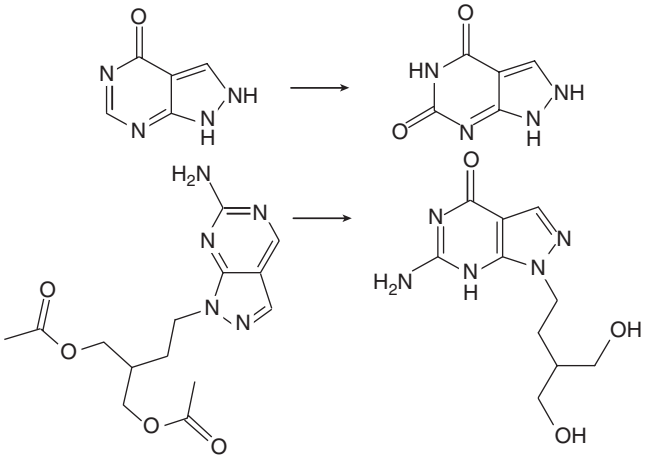

Figure 7.22 Example reactions catalyzed by AOX.

[179]. Additional factors must play a role in metabolite regioselectivity as illustrated by the fact that the most electropositive carbon is not always the site of metabolism. The DFT calculations from Torress *et al*. suggest that oxidation of substrates by AO appears reliant on the electronic effects of the substituents. The use of 6-substituted quinazolinones demonstrate the electronic effects and increase in reaction rates with increased electron-withdrawing groups at the 6-position [180,181]. The calculated results provide a rank ordering of potential products by evaluating the individual tetrahedral intermediates precluding metabolite formation. For the compounds examined, >90% of AO metabolites were correctly predicted. The calculations were also able to differentiate the metabolites generated by XO compared to AO for a series of closely related molecules.

7.2.4 Monoamine Oxidase

Mammalian monoamine oxidases (MAOs) are flavin-containing enzymes that catalyze the oxidation of amines to aldehydes (Fig. 7.23) [182,183]. Two isozymes are known, MAO-A and MAO-B, which differ in substrate and inhibitor selectivity [184]. MAOs are expressed in many mammalian tissues, with high expression in both the liver and placenta [185]. MAOs are also present in the brain; they are believed to have an important biological function for the inactivation of neurotransmitters [186].

The requirements for MAO oxidation are a basic nitrogen and an adjacent carbon with two α-hydrogens (Fig. 7.24). The substrate-binding region is a flat cavity lined with hydrophobic residues [187]. Structure–activity relationships (SARs) suggest that

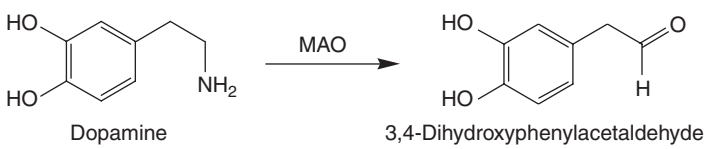

Figure 7.23 Example of MAO metabolism reactions with dopamine.

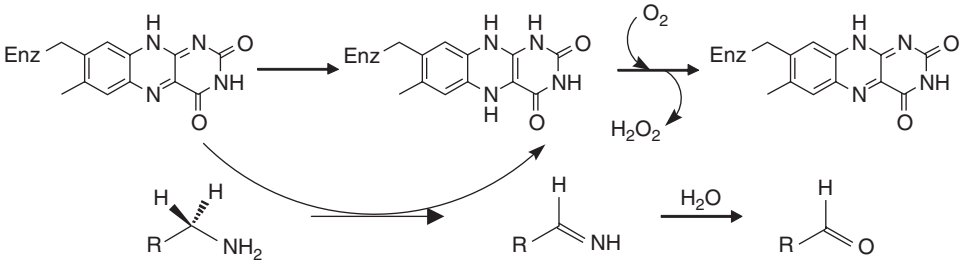

Figure 7.24 MAO catalytic cycle.

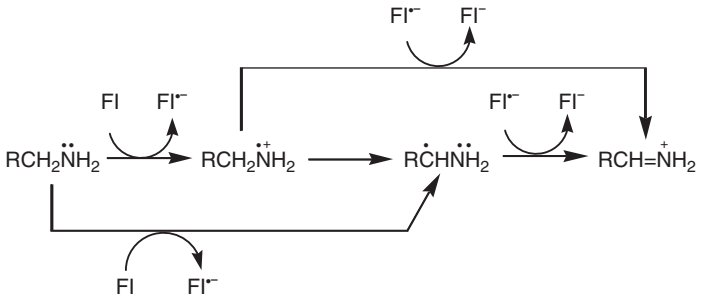

Figure 7.25 Proposed mechanisms of MAO-mediated reactions: single-electron transfer and hydrogen atom abstraction.

the size and shape of potential substrates determine access to the enzyme's active site [188]. The mechanisms of MAO-catalyzed reactions are generally similar; therefore, differences in observed kinetics are due to specific interactions between the enzyme and the substrate [189]. The influence of active-site topography is particularly important due to the stereochemical requirements for MAO oxidation. In the 1980s, Yu and coworkers found that the pro-(*R*)-hydrogen of MAO substrates was lost exclusively based on the reactivity of stereoselectively deuterated dopamine analogs [190,191]. In this sense, the active site dictates reaction stereochemistry. However, the aldehyde moiety resulting from substrate oxidation is not chiral, such that MAOs do not produce an inherently chiral product.

MAO-mediated oxidation has been proposed to proceed by three mechanisms: SET [192], HAT [193], and a polar/covalent mechanism (Fig. 7.25) [194]. The SET mechanism begins with transfer of an electron from the substrate nitrogen, forming an aminyl radical cation and a flavone semiquinone radical. Loss of an α-hydrogen creates a carbon-centered radical, which can then transfer an electron to form an imminium ion and a flavone semiquinone. On the basis of the results of SAR studies, the reactive carbon is positioned in front of the N5-C4a locus, with its α-hydrogens located ~3.6 Å from the flavin N5. The imminium ion is released from the active site and undergoes hydrolysis to form the aldehyde product. The HAT mechanism proceeds through a similar pathway, but begins with direct loss of an α-hydrogen. In the polar/covalent mechanism, the substrate forms a covalent bond with FAD (Fig. 7.26). Cleavage of the bond results in formation of an imminium ion and $FADH_2$.

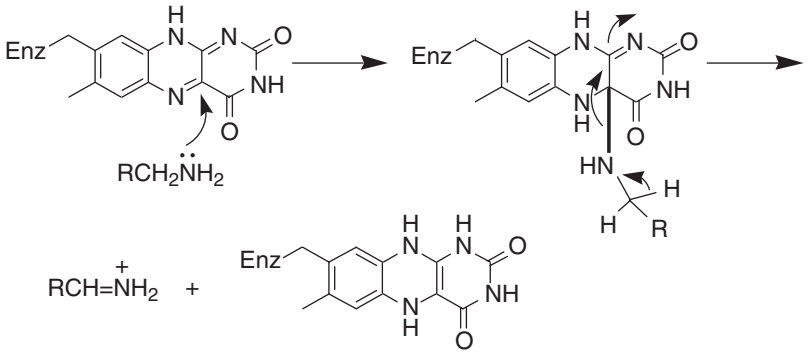

Figure 7.26 Proposed polar/covalent mechanism for MAO-mediated reactions.

MAO-A and MAO-B differ in both inhibitor and substrate selectivity. Substrates for MAO-A include 5-hydroxytryptamine and epinephrine; clorgyline is a selective inhibitor of MAO-A [195]. Substrates for MAO-B include benzyl amine and β-phenylethylamine; deprenyl is a selective inhibitor of MAO-B [196]. Differences in substrate selectivity may partially be explained by a smaller entrance cavity for MAO-B, although results from site-directed mutagenesis studies suggest that the Tyr326Ile MAO-B mutation conferred MAO-A activity and the Ile335Tyr MAO-A mutation conferred MAO-B activity [197].

7.2.5 Carboxylesterase

Carboxylesterases (CEs) metabolize and eliminate endogenous and xenobiotic esters. In humans, the highest hydrolase activity is found in the liver [198–200]. The mechanism for catalysis is similar to that of other α/β hydrolases that employ an active-site serine, histidine, and acidic (glutamic or aspartic acid) residue that are spatially oriented to form a catalytic triad (Fig. 7.27) [198,201–204]. The general mechanism occurs in two steps: first, the serine hydroxyl forms an acyl intermediate with the substrate. The acyl intermediate is then hydrolyzed to form a product. Like other drug-metabolizing enzymes, CEs display broad substrate specificity mediating the hydrolysis of esters, amides, and thioester substrates (Fig. 7.28) [205,206]. CEs have also demonstrated the ability to transesterify compounds such as cocaine, methylphenidate, and meperidine [207,208]. The inhibition of CEs has attracted attention as a mechanism of therapeutic intervention or modulation of coadministered prodrugs [209–211]. Furthermore, inhibition of CE is a primary off-target concern for therapeutics aimed toward inhibiting other esterase and hydrolase enzymes [212]. Differences in catalytic efficiencies have been observed when comparing human CE to CE found in preclinical species [199,213]. The mechanistic understanding of CE in drug metabolism has been established through a variety of techniques including ligand-based SAR, crystallography, and site-directed mutagenesis studies.

The strategically positioned amino acids for hydrolysis combined with the observed substrate promiscuity presents a unique dichotomy. One explanation is that CE displays significant induced fit of protein that is predicated on the proper spatial orientation of the substrate [214]. On substrate induced fit, the conformation of the catalytic triad

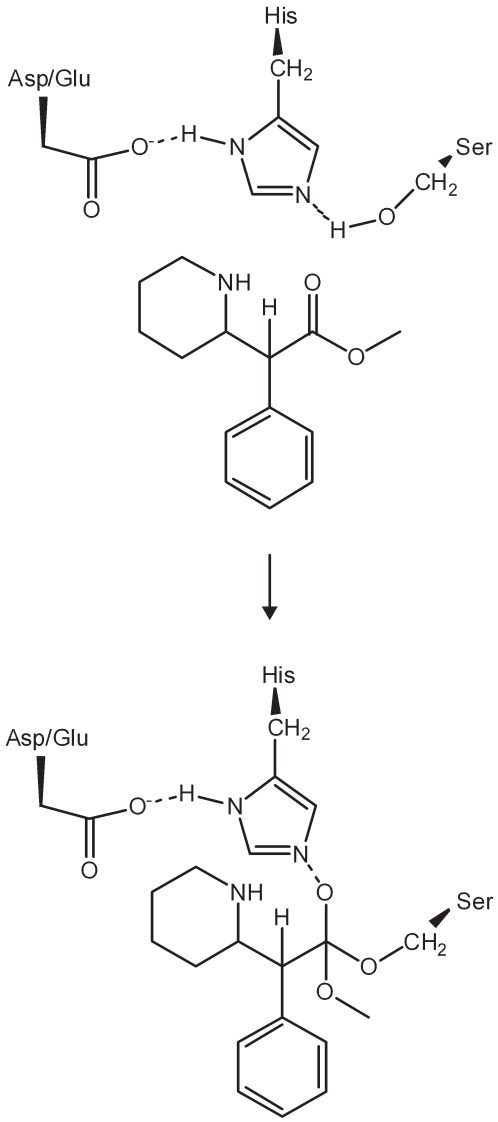

Figure 7.27 The catalytic triad binding methylphenidate to form tetrahedral transition state complex.

is postulated to form a strong hydrogen bond also known as a *low barrier hydrogen bond* between the catalytic His and acidic residue to yield an increased reactivity of His as a general base [215–217]. As might be expected, subtle changes in chemical structure of substrates and inhibitors can have a profound impact CE activity. For example, a series of cypermethrin analogs were examined to understand the role of stereochemistry on CE catalysis. Huang *et al*. [218] demonstrated a >20-fold difference in specific activity between *cis*- and *trans*-cypermethrin analogs. CE is the major first-pass enzymatic pathway for methylphenidate with higher activity toward the

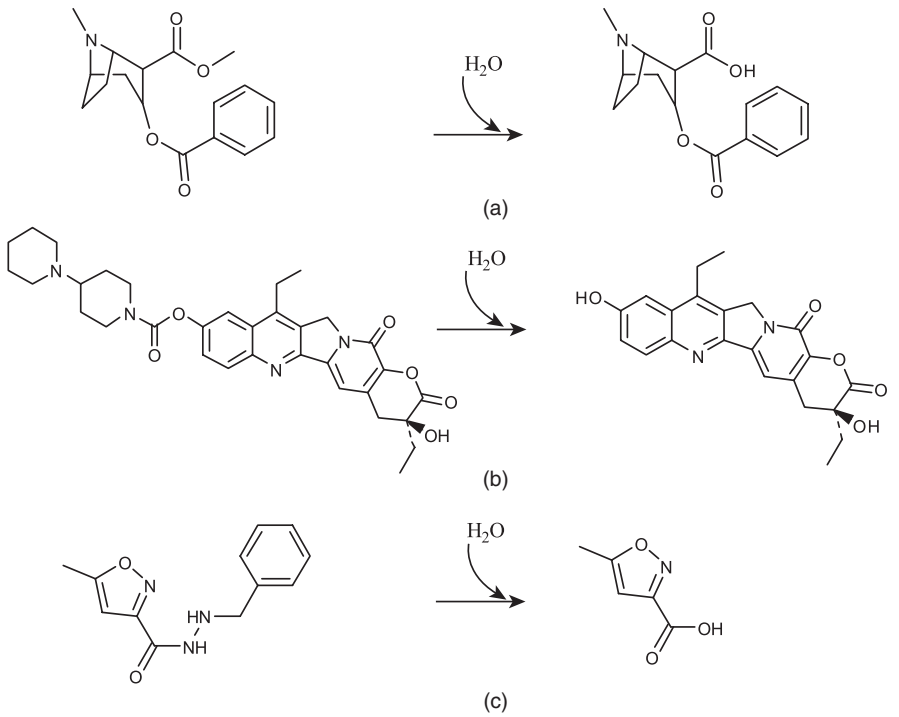

Figure 7.28 (a) Hydrolysis of cocaine ester, (b) hydrolysis of CPT-11 to bioactive SN-38, and (c) amide hydrolysis of isocarboxazid.

L-isomer compared to the D-isomer [219]. The stereochemistry leads to a subtle change in orientation of enzyme–substrate complex leading to profound changes in catalytic efficiency. This may be expected for CE based on the specific distance requirements for all three residues to act in concert with one another. The activity of the potent anticancer drug CPT-11 requires activation by hCE (Fig. 7.28). CPT-11 is the carbamate prodrug of the active SN-38 hCE-derived metabolite [206,220]. The conversion, however, is relatively inefficient where typically <5% of CPT-11 is converted to SN-38 [221]. Additional characterization of CE active site has been established with various competitive inhibitors. Trifluoromethyl ketones (TFKs) represent a class of compounds that display some of the most potent inhibitors of CE [222]. In general, the potency of TFK analogs is attributed to the enhanced electrophilicity of carbonyl carbon as a result of the electron-withdrawing nature of the CF_3 moiety (Fig. 7.29). In addition, TFK inhibitors also bind in the favored conformation of the transition state as a tetrahedral intermediate and thus are termed *transition state analog inhibitors*. Wheelock *et al*. [222] nicely demonstrated that TFK analogs were more amenable to mimicking the transition state through the formation of the gem diol (sp3 hybridized conformation; tetrahedral intermediate common to CE transition state), which lead to improved inhibitory potencies (Fig. 7.29). Other inhibitors include organophosphorus compounds, which also exploit the nucleophilic behavior of the catalytic serine to form an irreversible covalent acyl enzyme intermediate with compounds such as soman and tabin

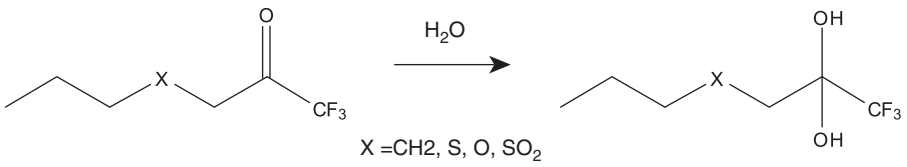

Figure 7.29 General structure of TFK inhibitor analogs where trifluoro substitution increase electrophilicity of carbonyl carbon favoring gem diol formation.

[223,224]. Interestingly, hCE does not seem to readily form the irreversible complex formed in rCE.

Site-directed mutagenesis of hCE identified key portions of the protein for substrate and metabolite entrance and exit channels from the active site [225,226]. Rational enzyme design was accomplished with site-directed mutagenesis studies in combination with crystal structure data to develop an hCE mutant with CPT-11 activity similar to that achievable with rCE. Modification of eight amino acids demonstrated improved CPT-11 hydrolysis, which was proposed to occur via an increased flexibility of the active-site cavity necessary to bind CPT-11.

The crystal structure of hCE in complex with the potent inhibitor benzil (45 nM) demonstrated the formation of covalent product [227]. Crystallization with modest inhibitor tamoxifen revealed binding at the *z*-site of the protein where in this may partially explain the partial inhibition properties of tamoxifen and provide evidence that the *z*-site may serve as an access channel for different substrates [227].

7.2.6 Epoxide Hydrolase

Mammalian epoxide hydrolases (EHs) catalyze the conversion of three-membered cyclic ethers, called *epoxides*, to diols (Fig. 7.30) [228]. EHs are expressed in many mammalian tissues with the highest concentrations found in the liver [229,230]. Several EHs are present in mammals; however, microsomal epoxide hydrolase (mEH) and soluble epoxide hydrolase (sEH) have been the focus of research efforts [231]. They differ in both subcellular localization and substrate specificity. mEH is found within the endoplasmic reticulum and metabolizes xenobiotic-derived epoxides [232]. sEH is found in the cytosol and metabolizes endogenous fatty acid epoxides [233]. The biological role of mEH is the detoxification of xenobiotics [234], while sEH appears to play a role in the hyperpolarization of vascular smooth muscle by controlling the levels of vasodiliatory epoxyeicosatrienoic acids [235,236].

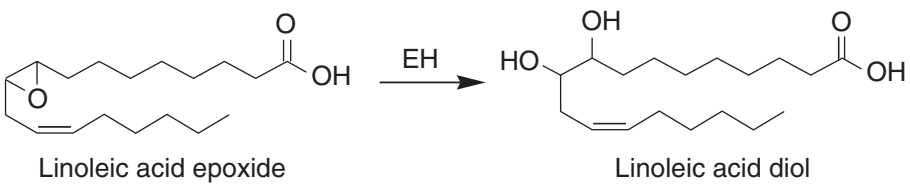

Figure 7.30 Example of EH metabolism reaction with linoleic acid epoxide.

Metabolism by EH requires the presence of an epoxide. The mechanisms of EH-mediated hydrolyses are similar; therefore, differences in observed kinetics are generally due to specific interactions between the enzyme and a potential substrate. SARs suggest that both the size and shape of a substrate are key factors in mediating access to the EH active site [237]. The active site of sEH contains a 25-Å long, L-shaped hydrophobic domain at the C-terminus where substrates bind for catalysis [231]. The influence of active-site topography on epoxide hydrolysis is particularly evident with regard to the stereoselectivity observed with many EH reactions. In the 1990s, Zeldin and coworkers [238] examined the stereochemistry of the conversion of *cis*-epoxyeicosatrienoic acids to diols by hepatic sEH and found that incubations containing the 8,9- or 14,15-epoxides formed diols stereoselectively, while incubations containing the 11,12-epoxide were not stereoselective. In this fashion, both the topography of the EH active site and the shape and orientation of the substrate within the EH active site influence the final stereochemistry of the product.

The catalytic cycle for EH is complex and involves several steps (Fig. 7.31). An underlying feature of this enzyme class is a catalytic triad containing a nucleophilic acid (usually Asp), an orienting acid (Asp or Glu), and a basic histidine [228]. In the first step of catalysis, polarization of the epoxide moiety by tyrosines located on the

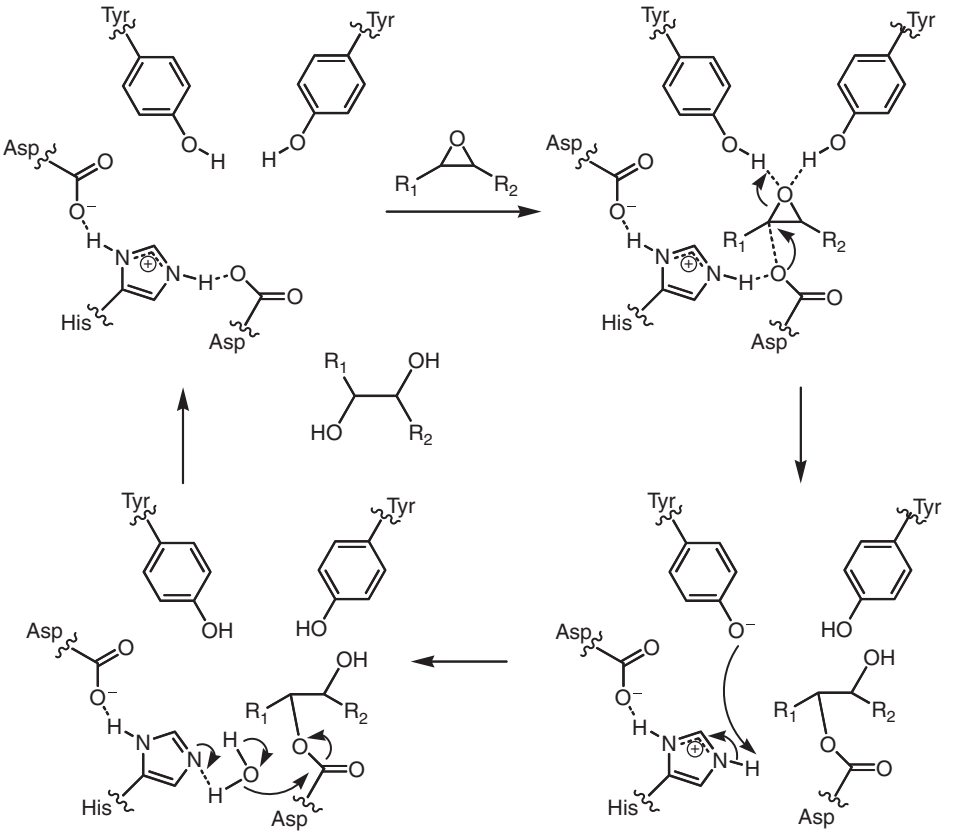

Figure 7.31 EH catalytic cycle.

top of the EH active site occurs concurrently with nucleophilic attack on an epoxide carbon by an acidic residue located on the opposite side of the active site [239]. This attack occurs preferentially at the least sterically hindered or most reactive carbon of the epoxide. Attack by the nucleophilic acid is aided and directed by a nearby histidine-orienting acid pair [240]. Ring opening of the epoxide results in formation of a covalent ester bond between the attacking acid and a carbon from the epoxide. This intermediate has been termed the *hydroxyl alkyl-enzyme intermediate* [228]. A water molecule, activated by the histidine-orienting acid pair, reacts with the hydroxyl alkyl-enzyme intermediate to release the enzyme and a diol as products.

Evidence for the mechanism of catalysis and the presence of a hydroxyl alkyl-enzyme intermediate comes from three sources. In a single turnover experiment using 1,10-phenanthrene-5,6-oxide as substrate, transfer of ^{18}O from hepatic mEH to the substrate was best explained through formation of a hydroxyl alkyl-enzyme intermediate [241]. Inhibition kinetics of EH-mediated reactions were well described using models based on formation of a covalent enzyme-inhibitor intermediate, whose half-life is inversely proportional to inhibition potency [242]. Additionally, a covalent adduct of hepatic mEH and [1-^{14}C]epoxystearic acid was detected after denaturing SDS gel electrophoresis [243]. Formation of the adduct was inhibited in the presence of 1,1,1-trichloropropylene oxide, an inhibitor of mEH.

7.2.7 Ketoreductase

The aldo-keto reductases (AKRs) comprise a superfamily of monomeric (monomer molecular weight = 34–37 kDa), NADPH-dependent oxidoreductases with similar physical and chemical properties [244]. Much more is known about the physiological roles of carbonyl-reducing enzymes (e.g., steroid and prostaglandin metabolism, housekeeping, and stress response) than their roles in drug metabolism [245]. With respect to drug metabolism, typically the AKR enzymes catalyze the reduction of aldehydes and ketones to the corresponding alcohol products (Fig. 7.32) and the subsequent products often times undergo further conjugation and elimination [246]. For example, AKRs play an important role in the metabolism of the therapeutic agent such as haloperidol, ketotifen, and oracin [247–249]. In humans, an important pathway of warfarin metabolism is reduction of the ketone to a secondary alcohol [250]. This reaction is catalyzed by cytosolic ketone reductases and is stereospecific, producing only the (S)-enantiomer of warfarin enantiomers [251].

A nomenclature system to group AKRs has been adopted and currently 14 subfamilies have been identified [252]. However, only four AKR subfamilies, namely, 1A, 1B, 1 C, and 7A, have documented roles in xenobiotic carbonyl metabolism [253]. To date, over 15 crystal structures of AKRs complexed with their ligands have been determined [254]. In each instance, the AKR structure reveal a $(\alpha/\beta)8$-folding pattern (triose isomerase or TIM barrel fold), where the central β-strands form the staves of a barrel, with large loops at the back that form the ligand-binding site [255]. The cofactor-binding site and the active site are highly conserved across the superfamily. The active site (Fig. 7.33) contains a conserved catalytic tetrad (Tyr, Asp, Lys, and His), which forms an oxyanion-binding site with the nicotinamide ring of the cofactor via a hydrogen bonding network [256–258]. In contrast, strong variation exists in the structure of the substrate-binding cavity, which is largely defined by the residues from the loops [259]. The reaction mechanism for this class of enzymes has been studied in

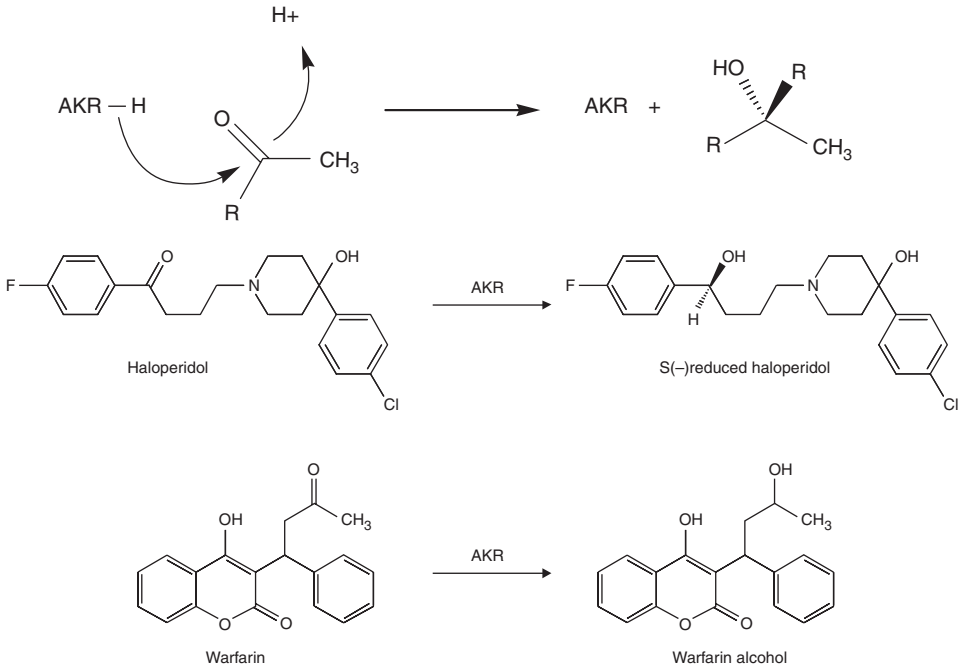

Figure 7.32 (a) Generic mechanism of ketone reduction. (b) Examples of AKR metabolism reactions with haloperidol and warfarin.

detail, revealing an ordered bi-bi mechanism [260], where the cofactor binds first and leaves last [261]. Interestingly, while the catalyzed reaction favors alcohol formation, it is possible for the reverse reaction to occurs, albeit to a limited extent.

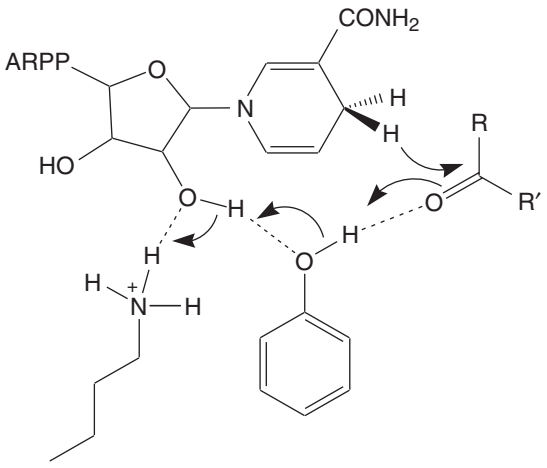

Figure 7.33 Proposed AKR active-site hydrogen bonding network to form the oxyanion-binding site with the nicotinamide ring in ketone reduction reaction.

A common feature of the carbonyl-reducing enzymes is their proposed two-electron reduction mechanism involving hydride transfer from the cofactor to the carbonyl carbon, which is facilitated by general acid [262]. In this fashion, unsymmetrical ketones generate chiral centers on reduction to alcohols. As a consequence, for many substrates, the stereoselectivity of carbonyl reductase-catalyzed ketone reduction is dependent on the steric situation of substrates and may be predicted with "Prelog's rule" [263]. Prelog's rule describes the reduction of ketone to yield optically active secondary alcohols. In this instance, the chirality of an alcohol arising from nucleophilic addition to a ketone depends on which prochiral face accepts the nucleophile and the sequence priority of the nucleophile relative to other substituents of the carbonyl function [264]. In hydride transfer reactions, the hydride nucleophile will always be the lowest priority group; thus, the reface addition of the hydride to a ketone will always generate an S-configuration alcohol [265].

7.3 PHASE II DRUG METABOLISM REACTIONS

7.3.1 Glucuronosyltransferase

The UGT family of enzymes catalyzes the conjugation of a glucuronic acid moiety from uridine diphosphoglucuronic acid (UDPGA) to a broad range of substrate molecules (Fig. 7.34) [266,267]. The glucuronidated compounds are more hydrophilic than their aglycone counterparts and thus more readily excreted from the body. Any functional group with sufficient nucleophilicity can be an acceptor for the glucuronic acid transfer, with the most common functional groups including phenols, aliphatic alcohols, carboxylic acids, amines, thiols, and nucleophilic carbon atoms [51]. Common substrates include endogenous compounds such as bilirubin, estrogens, and fatty acids as well as numerous xenobiotics.

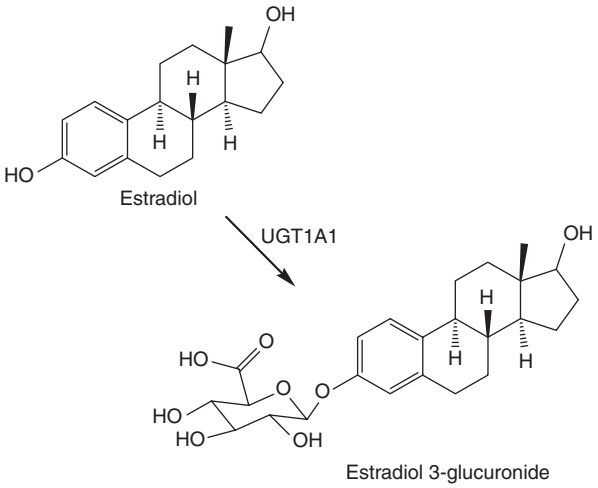

Figure 7.34 Example of UGT metabolism reaction with estradiol.

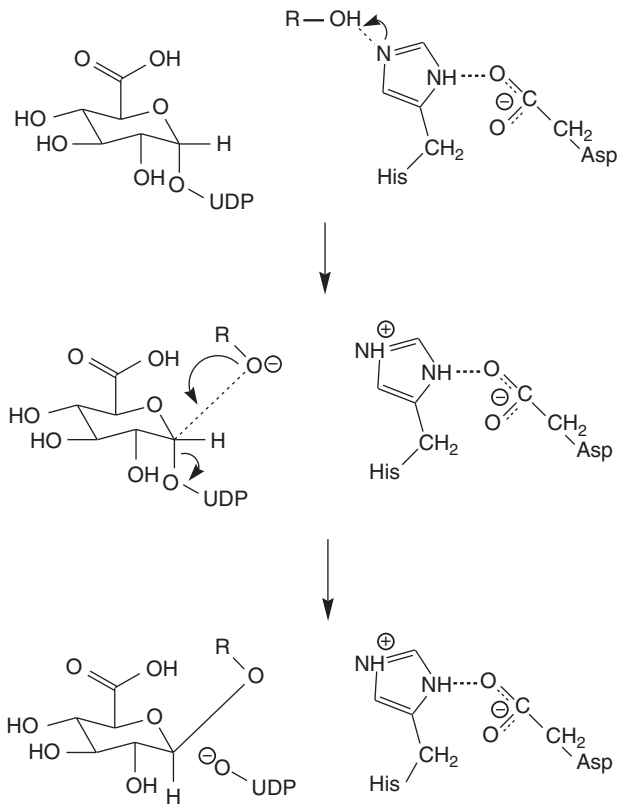

Figure 7.35 Proposed mechanism of UGT-catalyzed glucuronidation.

It is now generally accepted that UGT-catalyzed glucuronidation proceeds via an acid–base mechanism similar to that exhibited by serine hydrolases [268,269]. A conserved histidine residue serves as a catalytic base to deprotonate a nucleophilic site on the aglycone molecule, which then results in a nucleophilic substitution at the C1 atom of the glucuronic acid moiety. Consequently, the protonated histidine residue is stabilized through an interaction with a proximal aspartic acid residue that is also conserved across human UGTs (Fig. 7.35). The nucleophilic attack on the C1 carbon occurs through an S_N2 reaction mechanism with stereoinversion from the α-configuration at the C1 carbon of the glucuronic acid moiety in UDPGA to the β-configuration in the resulting glucuronide [270]. The reaction mechanism is supported by data showing a correlation between reaction rates and nucleophilicity for a series of phenol-containing compounds [271]. The order in which the aglycone and UDPGA bind during the UGT-catalyzed S_N2 reaction remains ambiguous and may be isoform dependent, with proposed mechanisms including a compulsory-ordered bi-bi mechanism, a random-ordered bi-bi mechanism, or a Theorell–Chance reaction mechanism [271–278].

A unique scenario exists following a nucleophilic attack on the C1 carbon by a carboxylic acid moiety. The resulting acyl glucuronides are more reactive than ether-linked glucuronides and present the possibility for additional reaction steps, where the aglycone migrates via intramolecular transesterification from the C1-hydroxyl group

of the glucuronic acid moiety to the C2-, C3-, or C4-hydroxyl groups [279,280]. All the steps in the migration are reversible, except for the first migration step from the C1 to the C2 position. On migration, acyl glucuronides can covalently adduct proteins and other macromolecules through one of two mechanisms. First, a direct nucleophilic attack on the glucuronic acid moiety by an amino acid residue results in binding of the aglycone to protein though a carbonyl linkage and liberation of D-glucuronic acid [281–285]. The second proposed mechanism for the irreversible binding of acyl glucuronides to protein involves the interaction of a protein nucleophile, such as an internal lysine residue or the N-terminus of a protein, and the free aldehyde of the open-chain glucuronic acid moiety to form an imine bond between the two functional groups. The initial interaction is reversible; however, it can subsequently be followed by an irreversible imine reduction or Amadori rearrangement, which occurs when the aglycone moiety has migrated to the C3 or C4 position, and is converted to the more stable 1-amino-2-keto product [286,287].

In addition to the observed stereochemistry observed at the C1 carbon of UDPGA during glucuronidation, the UGT family of enzymes also has also been shown to exhibit a high degree of stereoselectivity regarding the aglycone acceptor molecules. A recent study aimed at measuring the eudismic ratios of a series of chiral secondary alcohols for UGT2B7 and UGT2B17 demonstrated that the UGTs can display a degree of stereoselectivity that is similar to that generally reserved for highly specific receptor proteins [288]. Similarly, both isoforms have shown substrate specificities that are dependent on the configuration (α vs β) of the 17-hydroxyl group of steroids such as estradiol and testosterone [289,290]. Interestingly, the stereochemistry of the aglycone had a negligible effect on the affinity of the enzyme–substrate complex and thus may reflect the importance of substrate orientation in the transfer of the glucuronic acid moiety. Additional studies have also demonstrated the importance of the orientation of the glucuronic acid, uridine diphosphate, and aglycone groups in forming the ternary UGT-UDPGA-aglycone complex [291].

While substrate selectivities vary across the different UGT isoforms, it is generally accepted that the N-terminal domain plays an important role in substrate recognition [67,268, 292–302]. It has been suggested that a conserved histidine residue is generally required for glucuronidation through proton abstraction, while a proline residue is more likely involved in the glucuronidation of tertiary amines [303]. From the standpoint of the acceptor molecule, compounds that are hydrophobic in nature and contain a nucleophilic site generally make good substrates for glucuronidation. More recently, the effect of chemical substituents within close proximity to the nucleophile on the rate of glucuronidation has been examined. In general, an aromatic ring adjacent to the nucleophilic site appears to greatly increase the likelihood of glucuronidation at the nucleophilic site, possibly through electronic stabilization of the reaction intermediate or through π-stacking interactions within the active site of the enzyme, which serve to decrease the entropy of bond formation between the acceptor molecule and UDPGA [304,305]. It has also been noted that nucleophiles with a more negative partial charge combined with a higher Fukui function (describing the likelihood of electrophilic or nucleophilic attack at a given atom) are more prone to glucuronidation [305]. In addition to the nucleophilicity of the acceptor molecule (aglycone), glucuronidation by hepatic UGTs is also highly dependent on the hydrophobicity of the aglycone, with an optimal octanol–water partition coefficient (log P) of $\sim$2 having been reported [306]. Finally, steric interactions can also play a role in substrate selectivity as well as overall

rates of glucuronidation, as has been observed for a series of substituted phenols, where bulky substituents in the ortho-position to the hydroxyl group generally decreased the susceptibility of the nucleophile to glucuronidation [307,308].

7.3.2 Glutathione Transferase

Cytosolic and membrane-bound forms of glutathione-*S*-transferase (GST) are encoded by two distinct superfamilies [309]. The soluble protein form exists as two polypeptide subunits creating dimer with a molecular mass of 50 kDa. GSTs catalyze the transfer of the endogenous tripeptide, GSH to the electrophilic center of a diverse set of substrates to form a polar S-glutathionylated reaction product (R-SG). GST subunits contain a GSH-binding site (G-site) and a hydrophobic substrate site (H-site) (Fig. 7.36) [310,311]. On proper orientation of substrate and GSH, the reaction proceeds through the formation of a Meisenheimer complex (Fig. 7.37).

The G-site binds GSH extending the tripeptide in a conformation that points the sulfur toward the subunit in which it is bound. Electrostatic interactions with the glycine of GSH are favorable with the subunit it binds ($K_d = 20\,\mu M$). The spatial orientation of GSH in the active site is conserved across soluble forms of GST. However, the interactions stabilizing the GSH-GST subunit complex are unique to the isoform and isoform-specific interactions may contribute to differences in conjugate regioselectivity and catalytic activity of the different enzyme forms [312]. Ultimately, GSH binding at the G-site lowers the activation energy for the nucleophilic attack by reducing the thiol pK_a of GSH. The thiol pK_a of unbound GSH is 9.0 ($GSH \rightarrow GS^-$ in water) compared to GSH in complex with GST subunit where the pK_a is 6.0–7.5 [313–315]. A shift

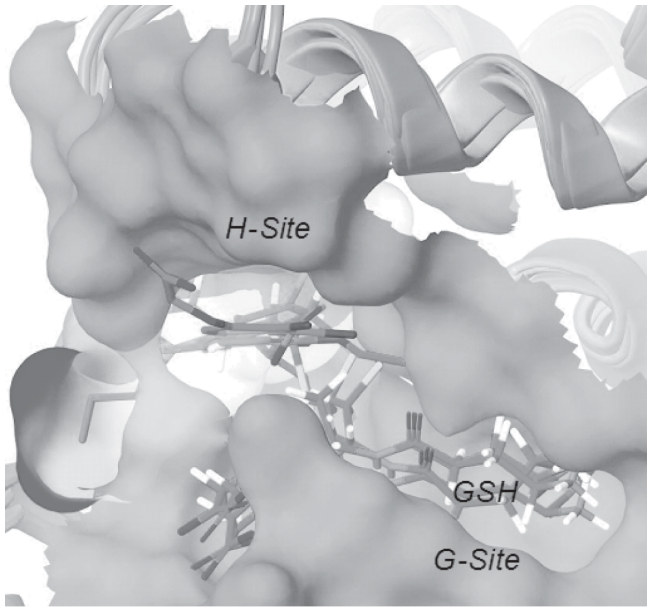

Figure 7.36 General binding site for GSH (G-site) and electrophilic substrate (H-site). (See color insert.)

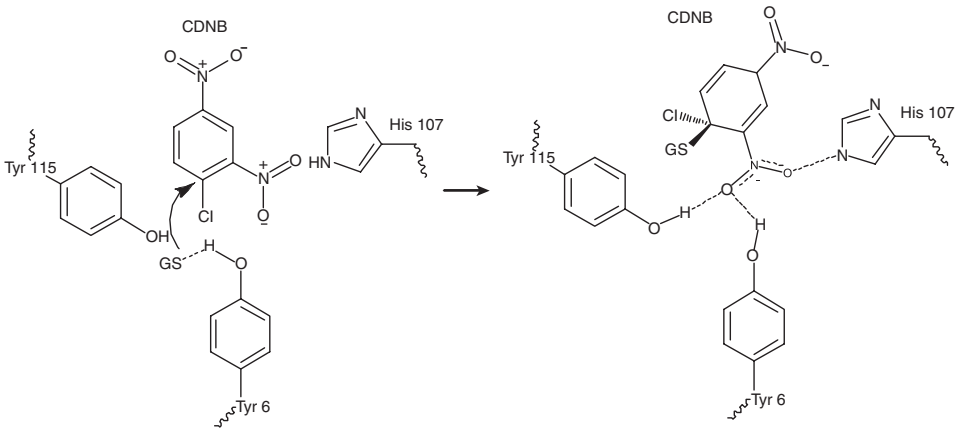

Figure 7.37 Meisenhemier complex formation with CDNB.

in pK_a of that magnitude requires ~3 kcal/mol of energy, which is generated through the binding of GSH at the G-site.

The H-site is composed of the C-terminal domain and displays greater primary sequence diversity providing the substrate diversity observed across the different enzyme forms. For example, α-class GSTs show substrate specificity for cumene hydroperoxide (CuOOH) and 7-chloro-4-nitrobenz-2-oxa-1,3-diazole (NBD-C1), due to unique structural component proximal to the H-site, there is a short three-residue β-strand near the C-terminal segment and a longer α-7 helix (due to insertions at the N-terminus and near to the middle of this helix); domain I is formed from two separate segments of the sequence. This occurs because an extra helix (α-11) formed via folding of the C-terminal region of the polypeptide chain is also part of this domain. This helix covers the substrate bound in the H-site, which is thought to explain the preference of α-class GSTs for more hydrophobic compounds. In fact, different GSTs have unique linear free energy plots relative to hydrophobicity in the form of alkyl chain length (Fig. 7.38) [316].

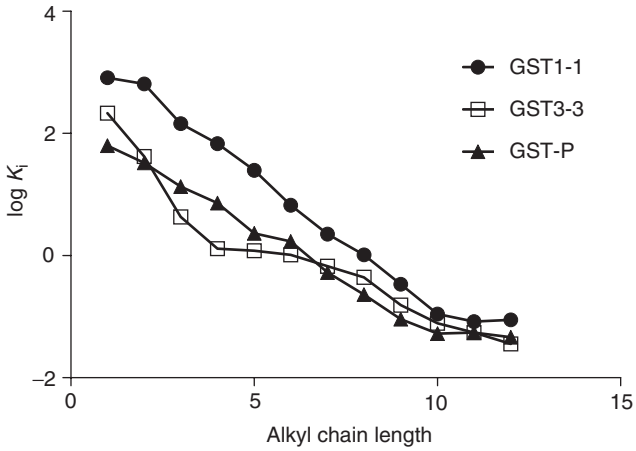

Figure 7.38 Linear free energy relationship between inhibitory potency and hydrophobicity.

Product inhibition and transition state analogs of GST metabolites provide information regarding structure function of GST enzymatic activity. Nucleophilic substitution between GSH and chlorodinitrobenzene leads to formation of Meisenheimer complex (σ-complex) (Fig. 7.37) [317]. The complex presents as a competitive inhibitor of rat isoform 3-3 with a $K_i = 20\,\mu M$. The generation of anionic tripeptide analogs of GSH where the thiol group was replaced with carboxylic acid functional group yielded competitive inhibitors to GSH [313]. Most notably the substitution of the cysteine residue for 2-aminomalonyl derivative yielded a K_i of $0.74\,\mu M$. Chen *et al*. [318] employed the use of GSH in comparison to three GSH analogs in concert with several 4-substituted L-halo-2-nitrobenzenes to investigate the catalytic mechanism of rat liver GSH transferase (isozyme 4-4). The observed substituent effects were consistent with a catalytic mechanism where the Meisenheimer complex formation is rate-limiting or partially rate-limiting step of conjugation (Fig. 7.37). Structural variants of GSH peptides affected the effective pK_a of the thiol and altered the orientation of the thiol toward the nucleophile [318]. The design of novel bivalent inhibitors have been used to realize the in-solution distance of the two H-sites from different dimerized forms of GST [319]. Endogenous ligands have also proven useful as tools to study structure function of GST. *S*-Nitroso glutathione serves as a carrier for NO and has been demonstrated to be a competitive reversible inhibitor of GSH with a K_i of $180\,\mu M$ [320].

In comparing the structural differences across GST classes, the helix α2 region displays significant variance and not surprisingly comprises part of the H-site. The helix α2 region has been established as a flexible region in the protein that influences catalysis in human GSTP1-1 [321,322]. For instance, S-nitrosoglutathione (GSNO) was shown to modify Cys47 in a temperature dependant fashion. Below physiological temperature, GSNO does not readily label the buried Cys residue, but under physiological conditions, the modification leads to enzyme inactivation. Mobility of the GST has also been identified and characterized by Atkins *et al*. [64].

Single-residue substitutions have also revealed significant information regarding active-site structure activity. Ile104 in GSTP1-1 is a critical residue affecting the binding at the H-site as demonstrated by unique binding of 6-(7-nitro-2,1,3-benzoxadiazol-4-ylthio)hexanol in the wild-type and mutant enzyme [323]. The significance of the histidine residue depicted in the catalytic mechanism of Fig. 7.37 was explored with hGSTM1a-1a and mutagenesis studies to demonstrate the critical role for His107 in catalysis [324]. Numerous other mutagenesis studies have highlighted important active-site residues in G- and H-sites [64,325,326].

7.3.3 Sulfotransferase

The cytosolic sulfotransferases catalyze the conjugation of a sulfate moiety to a nucleophilic acceptor molecule (Fig. 7.39). Sulfotransferases utilize 3′-phosphoadenosine-5′-phosphosulfate (PAPS) as the universal sulfuryl donor to increase the water solubility and decrease the biological activity of the acceptor substrate, though examples of bioactivation do exist [327–330]. Known acceptor moieties for sulfotransferase reactions include phenolic and aliphatic hydroxyl groups as well as N-substituted hydroxylamines [331]. Unprotonated amines can also undergo sulfation, resulting in the formation of a sulfamate product [332].

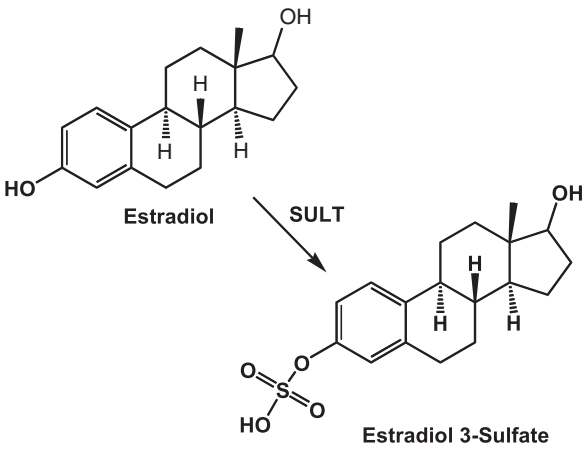

Figure 7.39 Example of sulfotransferase metabolism reaction with estradiol.

The proposed reaction mechanism for sulfotransferases involves an S_N2 nucleophilic attack on the sulfate moiety of PAPS by the acceptor substrate. As many of these substrates have pK_a values of ~6.4–9.0 and thus insufficient nucleophilicity at physiological pH, it has been suggested that a conserved histidine residue acts as a catalytic base to deprotonate the acceptor molecule [333], while active-site serine and lysine residues serve to orient PAPS in the sulfotransferase active site (Fig. 7.40) [334]. The overall basicity of the catalytic histidine residue is increased through hydrogen bonding with neighboring threonine residues, which serve to distribute the resulting charge on the histidine. Following the formation of a ternary sulfotransferase-PAPS-deprotonated acceptor molecule complex, a trigonal bi-pyramidal transition state intermediate has been proposed [335]. This transition state geometry may be stabilized by highly conserved serine and lysine residues that interact with the bridging oxygen of the 5′-phosphate group of PAP [333,334,336]. As the lysine residues may also directly catalyze the cleavage of the sulfate moiety from PAPS, an in-line displacement reaction mechanism has been proposed for sulfation. The ordering of the sulfation reaction appears to differ between species and sulfotransferase isoforms, as kinetic studies with rat aryl sulfotransferase suggest either a random bi-bi mechanism or an ordered Theorell–Chance mechanism [337], while a random bi-bi mechanism has been proposed for mouse and human SULT1E1 [338] and multiple studies with additional human sulfotransferases have suggested an ordered bi-bi mechanism in which PAPS binds before the acceptor molecule [339–341]. Interestingly, studies with bacterial sulfotransferases have implicated a random two-site ping-pong bi-bi mechanism, whereby PAPS and the sulfate acceptor molecule bind randomly and independently of each other [342].

Sulfotransferase enzymes can exhibit stereoselectivity among chiral substrates, as is observed with the increased sulfation rate of (*R*)-4′-hydroxypropranolol as compared to (*S*)-4′-hydroxypropranolol [343]. Additional examples include salbutamol, albuterol, isoprenaline, and various hydroxysteroid analogs [343–349]. While active-site characteristics may play a role in the preferred sulfation of one enantiomer over the other, steric interactions within the substrate molecule must also be considered. Studies with

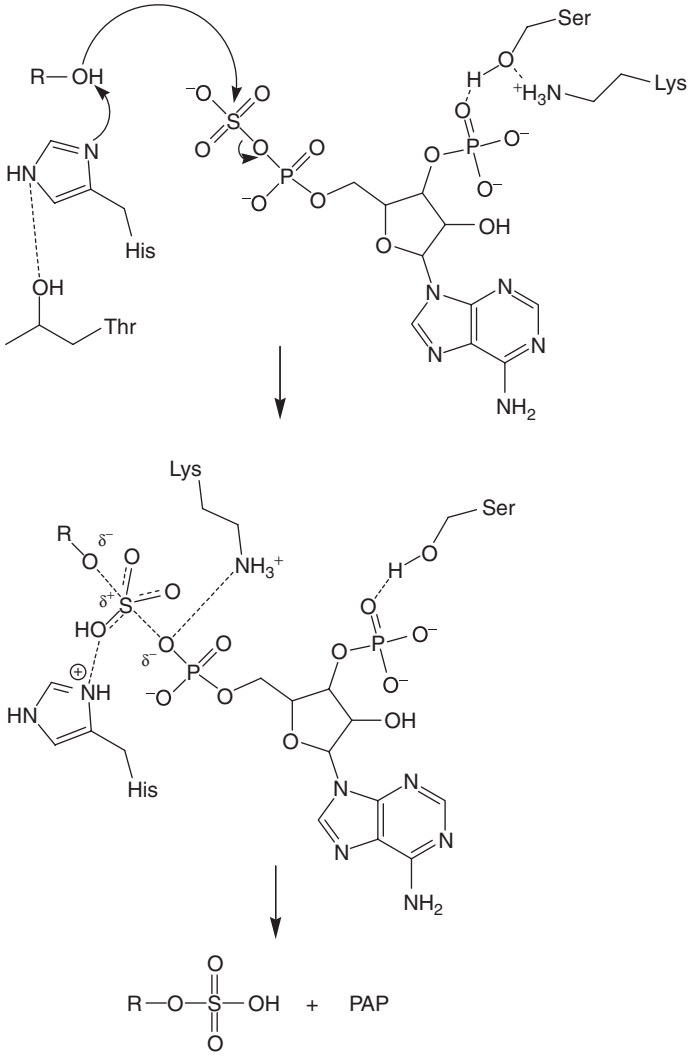

Figure 7.40 Proposed mechanism of SULT-catalyzed sulfation.

chiral aryl alcohols such as 1-(1-naphthyl)ethanol have suggested that spatial orientation may either sterically inhibit the interaction of the PAPS sulfate group with the nucleophilic site on the acceptor molecule or conversely, may orient the nucleophilic site in too distal a position to allow an S_N2 attack to occur on the sulfate group [344]. The resulting conformational rotation needed to overcome the stereoselectivity imposed by the spatial orientation of the substrate molecule would require a significant amount of energy and as such does not readily occur (Fig. 7.41).

From the standpoint of the acceptor molecule, substrate specificity appears to be linked to a number of molecular descriptors, including the size of the acceptor molecule, local structural features, lipophilicity, and electronic characteristics [350–352]. For example, both chain length as well as substituent positions (ortho-, meta-, and para-)

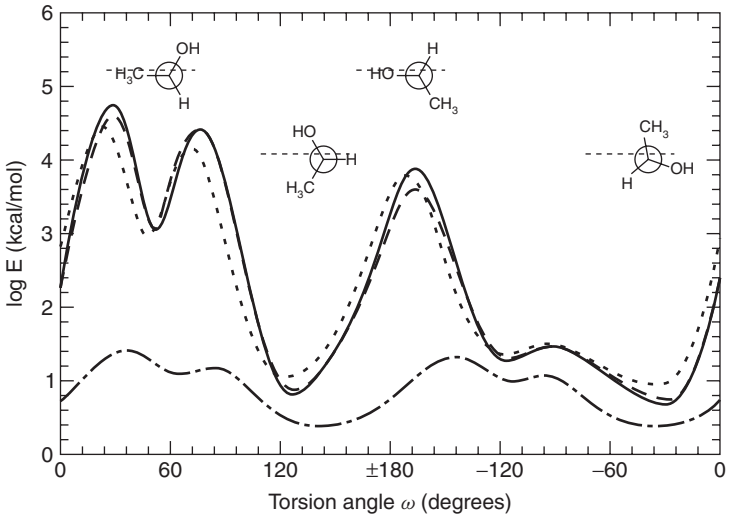

Figure 7.41 Conformational energies of chiral aryl alcohols. *Source:* Reproduced with permission from Banoglu E, Duffel MW. *Chem Res Toxicol* 1999;12(3):278–285.

have been shown to play a role in the substrate profiles of SULT1A1 and SULT1A2 [108,353]. Meanwhile, relationships have been developed between the K_m for a series of phenol sulfotransferase ligands and their respective log *P* values, molar refractivities, and Hammett constants [350]. Finally, the presence of a formal charge at physiological pH may also affect the substrate specificity for a given sulfotransferase, as observed for SULT1A3. Tyramine, which contains a primary amine that is positively charged at physiological pH, binds to SULT1A3 with an affinity that is 200-fold greater than that of *p*-ethylphenol, a structurally similar compound to tyramine that differs in only the lack of the primary amine [354].

7.3.4 *N*-Acetyltransferase

Mammalian *N*-acetyltransferases (NATs) are cytosolic proteins that transfer an acetyl group from acetyl coenzyme A to xenobiotics (Fig. 7.42) [355]. Two isozymes are known, NAT1 and NAT2, which differ in tissue localization and substrate selectivity. NAT1 is found in a variety of tissues including liver, colon, blood, and skeletal muscle [356]. NAT2 is present mainly in the liver and gut [357]. The biological function of NATs outside of xenobiotic metabolism is unclear; the only other known role of NATs is involvement in folate catabolism [358].

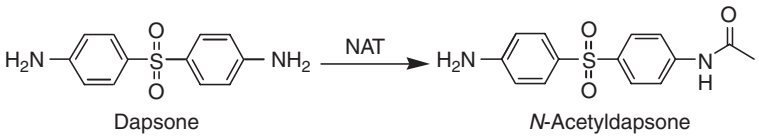

Figure 7.42 Example of NAT metabolism with dapsone.

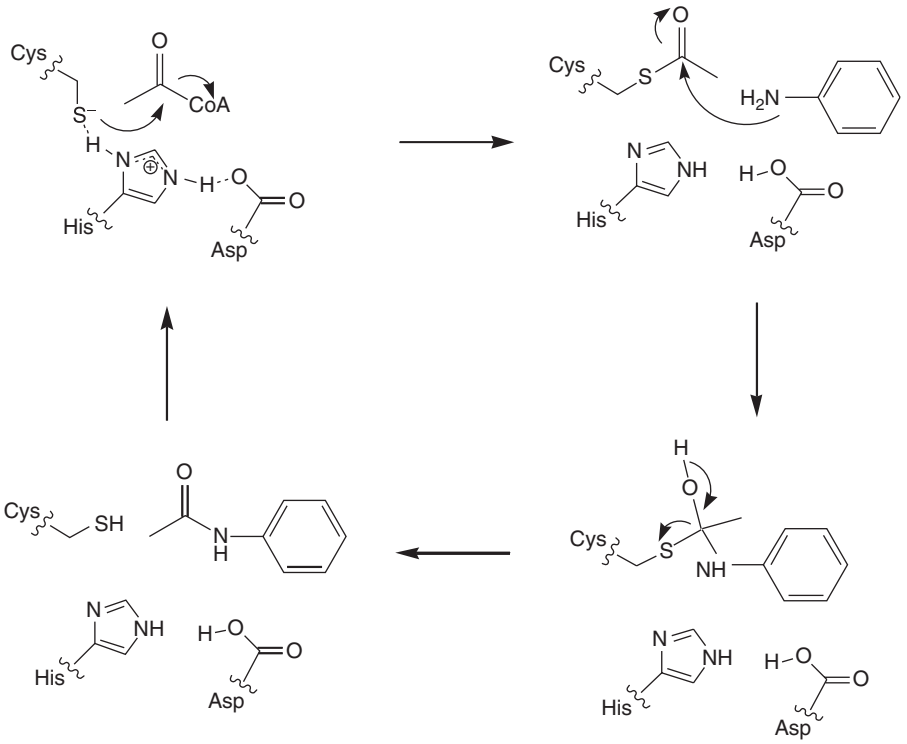

Figure 7.43 NAT catalytic cycle.

The general requirement for NAT conjugation is the presence of an aromatic amine. The catalytic cycle of NAT conjugation is complex and proceeds through a ping-pong bi-bi mechanism [355]. The reaction is initiated through acetylation of an active-site cysteine by acetyl-CoA (Fig. 7.43). Activation of the active-site cysteine is aided by adjacent histidine and acidic residues [359,360]. The positioning of the C-terminal region of human NATs may also facilitate interactions with acetyl-CoA, as a serine residue is within hydrogen bonding distance of the adenine ring (N6) of acetyl-CoA [361]. The acetyl group is then transferred from the enzyme to the substrate, forming an acetylated product and releasing the enzyme.

The hydrophobic nature of the active-site pocket may contribute to the stability of the acetylated enzyme intermediate [356]. While the lifetimes of these intermediates is NAT-dependent, the estimated half-life in hamster is 88 s [359]. Variable access of water to the active site, resulting in competing hydrolysis, may explain lifetime differences. Further evidence to support this hypothesis includes kinetic models, which are most consistent with reaction of unionized anilines with the reactive species. Ionized alkylamines, which tend to remain unionized at physiological pH, generally do not react with NATs [356].

NAT1 and NAT2 exhibit different substrate selectivity. Substrates for NAT1 include *p*-aminobenzoic acid and *p*-aminophenol [362]. Substrates for NAT2 include sulfmethazine, dapsone, and procainamide [363]. Substrate selectivity may be explained by differences in active-site topography. The active site of NAT1 is ~40% smaller than

NAT2 [364]. The NAT1 active site contains an arginine residue (Arg127) that is available for hydrogen bonding to acidic moieties and a phenylalanine residue (Phe125) that is closely located to orient linear, aromatic substrates toward the acetylated cysteine through π-stacking [365]. In contrast, docking studies based on the NAT2 crystal structure suggest that a phenylalanine residue (Phe93) is positioned to interact with hinged-aromatic substrates such as sulfmethazine [361]. The Phe125Ser mutation conferred NAT1 activity to NAT2 [366].

7.3.5 Acyl-CoA Synthetase

The acyl-CoA synthetases (also referred to as *acyl-CoA ligases*) catalyze the formation of thioester conjugates from carboxylic acids (Fig. 7.44). The activation of endogenous and xenobiotic acids to their thioester conjugates is often the first step in detoxification processes that end in amino acid conjugation and subsequent elimination [367]. The acyl-CoA synthetases are classified by their substrate specificity

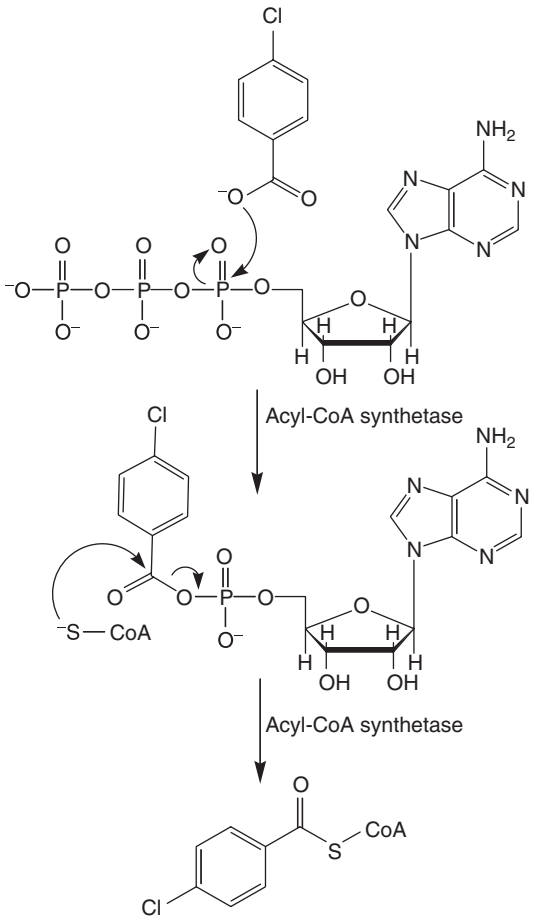

Figure 7.44 Example of acyl-CoA synthetase metabolism reaction with *p*-chlorobenzoic acid.

(short chain, medium chain, and long chain) and primary pharmacophores include aromatic carboxylic acids as well as some aliphatic and arylacetic acids [368]. Well-characterized substrates include nonsteroidal anti-inflammatory drugs such as ibuprofen and flunoxaprofen, hypolipidemic drugs such as clofibrate, and the environmental pollutant 4-chlorobenzoate [369–378].

The initial step in the acyl-CoA synthetase catalyzed reaction involves a nucleophilic attack of a carboxylate anion on the α-phosphate group of adenosine triphosphate (ATP) resulting in the formation of an acyl-adenylate intermediate, which does not dissociate from the acyl-CoA synthetase [379]. The acyl-adenylate intermediate then reacts with a deprotonated coenzyme A molecule resulting in the activated thioester conjugate and free adenosine monophosphate [380]. It has been proposed that the acetyl-CoA synthetase may adopt a different conformation for each step in the reaction [381]. The esterification of the carboxylate moiety has been proposed to proceed via a unidirectional bi-uni-uni-bi ping-pong mechanism [382]. Proper orientation of the reactants in the active site of acyl-CoA synthetase is achieved through hydrogen bonding with active-site residues as well as through coordination with a divalent magnesium ion [378,381–383].

A unique attribute of acyl-CoA synthetases is their involvement in the chiral inversion of nonsteroidal anti-inflammatory drugs such as ibuprofen, flunoxaprofen, and 2-phenylpropionic acid [373,375,377,384], resulting in a unidirectional inversion of the (R)-enantiomer to the (S)-enantiomer. In each case, the acyl-CoA enzyme displays a stereoselective preference for the formation of a thioester conjugate of the (R)-enantiomer, with a minimal amount of acyl-CoA transfer to the (S)-enantiomer. Using ibuprofen as an example, the first step in the chiral inversion process is the formation of an (*R*)-ibuprofen-CoA thioester intermediate (Fig. 7.45), as demonstrated through studies utilizing deuterium-labeled ibuprofen [385]. The next step involves the abstraction of the C2 proton of the ibuprofen-CoA conjugate by epimerase/carnitine dehydratase. Though the inherent acidity of this proton is increased by the presence of the thioester conjugate, the deprotonation step is not spontaneous at physiological pH and requires the presence of a catalytic base provided by epimerase [372,375,386]. The resulting carbanion tautomerizes to the planar and more stable enolate, allowing for a proton attack from either side of the double bond to form both enantiomers of the ibuprofen thioester conjugate. Finally, hydrolysis of the thioester bond by acyl-CoA hydrolase results in the formation of unconjugated (*S*)-ibuprofen [375,377,387].

While substrate specificities may vary among the different acyl-CoA synthetase homologs, the enzymes generally catalyze the thioester conjugation of aliphatic and aromatic carboxylic acids. For the aliphatic acids, the acyl chain length is often the determining factor in the specificity of individual acyl-CoA isoforms. In addition, both the pK_a of the carboxylic acid as well as the log P of the compound have been shown to be important determinants in the formation of thioester conjugates [368,388,389], though electronic and steric factors may also play a role. For example, examination of the rates of thioester formation for a series of cinnamic acid analogs with various electron-donating or electron-withdrawing groups in the para-position resulted in a biphasic Hammett plot (Fig. 7.46), implicating the importance of a negative charge in formation of the conjugate as well as a potential change in the rate-determining step in the reaction for electron-donating versus withdrawing groups [390]. Sterically, compounds with a flat hydrophobic region that is coplanar to the carboxylic acid moiety appear to be much better substrates for acyl-CoA synthetases [391]. It has been

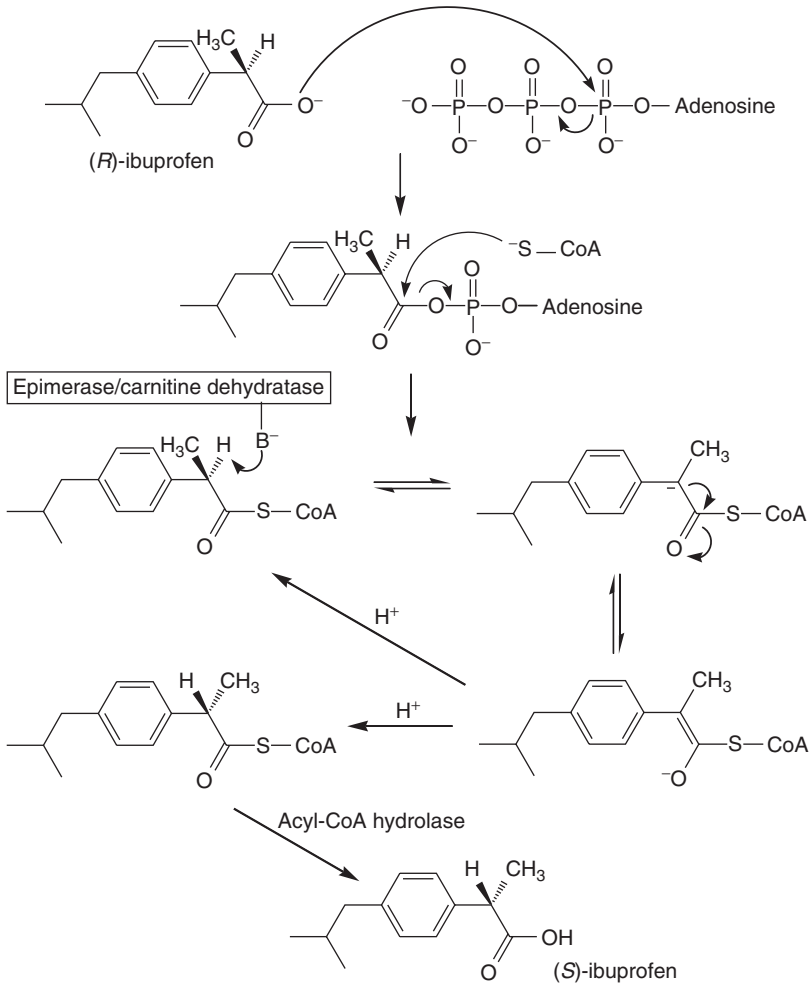

Figure 7.45 Proposed acyl-CoA synthetase reaction mechanism resulting in stereoinversion of (*R*)-ibuprofen to (*S*)-ibuprofen.

suggested that compounds that do not meet this coplanar criteria may have difficulty accessing the active site of the enzyme.

7.3.6 Methyltransferase

The methyltransferase family of enzymes (including thiopurine-*S*-methyl transferase, thiol methyltransferase, catechol-*O*-methyltransferase, phenethanolamine-*N*-methyltransferase, and multiple other forms involved in biological homeostasis) catalyze the transfer of a methyl group from *S*-adenosyl methionine to nucleophilic substrate [392–394]. Drugs that are metabolized by methyltransferases include 6-mercaptopurine, 6-thioguanine, and azathioprine (thiopurine-*S*-methyl

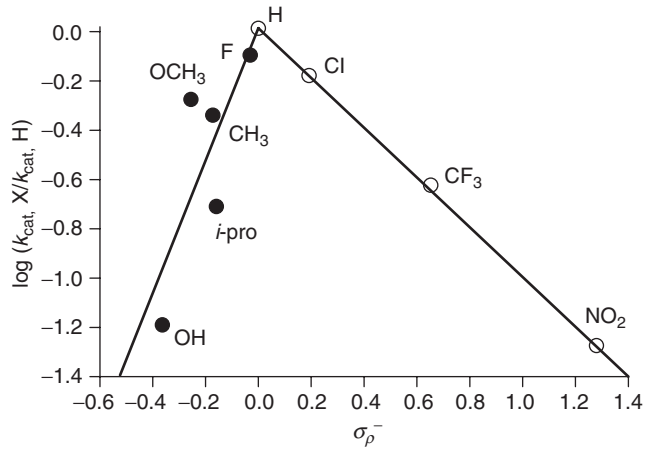

Figure 7.46 A Hammett plot for acyl-CoA synthetase reactions with para-substituted cinnamic acids. *Source:* Reproduced with permission from Koetsier MJ, *et al*. *Biochem J* 2009;417:467–476. © The Biochemical Society, http://www.biochemj.org.

transferase), dopamine, L-3,4-dihydroxyphenylalanine and isoprenaline (catechol-*O*-methyltransferase), captopril and D-penicillamine (thiol methyltransferase), and norepinephrine (phenethanolamine-*N*-methyltransferase) [395–404].

The mechanism by which methyltransferases catalyze the addition of a methyl group to a substrate proceeds via an S_N2 nucleophilic attack on the methyl carbon of *S*-adenosyl methionine by the substrate (Fig. 7.47). The reaction may require the presence of Mg^{2+} (catechol-*O*-methyltransferase) and has strict geometrical requirements for the orientation of substrate and cofactor [396,405,406]. An ordered mechanism has been suggested for the transfer of the methyl group, with the order of binding

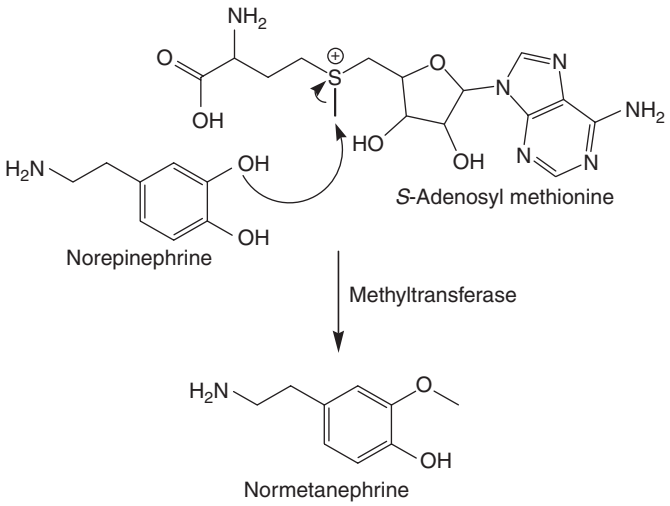

Figure 7.47 Example of methyltransferase metabolism reaction with norepinephrine.

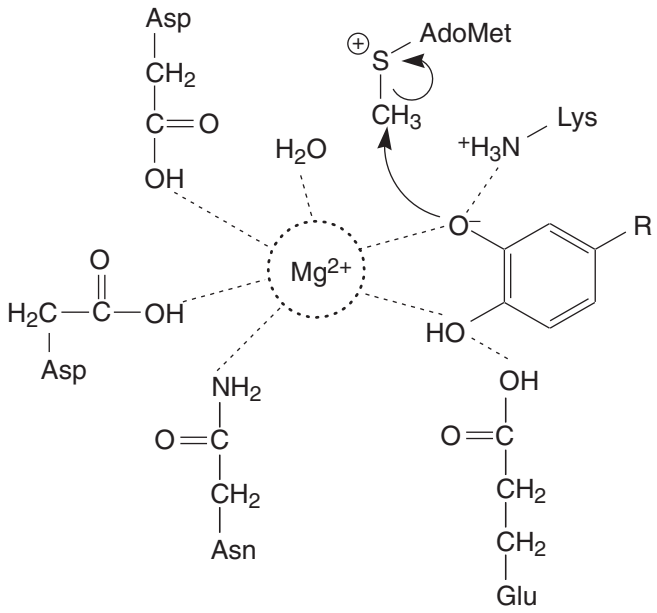

Figure 7.48 Proposed methyltransferase reaction mechanism.

being (i) *S*-adenosyl methionine; (ii) Mg^{2+}; and (iii) substrate [407–409]. Following transfer of the methyl group, *S*-adenosyl homocysteine (the demethylated byproduct of *S*-adenosyl methionine) is the last ligand to dissociate from the binding pocket of the methyltransferase [410,411]. Kinetic isotope effect studies and hybrid density functional theory models have been used to identify the transfer of the methyl group as the rate-limiting step in the reaction [393,412,413]. In a similar manner to other enzyme-catalyzed S_N2 reactions (i.e., glucuronidation and sulfation), a conserved active-site lysine residue (catechol-*O*-methyltransferase) or arginine residue (thiopurine-*S*-methyltransferase) acts as a catalytic base to deprotonate the nucleophile before the S_N2 attack (Fig. 7.48) [398,414].

Substrate selectivity varies widely across the range of methyltransferases. For catechol-*O*-methyltransferases, which catalyze the transfer of a methyl group to catechols and catecholestrogens, it appears that the presence of vicinal aromatic hydroxyl groups is a requirement for catalysis, as the enzyme does not bind the nonaromatic dihydroxyl cyclohexane analogs [415,416]. In addition, the presence of a strong electron-withdrawing group on the catechol has been shown to greatly decrease the rate of O-methylation, though the compounds can still bind and inhibit the enzyme [417–419]. Orientation of the substrate within the active site is controlled by the bound magnesium ion, which is coordinated to active-site aspartate and asparagine residues, a bound water molecule, and both hydroxyl groups of the catechol, while overall substrate selectivity may be conferred by hydrophobic "gatekeeper" residues (Fig. 7.48). For thiol methyltransferases, the preferred substrates are aliphatic sulfhydryl-containing compounds, such as 2-mercaptoethanol [420]. Potent inhibitors of thiol methyltransferase include the calcium channel blocker SKF 525A [421]. Lastly, while thiopurine methyltransferases catalyze the methylation of

thiopurines, thiopyrimidines and aromatic sulfhydryl compounds, a natural substrate has not yet been identified [402,414,422]. Though compounds with a purine moiety are understandably the primary substrates for thiopurine methyltransferase, the presence of a heterocyclic aromatic functional group is not a requirement for substrate recognition, as demonstrated by studies with thiophenol-containing compounds [402,423]. Substrate recognition by thiopurine methyltransferases also appears to be dependent on the ability of the acceptor molecule to achieve proper orientation within the substrate-binding site of thiopurine methyltransferase through hydrophobic and van der Waals interactions [414].

Methyltransferases are also known to display both stereoselectivity and regioselectivity in the transfer of a methyl group to an acceptor molecule. Regioselectivity by methyltransferases has been observed for the methylation of catechols by catechol-O-methyltransferase, with 3-O-methylation (meta) generally preferred over 4-O-methylation (para), especially *in vivo* [398,407]. Furthermore, dimethylation is not readily observed. This observed phenomenon may be due in part to the unfavorable interactions required between the substrate and hydrophobic active-site residues to allow the 4-hydroxy position to gain proper alignment for an S_N2 attack on *S*-adenosyl methionine. The catechol-*O*-methyltransferases also exhibit stereoselectivity in the methylation reaction, as noted with a series of β-adrenoceptor agents, where the enzyme preferentially catalyzed the methylation of (−)-isoprenaline and (−)-noradrenaline over their respective (+) counterparts [424].

7.4 CONCLUSION

Understanding the biochemistry of drug metabolism is one of the most critical aspects of new drug development to assure safe and efficacious medicines of the future. As described in this chapter, drug metabolism is heavily dependent on the molecular properties of the substrate and the topography of the enzyme's active site. Considerable advances have been made in recent years, such that basic rules can be applied to determine the fate of a compound in man based on physicochemistry character and structure of a drug metabolite. In this light, the impact of the identification of drug metabolites allows the drug metabolism scientist to predict drug clearance pathways and factors affecting drug/metabolite exposures early in the drug development process. Moreover, it is anticipated that a strong understanding of the chemical basis for metabolite formation will greatly enhance our ability to elucidate the mechanisms involved in idiosyncratic drug reactions and off-target toxicity.

In addition to gaining greater insights into the biochemical factors that influence the chemistry of drug metabolism, other technological and analytical advances will continue to be made and their application will continue to grow, which should enable scientists to have even greater impact in the area of drug metabolism. Of course, in order to have the greatest benefits from these advances, drug metabolism scientists need to embrace and incorporate emerging trends in science and technology, select the appropriate tools, and accurately interpret data generated from drug metabolism studies with a link toward the fundamental chemistry associated with the observed biotransformation. We hope the present work provides a reasonable chemical foundation for the biochemistry of drug metabolism on which both experienced and newly initiated drug metabolism scientists may rely on.

REFERENCES

1. Wienkers LC, Heath TG. Predicting *in vivo* drug interactions from *in vitro* drug discovery data. Nat Rev 2005;4:825–833.
2. Lipinski CA, Lombardo F, Dominy BW, *et al*. Experimental and computational approaches to estimate solubility and permeability in drug discovery and development settings. Adv Drug Deliv Rev 2001;46:3–26.
3. Van de Waterbeemd H, el Tayar N, Testa B, *et al*. Quantitative structure-activity relationships and eudismic analyses of the presynaptic dopaminergic activity and dopamine D2 and sigma receptor affinities of 3-(3-hydroxyphenyl)piperidines and octahydrobenzo[f]quinolines. J Med Chem 1987;30:2175–2181.
4. Davson H, Danielli JF. Studies on the permeability of erythrocytes: the alleged reversal of ionic permeability at alkaline reaction. Biochem J 1936;30:316–320.
5. Davson H, Danielli JF. Studies on the permeability of erythrocytes: factors in cation permeability. Biochem J 1938;32:991–1001.
6. Hirom PC, Millburn P, Smith RL. Bile and urine as complementary pathways for the excretion of foreign organic compounds. Xenobiotica 1976;6:55–64.
7. Smith DA, Brown K, Neale MG. Chromone-2-carboxylic acids: roles of acidity and lipophilicity in drug disposition. Drug Metab Rev 1985;16:365–388.
8. Varma MV, Feng B, Obach RS, *et al*. Physicochemical determinants of human renal clearance. J Med Chem 2009;52:4844–4852.
9. Rollins DE, Klaassen CD. Biliary excretion of drugs in man. Clin Pharmacokinet 1979;4:368–379.
10. Alrefai WA, Gill RK. Bile acid transporters: structure, function, regulation and pathophysiological implications. Pharm Res 2007;24:1803–1823.
11. Nies AT, Schwab M, Keppler D. Interplay of conjugating enzymes with OATP uptake transporters and ABCC/MRP efflux pumps in the elimination of drugs. Expert Opin Drug Metab Toxicol 2008;4:545–568.
12. Abou-El-Makarem MM, Millburn P, Smith RL, *et al*. Biliary excretion in foreign compounds. Species difference in biliary excretion. Biochem J 1967;105:1289–1293.
13. Abou-El-Makarem MM, Millburn P, Smith RL, *et al*. Biliary excretion of foreign compounds. Benzene and its derivatives in the rat. Biochem J 1967;105:1269–1274.
14. Penniston JT, Beckett L, Bentley DL, *et al*. Passive permeation of organic compounds through biological tissue: a non-steady-state theory. Mol Pharmacol 1969;5:333–341.
15. Goodwin JT, Conradi RA, Ho NF, *et al*. Physicochemical determinants of passive membrane permeability: role of solute hydrogen-bonding potential and volume. J Med Chem 2001;44:3721–3729.
16. Hansch C, Kim D, Leo AJ, *et al*. Toward a quantitative comparative toxicology of organic compounds. Crit Rev Toxicol 1989;19:185–226.
17. Abraham MH, Le J. The correlation and prediction of the solubility of compounds in water using an amended solvation energy relationship. J Pharm Sci 1999;88:868–880.
18. Amidon GL, Anik ST. Comparison of several molecular topological indexes with molecular surface area in aqueous solubility estimation. J Pharm Sci 1976;65:801–806.
19. Gronwall TH. On the Determination of the Apparent Diameters of the Ions in the Debye-Huckel Theory of Strong Electrolytes. Proc Natl Acad Sci U S A 1927;13:198–202.
20. Koppenol WH. Effect of a molecular dipole on the ionic strength dependence of a biomolecular rate constant. Identification of the site of reaction. Biophys J 1980;29:493–507.
21. Cohen BE, Bangham AD. Diffusion of small non-electrolytes across liposome membranes. Nature 1972;236:173–174.
22. McDaniel DH, Brown HC. Hydrogen Bonding as a Factor in the Ionization of Dicarboxylic Acids. Science (New York) 1953;118:370–372.
23. Williams RT. The fate of foreign compounds in man and animals. Pure Appl Chem 1969;18:129–141.

24. Gillette JR, Brodie BB, La Du BN. The oxidation of drugs by liver microsomes: on the role of TPNH and oxygen. J Pharmacol Exp Ther 1957;119:532–540.
25. Smith JN, Smithies RH, Williams RT. Studies in detoxication. 59. The metabolism of alkylbenzenes; the biological reduction of ketones derived from alkylbenzenes. Biochem J 1954;57:74–76.
26. Burns JJ, Weiner M, Simson G, *et al*. The biotransformation of ethyl biscoumacetate (tromexan) in man, rabbit and dog. J Pharmacol Exp Ther 1953;108:33–41.
27. Dutton GJ, Storey ID. Uridine compounds in glucuronic acid metabolism. I. The formation of glucuronides in liver suspensions. Biochem J 1954;57:275–283.
28. Brodie BB, Axelrod J. The fate of aminopyrine (pyramidon) in man and methods for the estimation of aminopyrine and its metabolites in biological material. J Pharmacol Exp Ther 1950;99:171–184.
29. Brodie BB, Axelrod J. The fate of acetanilide in man. J Pharmacol Exp Ther 1948; 94:29–38.
30. Daly J, Inscoe JK, Axelrod J. The formation of O-methylated catechols by microsomal hydroxylation of phenols and subsequent enzymatic catechol O-methylation. Substrate specificity. J Med Chem 1965;8:153–157.
31. Barnes MM, James SP, Wood PB. The formation of mercapturic acids. 1. Formation of mercapturic acid and the levels of glutathione in tissues. Biochem J 1959;71:680–690.
32. Albery WJ, Knowles JR. Evolution of enzyme function and the development of catalytic efficiency. Biochemistry 1976;15:5631–5640.
33. Storm DR, Koshland DE. A Source for the Special Catalytic Power of Enzymes: Orbital Steering. Proc Natl Acad Sci U S A 1970;66:445–452.
34. Koshland DE Jr. The evolution of function in enzymes. Fed Proc 1976;35:2104–2111.
35. Pauling L, Delbruck M. The nature of the intermolecular forces operative in biological processes. Science (New York) 1940;92:77–79.
36. Lienhard GE. Enzymatic catalysis and transition-state theory. Science (New York) 1973;180:149–154.
37. Jehle H. Intermolecular forces and biological specificity. Proc Natl Acad Sci U S A 1963;50:516–524.
38. Bartlett GJ, Porter CT, Borkakoti N, *et al*. Analysis of catalytic residues in enzyme active sites. J Mol Biol 2002;324:105–121.
39. Prasad S, Cantwell AM, Bush LA, *et al*. Residue Asp-189 controls both substrate binding and the monovalent cation specificity of thrombin. J Biol Chem 2004;279:10103–10108.
40. Meloche HP, Glusker JP. Aldolase catalysis: single base-mediated proton activation. Science (New York) 1973;181:350–352.
41. Ghisla S, Massey V, Lhoste JM, *et al*. Fluorescence and optical characteristics of reduced flavines and flavoproteins. Biochemistry 1974;13:589–597.
42. Sabourin PJ, Hodgson E. Characterization of the purified microsomal FAD-containing monooxygenase from mouse and pig liver. Chem Biol Interact 1984;51:125–139.
43. Groves JT. High-valent iron in chemical and biological oxidations. J Inorg Biochem 2006;100:434–447.
44. Hayaishi O, Rothberg S, Mehler AH, *et al*. Studies on oxygenases; enzymatic formation of kynurenine from tryptophan. J Biol Chem 1957;229:889–896.
45. Hayano M, Lindberg MC, Dorfman RI, *et al*. On the mechanism of the c-11beta-hydroxylation of steroids; a study with H2O18 and O218. Arch Biochem Biophys 1955;59:529–532.
46. Mason HS, Onopryenko I, Buhler D. Hydroxylation; the activation of oxygen by peroxidase. Biochim Biophys Acta 1957;24:225–226.
47. Axelrod J. The enzymatic deamination of amphetamine (benzedrine). J Biol Chem 1955;214:753–763.

48. La Du BN, Gaudette L, Trousof N, *et al*. Enzymatic dealkylation of aminopyrine (pyramidon) and other alkylamines. J Biol Chem 1955;214:741–745.
49. Dolphin D. Cytochrome P450: substrate and prosthetic-group free radicals generated during the enzymatic cycle. Philos Trans R Soc Lond B Biol Sci 1985;311:579–591.
50. Kadlubar FF, Morton KC, Ziegler DM. Microsomal-catalyzed hydroperoxide-dependent C-oxidation of amines. Biochem Biophys Res Commun 1973;54:1255–1261.
51. Tukey RH, Strassburg CP. Human UDP-glucuronosyltransferases: metabolism, expression, and disease. Annu Rev Pharmacol Toxicol 2000;40:581–616.
52. Weinshilboum RM, Otterness DM, Aksoy IA, *et al*. Sulfation and sulfotransferases 1: sulfotransferase molecular biology: cDNAs and genes. FASEB J 1997;11:3–14.
53. Cleland WW. The use of isotope effects to determine enzyme mechanisms. Arch Biochem Biophys 2005;433:2–12.
54. Northrop DB. Deuterium and tritium kinetic isotope effects on initial rates. Methods Enzymol 1982;87:607–625.
55. Sugiyama K, Trager WF. Prochiral selectivity and intramolecular isotope effects in the cytochrome P-450 catalyzed omega-hydroxylation of cumene. Biochemistry 1986; 25:7336–7343.
56. Darbyshire JF, Iyer KR, Grogan J, *et al*. Substrate probe for the mechanism of aromatic hydroxylation catalyzed by cytochrome P450. Drug Metab Dispos 1996;24: 1038–1045.
57. Boyd DR, Daly JW, Jerina DM. Rearrangement of (1- 2 H)- and (2- 2 H)naphthalene 1,2-oxides to 1-naphthol. Mechanism of the NIH shift. Biochemistry 1972;11:1961–1966.
58. Guroff G, Daly JW, Jerina DM, *et al*. Hydroxylation-induced migration: the NIH shift. Recent experiments reveal an unexpected and general result of enzymatic hydroxylation of aromatic compounds. Science (New York) 1967;157:1524–1530.
59. Decker CJ, Doerge DR, Cashman JR. Metabolism of benzimidazoline-2-thiones by rat hepatic microsomes and hog liver flavin-containing monooxygenase. Chem Res Toxicol 1992;5:726–733.
60. Skiles GL, Yost GS. Mechanistic studies on the cytochrome P450-catalyzed dehydrogenation of 3-methylindole. Chem Res Toxicol 1996;9:291–297.
61. Holtzman JL, Gillette JR, Milne GW. The incorporation of 18-O into naphthalene in the enzymatic formation of 1,2-dihydronaphthalene-1,2-diol. J Biol Chem 1967; 242:4386–4387.
62. Jerina DM, Daly JW, Witkop B, *et al*. The role of arene oxide-oxepin systems in the metabolism of aromatic substrates. 3. Formation of 1,2-naphthalene oxide from naphthalene by liver microsomes. J Am Chem Soc 1968;90:6525–6527.
63. Spatzenegger M, Liu H, Wang Q, *et al*. Analysis of differential substrate selectivities of CYP2B6 and CYP2E1 by site-directed mutagenesis and molecular modeling. J Pharmacol Exp Ther 2003;304:477–487.
64. Balogh LM, Le Trong I, Kripps KA, *et al*. Structural analysis of a glutathione transferase A1-1 mutant tailored for high catalytic efficiency with toxic alkenals. Biochemistry 2009;48:7698–7704.
65. Zheng YM, Henne KR, Charmley P, *et al*. Genotyping and site-directed mutagenesis of a cytochrome P450 meander Pro-X-Arg motif critical to CYP4B1 catalysis. Toxicol Appl Pharmacol 2003;186:119–126.
66. Adali O, Carver GC, Philpot RM. Modulation of human flavin-containing monooxygenase 3 activity by tricyclic antidepressants and other agents: importance of residue 428. Arch Biochem Biophys 1998;358:92–97.
67. Dubois SG, Beaulieu M, Levesque E, *et al*. Alteration of human UDP-glucuronosyltransferase UGT2B17 regio-specificity by a single amino acid substitution. J Mol Biol 1999;289:29–39.

68. Pearson JT, Wahlstrom JL, Dickmann LJ, *et al*. Differential time-dependent inactivation of P450 3A4 and P450 3A5 by raloxifene: a key role for C239 in quenching reactive intermediates. Chem Res Toxicol 2007;20:1778–1786.
69. Radominska-Pandya A, Czernik PJ, Little JM, *et al*. Structural and functional studies of UDP-glucuronosyltransferases. Drug Metab Rev 1999;31:817–899.
70. van der Aar EM, Tan KT, Commandeur JN, *et al*. Strategies to characterize the mechanisms of action and the active sites of glutathione S-transferases: a review. Drug Metab Rev 1998;30:569–643.
71. Battaglia E, Pritchard M, Ouzzine M, *et al*. Chemical modification of human UDP-glucuronosyltransferase UGT1*6 by diethyl pyrocarbonate: possible involvement of a histidine residue in the catalytic process. Arch Biochem Biophys 1994;309:266–272.
72. Battaglia E, Senay C, Fournel-Gigleux S, *et al*. The chemical modification of human liver UDP-glucuronosyltransferase UGT1*6 reveals the involvement of a carboxyl group in catalysis. FEBS Lett 1994;346:146–150.
73. Patana AS, Kurkela M, Finel M, *et al*. Mutation analysis in UGT1A9 suggests a relationship between substrate and catalytic residues in UDP-glucuronosyltransferases. Protein Eng Des Sel 2008;21:537–543.
74. Ryan D, Lu AY, West S, *et al*. Multiple forms of cytochrome P-450 in phenobarbital- and 3-methylcholanthrene-treated rats. Separation and spectral properties. J Biol Chem 1975;250:2157–2163.
75. Zakim D, Vessey DA. Regulation of microsomal UDP-glucuronyltransferase by metal ions. Differential effects of Mn2+ on forward and reverse reactions. Eur J Biochem/FEBS 1976;64:459–463.
76. Nebert DW. Suggestions for the nomenclature of human alleles: relevance to ecogenetics, pharmacogenetics and molecular epidemiology. Pharmacogenetics 2000;10:279–290.
77. Nelson DR, Zeldin DC, Hoffman SM, *et al*. Comparison of cytochrome P450 (CYP) genes from the mouse and human genomes, including nomenclature recommendations for genes, pseudogenes and alternative-splice variants. Pharmacogenetics 2004;14:1–18.
78. Wienkers LC, Wynalda MA. Multiple cytochrome P450 enzymes responsible for the oxidative metabolism of the substituted (S)-3-phenylpiperidine, (S,S)-3-[3-(methylsulfonyl)phenyl]-1-propylpiperidine hydrochloride, in human liver microsomes. Drug Metab Dispos 2002;30:1372–1377.
79. Wynalda MA, Hutzler JM, Koets MD, *et al*. *In vitro* metabolism of clindamycin in human liver and intestinal microsomes. Drug Metab Dispos 2003;31:878–887.
80. Ortiz de Montellano PR, De Voss JJ. Oxidizing species in the mechanism of cytochrome P450. Nat Prod Rep 2002;19:477–493.
81. Iyanagi T, Mason HS. Some properties of hepatic reduced nicotinamide adenine dinucleotide phosphate-cytochrome c reductase. Biochemistry 1973;12:2297–2308.
82. Vermilion JL, Ballou DP, Massey V, *et al*. Separate roles for FMN and FAD in catalysis by liver microsomal NADPH-cytochrome P-450 reductase. J Biol Chem 1981;256:266–277.
83. Vermilion JL, Coon MJ. Identification of the high and low potential flavins of liver microsomal NADPH-cytochrome P-450 reductase. J Biol Chem 1978;253:8812–8819.
84. Schenkman JB, Jansson I. Interactions between cytochrome P450 and cytochrome b5. Drug Metab Rev 1999;31:351–364.
85. Evans WE, Relling MV. Pharmacogenomics: translating functional genomics into rational therapeutics. Science (New York) 1999;286:487–491.
86. Ding X, Kaminsky LS. Human extrahepatic cytochromes P450: function in xenobiotic metabolism and tissue-selective chemical toxicity in the respiratory and gastrointestinal tracts. Annu Rev Pharmacol Toxicol 2003;43:149–173.
87. Nebert DW, Russell DW. Clinical importance of the cytochromes P450. Lancet 2002;360:1155–1162.

88. Schlichting I, Berendzen J, Chu K, *et al*. The catalytic pathway of cytochrome p450cam at atomic resolution. Science (New York) 2000;287:1615–1622.
89. Guengerich FP. Reactions and significance of cytochrome P-450 enzymes. J Biol Chem 1991;266:10019–10022.
90. Estabrook RW, Baron J, Hildebrandt A. A new spectral species associated with cytochrome P-450 in liver microsomes. Chem Biol Interact 1971;3:260–261.
91. Isin EM, Guengerich FP. Substrate binding to cytochromes P450. Anal Bioanal Chem 2008;392:1019–1030.
92. Makris TM, Denisov IG, Sligar SG. Haem-oxygen reactive intermediates: catalysis by the two-step. Biochem Soc Trans 2003;31:516–519.
93. Tajima K, Edo T, Ishizu K, *et al*. Cytochrome P-450-butyl peroxide complex detected by ESR. Biochem Biophys Res Commun 1993;191:157–164.
94. Davydov R, Macdonald IDG, Makris TM, *et al*. EPR and ENDOR of catalytic intermediates in cyroreduced native and mutant oxy-cytochromes P450cam: mutation-induced changes in the proton delivery system. J Am Chem Soc 1999;121:10654–10655.
95. Davydov R, Makris TM, Kofman V, *et al*. Hydroxylation of camphor by reduced oxy-cytochrome p450cam: mechanistic implication of EPR and ENDOR studies of catalytic intermediates in native and mutant enzymes. J Am Chem Soc 2001;123:1403–1415.
96. Dolphin D, Forman A, Borg DC, *et al*. Compounds I of catalase and horse radish peroxidase: pi-cation radicals. Proc Natl Acad Sci U S A 1971;68:614–618.
97. Groves JT, McClusky GA. Aliphatic hydroxylation by highly purified liver microsomal cytochrome P-450. Evidence for a carbon radical intermediate. Biochem Biophys Res Commun 1978;81:154–160.
98. Vaz AD, McGinnity DF, Coon MJ. Epoxidation of olefins by cytochrome P450: evidence from site-specific mutagenesis for hydroperoxo-iron as an electrophilic oxidant. Proc Natl Acad Sci U S A 1998;95:3555–3560.
99. Lovern MR, Turner MJ, Meyer M, *et al*. Identification of benzene oxide as a product of benzene metabolism by mouse, rat, and human liver microsomes. Carcinogenesis 1997;18:1695–1700.
100. Volz TJ, Rock DA, Jones JP. Evidence for two different active oxygen species in cytochrome P450 BM3 mediated sulfoxidation and N-dealkylation reactions. J Am Chem Soc 2002;124:9724–9725.
101. Hjelmeland LM, Aronow L, Trudell JR. Intramolecular determination of substituent effects in hydroxylations catalyzed by cytochrome P-450. Mol Pharmacol 1977;13:634–639.
102. White RE, Miller JP, Favreau LV, *et al*. Stereochemical dynamics of aliphatic hydroxylation by cytochrome P-450. J Am Chem Soc 1986;108:6024–6031.
103. Gelb MH, Heimbrook DC, Malkonen P, *et al*. Stereochemistry and deuterium isotope effects in camphor hydroxylation by the cytochrome P450cam monoxygenase system. Biochemistry 1982;21:370–377.
104. Ortiz de Montellano PR, Stearns RA. Timing of the radical recombination step in cytochrome P-450 catalysis with ring strained probes. J Am Chem Soc 1987;109: 3415–3420.
105. Atkinson JK, Hollenberg PF, Ingold KU, *et al*. Cytochrome P450-catalyzed hydroxylation of hydrocarbons: kinetic deuterium isotope effects for the hydroxylation of an ultrafast radical clock. Biochemistry 1994;33:10630–10637.
106. Bowry VW, Ingold KU. A radical clock investigation of microsomal cytochrome P-450 hydroxylation of hydrocarbons. Rate of oxygen rebound. J Am Chem Soc 1991; 113:5699–5707.
107. Newcomb M, Le Tadic-Biadatti M-H, Chestney DL, *et al*. An incredibly fast apparent oxygen rebound rate constant for hydrocarbon hydroxylation by cytochrome P-450 enzymes. J Am Chem Soc 1995;117:3312–3313.

108. Harris RM, Waring RH, Kirk CJ, *et al*. Sulfation of "estrogenic" alkylphenols and 17beta-estradiol by human platelet phenol sulfotransferases. J Biol Chem 2000;275:159–166.
109. Watabe T, Akamatsu K. Microsomal epoxidation of cis-stilbene: decrease in epoxidase activity related to lipid peroxidation. Biochem Pharmacol 1974;23:1079–1085.
110. Ortiz de Montellano PR, Kunze KL, Mico BA. Destruction of cytochrome P-450 by olefins: N-alkylation of prosthetic heme. Mol Pharmacol 1980;18:602–605.
111. Ortiz de Montellano PR, Mico BA. Destruction of cytochrome P-450 by ethylene and other olefins. Mol Pharmacol 1980;18:128–135.
112. Miller RE, Guengerich FP. Oxidation of trichloroethylene by liver microsomal cytochrome P-450: evidence for chlorine migration in a transition state not involving trichloroethylene oxide. Biochemistry 1982;21:1090–1097.
113. de Visser SP, Ogliaro F, Harris N, *et al*. Multi-state epoxidation of ethene by cytochrome P-450: a quantum chemical study. J Am Chem Soc 2001;123:3037–3047.
114. Ortiz de Montellano PR, Kunze KL. Shift of the acetylenic hydrogen during chemical and enzymatic oxidation of the biphenylacetylene triple bond. Arch Biochem Biophys 1981;209:710–712.
115. McMahon RE, Turner JC, Whitaker GW, *et al*. Deuterium-isotope effect in the biotransformation of 4-ethynylbiphenyls to 4-biphenylylacetic acids by rat hepatic microsomes. Biochem Biophys Res Commun 1981;99:662–667.
116. Jerina DM, Daly JW. Arene oxides: a new aspect of drug metabolism. Science (New York) 1974;185:573–582.
117. Koerts J, Soffers AE, Vervoort J, *et al*. Occurrence of the NIH shift upon the cytochrome P450-catalyzed *in vivo* and *in vitro* aromatic ring hydroxylation of fluorobenzenes. Chem Res Toxicol 1998;11:503–512.
118. Hanzlik RP, Ling K-HJ. Active site dynamics of xylene hydroxylation by cytochrome P-450 as revealed by kinetic deuterium isotope effects. J Am Chem Soc 1993; 115:9363–9370.
119. Riley P, Hanzlik RP. Electron transfer in P450 mechanisms. Microsomal metabolism of cyclopropylbenzene and p-cyclopropylanisole. Xenobiotica 1994;24:1–16.
120. Miwa GT, Walsh JS, Kedderis GL, *et al*. The use of intramolecular isotope effects to distinguish between deprotonation and hydrogen atom abstraction mechanisms in cytochrome P-450- and peroxidase-catalyzed N-demethylation reactions. J Biol Chem 1983;258:14445–14449.
121. Griller D, Howard JA, Marriott PR, *et al*. Absolute rate constants for the reactions of tert-butoxyl, tert-butylperoxyl, and benzophenone triplet with amines: the importance of a stereoelectronic effect. J Am Chem Soc 1981;103:619–623.
122. Dinnocenzo JP, Karki SB, Jones JP. On isotope effects for the cytochrome P-450 oxidation of substituted N,N-dimethylanilines. J Am Chem Soc 1993;115:7111–7116.
123. Karki SB, Dinnocenzo JP. On the mechanism of amine oxidations by P450. Xenobiotica 1995;25:711–724.
124. Shaffer CL, Harriman S, Koen YM, *et al*. Formation of cyclopropanone during cytochrome P450-catalyzed N-dealkylation of a cyclopropylamine. J Am Chem Soc 2002; 124:8268–8274.
125. Shaffer CL, Morton MD, Hanzlik RP. Enzymatic N-dealkylation of an N-cyclopropyl amine: an unusual fate for the cyclopropyl group. J Am Chem Soc 2000;123:349–350.
126. Shaffer CL, Morton MD, Hanzlik RP. N-Dealkylation of an N-cyclopropylamine by horseradish peroxidase. Fate of the Cyclopropyl Group. J Am Chem Soc 2001;123: 8502–8508.
127. Dowers TS, Rock DA, Rock DA, *et al*. An analysis of the regioselectivity of aromatic hydroxylation and N-oxygenation by cytochrome P450 enzymes. Drug Metab Dispos 2004; 32:328–332.

128. Miwa GT, Walsh JS, Lu AY. Kinetic isotope effects on cytochrome P-450-catalyzed oxidation reactions. The oxidative O-dealkylation of 7-ethoxycoumarin. J Biol Chem 1984; 259:3000–3004.
129. Dowers TS, Jones JP. Kinetic isotope effects implicate a single oxidant for cytochrome P450-mediated O-dealkylation, N-oxygenation, and aromatic hydroxylation of 6-methoxyquinoline. Drug Metab Dispos 2006;34:1288–1290.
130. Jones JP, Korzekwa KR. Predicting the rates and regioselectivity of reactions mediated by the P450 superfamily. Methods Enzymol 1996;272:326–335.
131. Jones JP, Mysinger M, Korzekwa KR. Computational models for cytochrome P450: a predictive electronic model for aromatic oxidation and hydrogen atom abstraction. Drug Metab Dispos 2002;30:7–12.
132. Ziegler DM. Flavin-containing monooxygenases: enzymes adapted for multisubstrate specificity. Trends Pharmacol Sci 1990;11:321–324.
133. Chen GP, Poulsen LL, Ziegler DM. Oxidation of aldehydes catalyzed by pig liver flavin-containing monooxygenase. Drug Metab Dispos 1995;23:1390–1393.
134. Chen GP, Ziegler DM. Liver microsome and flavin-containing monooxygenase catalyzed oxidation of organic selenium compounds. Arch Biochem Biophys 1994;312:566–572.
135. Lang DH, Yeung CK, Peter RM, *et al*. Isoform specificity of trimethylamine N-oxygenation by human flavin-containing monooxygenase (FMO) and P450 enzymes: selective catalysis by FMO3. Biochem Pharmacol 1998;56:1005–1012.
136. Rettie AE, Lawton MP, Sadeque AJ, *et al*. Prochiral sulfoxidation as a probe for multiple forms of the microsomal flavin-containing monooxygenase: studies with rabbit FMO1, FMO2, FMO3, and FMO5 expressed in Escherichia coli. Arch Biochem Biophys 1994;311:369–377.
137. Smyser BP, Hodgson E. Metabolism of phosphorus-containing compounds by pig liver microsomal FAD-containing monooxygenase. Biochem Pharmacol 1985;34:1145–1150.
138. Yanni SB, Annaert PP, Augustijns P, *et al*. Role of flavin-containing monooxygenase in oxidative metabolism of voriconazole by human liver microsomes. Drug Metab Dispos 2008;36:1119–1125.
139. Kim YM, Ziegler DM. Size limits of thiocarbamides accepted as substrates by human flavin-containing monooxygenase 1. Drug Metab Dispos 2000;28:1003–1006.
140. Ripp SL, Overby LH, Philpot RM, *et al*. Oxidation of cysteine S-conjugates by rabbit liver microsomes and cDNA-expressed flavin-containing mono-oxygenases: studies with S-(1,2-dichlorovinyl)-L-cysteine, S-(1,2,2-trichlorovinyl)-L-cysteine, S-allyl-L-cysteine, and S-benzyl-L-cysteine. Mol Pharmacol 1997;51:507–515.
141. Krueger SK, Henderson MC, Siddens LK, *et al*. Characterization of sulfoxygenation and structural implications of human flavin-containing monooxygenase isoform 2 (FMO2.1) variants S195L and N413K. Drug Metab Dispos 2009;37:1785–1791.
142. Rettie AE, Meier GP, Sadeque AJ. Prochiral sulfides as *in vitro* probes for multiple forms of the flavin-containing monooxygenase. Chem Biol Interact 1995;96:3–15.
143. Cashman JR, Williams DE. Enantioselective S-oxygenation of 2-aryl-1,3-dithiolanes by rabbit lung enzyme preparations. Mol Pharmacol 1990;37:333–339.
144. Hamman MA, Haehner-Daniels BD, Wrighton SA, *et al*. Stereoselective sulfoxidation of sulindac sulfide by flavin-containing monooxygenases. Comparison of human liver and kidney microsomes and mammalian enzymes. Biochem Pharmacol 2000;60:7–17.
145. Light DR, Waxman DJ, Walsh C. Studies on the chirality of sulfoxidation catalyzed by bacterial flavoenzyme cyclohexanone monooxygenase and hog liver flavin adenine dinucleotide containing monooxygenase. Biochemistry 1982;21:2490–2498.
146. Waxman DJ, Light DR, Walsh C. Chiral sulfoxidations catalyzed by rat liver cytochromes P-450. Biochemistry 1982;21:2499–2507.
147. Hai X, Adams E, Hoogmartens J, *et al*. Enantioselective in-line and off-line CE methods for the kinetic study on cimetidine and its chiral metabolites with reference to flavin-containing monooxygenase genetic isoforms. Electrophoresis 2009;l30:1248–1257.

148. Beaty NB, Ballou DP. Transient kinetic study of liver microsomal FAD-containing monooxygenase. J Biol Chem 1980;255:3817–3819.
149. Canepa C, Bach RD, Dmitrenko O. Neutral versus charged species in enzyme catalysis. Classical and free energy barriers for oxygen atom transfer from C4a-hydroperoxyflavin to dimethyl sulfide. J Org Chem 2002;67:8653–8661.
150. Denisov IG, Grinkova YV, Baas BJ, *et al*. The ferrous-dioxygen intermediate in human cytochrome P450 3A4. Substrate dependence of formation and decay kinetics. J Biol Chem 2006;281:23313–23318.
151. Poulsen LL, Ziegler DM. The liver microsomal FAD-containing monooxygenase. Spectral characterization and kinetic studies. J Biol Chem 1979;254:6449–6455.
152. Williams RF, Shinkai S, Bruice TC. Radical mechanisms for 1,5-dihydroflavin reduction of carbonyl compounds. Proc Natl Acad Sci U S A 1975;72:1763–1767.
153. Ziegler DM. The 1990 Bernard B. Brodie Award Lecture. Unique properties of the enzymes of detoxication. Drug Metab Dispos 1991;19:847–852.
154. Orf HW, Dolphin D. Oxaziridines as possible intermediates in flavin monooxygenases. Proc Natl Acad Sci U S A 1974;71:2646–2650.
155. Ryan KS, Chakraborty S, Howard-Jones AR, *et al*. The FAD cofactor of RebC shifts to an IN conformation upon flavin reduction. Biochemistry 2008;47:13506–13513.
156. Baron R, Riley C, Chenprakhon P, *et al*. Multiple pathways guide oxygen diffusion into flavoenzyme active sites. Proc Natl Acad Sci U S A 2009;106:10603–10608.
157. Jones KC, Ballou DP. Reactions of the 4a-hydroperoxide of liver microsomal flavin-containing monooxygenase with nucleophilic and electrophilic substrates. J Biol Chem 1986;261:2553–2559.
158. Suh JK, Poulsen LL, Ziegler DM, *et al*. Lysine 219 participates in NADPH specificity in a flavin-containing monooxygenase from Saccharomyces cerevisiae. Arch Biochem Biophys 1999;372:360–366.
159. Eswaramoorthy S, Bonanno JB, Burley SK, *et al*. Mechanism of action of a flavin-containing monooxygenase. Proc Natl Acad Sci U S A 2006;103:9832–9837.
160. Alfieri A, Malito E, Orru R, *et al*. Revealing the moonlighting role of NADP in the structure of a flavin-containing monooxygenase. Proc Natl Acad Sci U S A 2008; 105:6572–6577.
161. Guengerich FP, Krauser JA, Johnson WW. Rate-limiting steps in oxidations catalyzed by rabbit cytochrome P450 1A2. Biochemistry 2004;43:10775–10788.
162. Obach RS. Potent inhibition of human liver aldehyde oxidase by raloxifene. Drug Metab Dispos 2004;32:89–97.
163. Obach RS, Huynh P, Allen MC, *et al*. Human liver aldehyde oxidase: inhibition by 239 drugs. J Clin Pharmacol 2004;44:7–19.
164. Cohen P. Protein kinases–the major drug targets of the twenty-first century? Nat Rev 2002;1:309–315.
165. Torres RA, Korzekwa KR, *et al*. Use of density functional calculations to predict the regioselectivity of drugs and molecules metabolized by aldehyde oxidase. J Med Chem 2007;50:4642–4647.
166. Kitamura S, Sugihara K, Ohta S. Drug-metabolizing ability of molybdenum hydroxylases. Drug Metab Pharmacokinet 2006;21:83–98.
167. Hille R. Molybdenum-containing hydroxylases. Arch Biochem Biophys 2005;433: 107–116.
168. Alfaro JF, Jones JP. Studies on the mechanism of aldehyde oxidase and xanthine oxidase. J Org Chem 2008;73:9469–9472.
169. Miners JO, Birkett DJ. The use of caffeine as a metabolic probe for human drug metabolizing enzymes. Gen Pharmacol 1996;27:245–249.

170. Okamoto K, Eger BT, Nishino T, *et al*. Mechanism of inhibition of xanthine oxidoreductase by allopurinol: crystal structure of reduced bovine milk xanthine oxidoreductase bound with oxipurinol. Nucleosides Nucleotides Nucleic Acids 2008;27: 888–893.
171. Massey V, Edmondson D. On the mechanism of inactivation of xanthine oxidase by cyanide. J Biol Chem 1970;245:6595–6598.
172. Sato T, Ashizawa N, Matsumoto K, *et al*. Discovery of 3-(3-cyano-4-pyridyl)-5-(4-pyridyl)-1,2,4-triazole, FYX-051–a xanthine oxidoreductase inhibitor for the treatment of hyperuricemia. Bioorg Med Chem Lett 2009;19:6225–6229.
173. Okamoto K, Eger BT, Nishino T, *et al*. An extremely potent inhibitor of xanthine oxidoreductase. Crystal structure of the enzyme-inhibitor complex and mechanism of inhibition. J Biol Chem 2003;278:1848–1855.
174. Fukunari A, Okamoto K, Nishino T, *et al*. Y-700 [1-[3-Cyano-4-(2,2-dimethyl propoxy)phenyl]-1H-pyrazole-4-carboxylic acid]: a potent xanthine oxidoreductase inhibitor with hepatic excretion. J Pharmacol Exp Ther 2004;311:519–528.
175. Rooseboom M, Commandeur JN, Vermeulen NP. Enzyme-catalyzed activation of anticancer prodrugs. Pharmacol Rev 2004;56:53–102.
176. LoRusso PM, Prakash S, Wozniak A, *et al*. Phase I clinical trial of 5-fluoro-pyrimidinone (5FP), an oral prodrug of 5-fluorouracil (5FU). Invest New Drugs 2002;20:63–71.
177. Vere Hodge RA, Sutton D, Boyd MR, *et al*. Selection of an oral prodrug (BRL 42810; famciclovir) for the antiherpesvirus agent BRL 39123 [9-(4-hydroxy-3-hydroxymethylbutl-yl)guanine; penciclovir. Antimicrob Agents Chemother 1989;33:1765–1773.
178. Filer CW, Allen GD, Brown TA, *et al*. Metabolic and pharmacokinetic studies following oral administration of 14C-famciclovir to healthy subjects. Xenobiotica 1994;24:357–368.
179. Beedham C. Molybdenum hydroxylases: biological distribution and substrate-inhibitor specificity. Prog Med Chem 1987;24:85–127.
180. Alfaro JF, Joswig-Jones CA, Ouyang W, *et al*. Purification and mechanism of human aldehyde oxidase expressed in Escherichia coli. Drug Metab Dispos 2009;37:2393–2398.
181. Skibo EB, Gilchrist JH, Lee CH. Electronic probes of the mechanism of substrate oxidation by buttermilk xanthine oxidase: role of the active-site nucleophile in oxidation. Biochemistry 1987;26:3032–3037.
182. Kanazawa I. Short review on monoamine oxidase and its inhibitors. Eur Neurol 1994;34, Suppl 3: 36–39.
183. Greenawalt JW, Schnaitman C. An appraisal of the use of monoamine oxidase as an enzyme marker for the outer membrane of rat liver mitochondria. J Cell Biol 1970;46:173–179.
184. Tipton KF. Monoamine oxidase inhibition. Biochem Soc Trans 1994;22:764–768.
185. O'Carroll AM, Anderson MC, Tobbia I, *et al*. Determination of the absolute concentrations of monoamine oxidase A and B in human tissues. Biochem Pharmacol 1989;38:901–905.
186. Thorpe LW, Westlund KN, Kochersperger LM, *et al*. Immunocytochemical localization of monoamine oxidases A and B in human peripheral tissues and brain. J Histochem Cytochem 1987;35:23–32.
187. Binda C, Newton-Vinson P, Hubalek F, *et al*. Structure of human monoamine oxidase B, a drug target for the treatment of neurological disorders. Nat Struct Biol 2002;9:22–26.
188. Miller JR, Edmondson DE. Structure-activity relationships in the oxidation of para-substituted benzylamine analogues by recombinant human liver monoamine oxidase A. Biochemistry 1999;38:13670–13683.
189. Ramsay RR. Kinetic mechanism of monoamine oxidase A. Biochemistry 1991;30: 4624–4629.
190. Yu PH, Bailey BA, Durden DA, *et al*. Stereospecific deuterium substitution at the alpha-carbon position of dopamine and its effect on oxidative deamination catalyzed by MAO-A and MAO-B from different tissues. Biochem Pharmacol 1986;35:1027–1036.

191. Yu PH, Davis BA. Stereospecific deamination of benzylamine catalyzed by different amine oxidases. Int J Biochem 1988;20:1197–1201.
192. Silverman R. Radical ideas about monoamine oxidase. Acc Chem Res 1995;28:335–342.
193. Walker MC, Edmonson DE. Structure-activity relationships in the oxidation of benzylamine analogues by bovine liver mitochondrial monoamine oxidase B. Biochemistry 1994;33:7088–7098.
194. Kim JM, Hoegy SE, Mariano PS. Flavin chemical models for monoamine oxidase inactivation by cyclopropylamines, a-silylamines, and hydrazines. J Am Chem Soc 1995; 117:100–105.
195. Johnston JP. Some observations upon a new inhibitor of monoamine oxidase in brain tissue. Biochem Pharmacol 1968;17:1285–1297.
196. Cesura AM, Imhof R, Galva MD, *et al*. Interactions of the novel inhibitors of MAO-B Ro 19-6327 and Ro 16-6491 with the active site of the enzyme. Pharmacol Res Commun 1988;20, Suppl 4: 51–61.
197. Geha RM, Rebrin I, Chen K, *et al*. Substrate and inhibitor specificities for human monoamine oxidase A and B are influenced by a single amino acid. J Biol Chem 2001; 276:9877–9882.
198. Kaphalia BS, Mericle KA, Ansari GA. Mechanism of differential inhibition of hepatic and pancreatic fatty acid ethyl ester synthase by inhibitors of serine-esterases: *in vitro* and cell culture studies. Toxicol Appl Pharmacol 2004;200:7–15.
199. Lotti M, Ketterman A, Waskell L, *et al*. Meperidine carboxylesterase in mouse and human livers. Biochem Pharmacol 1983;32:3735–3738.
200. Munger JS, Shi GP, Mark EA, *et al*. A serine esterase released by human alveolar macrophages is closely related to liver microsomal carboxylesterases. J Biol Chem 1991;266:18832–18838.
201. De Simone G, Menchise V, Alterio V, *et al*. The crystal structure of an EST2 mutant unveils structural insights on the H group of the carboxylesterase/lipase family. J Mol Biol 2004;343:137–146.
202. Jbilo O, L'Hermite Y, Talesa V, *et al*. Acetylcholinesterase and butyrylcholinesterase expression in adult rabbit tissues and during development. Eur J Biochem/FEBS 1994; 225:115–124.
203. Mori M, Hosokawa M, Ogasawara Y, *et al*. cDNA cloning, characterization and stable expression of novel human brain carboxylesterase. FEBS Lett 1999;458:17–22.
204. Saboulard D, Naesens L, Cahard D, *et al*. Characterization of the activation pathway of phosphoramidate triester prodrugs of stavudine and zidovudine. Mol Pharmacol 1999;56:693–704.
205. Nishi K, Huang H, Kamita SG, *et al*. Characterization of pyrethroid hydrolysis by the human liver carboxylesterases hCE-1 and hCE-2. Arch Biochem Biophys 2006; 445:115–123.
206. Humerickhouse R, Lohrbach K, Li L, *et al*. Characterization of CPT-11 hydrolysis by human liver carboxylesterase isoforms hCE-1 and hCE-2. Cancer Res 2000; 60:1189–1192.
207. Boyer CS, Petersen DR. Enzymatic basis for the transesterification of cocaine in the presence of ethanol: evidence for the participation of microsomal carboxylesterases. J Pharmacol Exp Ther 1992;260:939–946.
208. Bourland JA, Martin DK, Mayersohn M. Carboxylesterase-mediated transesterification of meperidine (Demerol) and methylphenidate (Ritalin) in the presence of [2H6]ethanol: preliminary *in vitro* findings using a rat liver preparation. J Pharm Sci 1997;86:1494–1496.
209. Redinbo MR, Bencharit S, Potter PM. Human carboxylesterase 1: from drug metabolism to drug discovery. Biochem Soc Trans 2003;31:620–624.
210. Morishita Y, Fujii M, Kasakura Y, *et al*. Effect of carboxylesterase inhibition on the anti-tumour effects of irinotecan. J Int Med Res 2005;33:84–89.

211. Wadkins RM, Hyatt JL, Yoon KJ, *et al*. Discovery of novel selective inhibitors of human intestinal carboxylesterase for the amelioration of irinotecan-induced diarrhea: synthesis, quantitative structure-activity relationship analysis, and biological activity. Mol Pharmacol 2004;65:1336–1343.
212. Zhang D, Saraf A, Kolasa T, *et al*. Fatty acid amide hydrolase inhibitors display broad selectivity and inhibit multiple carboxylesterases as off-targets. Neuropharmacology 2007;52:1095–1105.
213. Takai S, Matsuda A, Usami Y, *et al*. Hydrolytic profile for ester- or amide-linkage by carboxylesterases pI 5.3 and 4.5 from human liver. Biol Pharm Bull 1997;20:869–873.
214. Vistoli G, Pedretti A, Mazzolari A, *et al*. Influence of ionization state on the activation of temocapril by hCES1: a molecular-dynamics study. Chem Biodiv 2009;6:2092–2100.
215. Satoh T, Hosokawa M. The mammalian carboxylesterases: from molecules to functions. Annu Rev Pharmacol Toxicol 1998;38:257–288.
216. Frey PA, Whitt SA, Tobin JB. A low-barrier hydrogen bond in the catalytic triad of serine proteases. Science (New York) 1994;264:1927–1930.
217. Cleland WW, Kreevoy MM. Low-barrier hydrogen bonds and enzymic catalysis. Science (New York) 1994;264:1887–1890.
218. Huang H, Fleming CD, Nishi K, *et al*. Stereoselective hydrolysis of pyrethroid-like fluorescent substrates by human and other mammalian liver carboxylesterases. Chem Res Toxicol 2005;18:1371–1377.
219. Sun Z, Murry DJ, Sanghani SP, *et al*. Methylphenidate is stereoselectively hydrolyzed by human carboxylesterase CES1A1. J Pharmacol Exp Ther 2004;310:469–476.
220. Guichard S, Terret C, Hennebelle I, *et al*. CPT-11 converting carboxylesterase and topoisomerase activities in tumour and normal colon and liver tissues. Br J Cancer 1999;80:364–370.
221. Satoh T, Hosokawa M, Atsumi R, *et al*. Metabolic activation of CPT-11, 7-ethyl-10-[4-(1-piperidino)-1-piperidino]carbonyloxycamptothecin, a novel antitumor agent, by carboxylesterase. Biol Pharm Bull 1994;17:662–664.
222. Wheelock CE, Severson TF, Hammock BD. Synthesis of new carboxylesterase inhibitors and evaluation of potency and water solubility. Chem Res Toxicol 2001;14:1563–1572.
223. Cohen SD. Carboxylesterase inhibition and potentiation of soman toxicity. Arch Toxicol 1981;49:105–106.
224. Luttrell WE, Castle MC. Species differences in the hydrolysis of meperidine and its inhibition by organophosphate compounds. Fundam Appl Toxicol 1988;11:323–332.
225. Wallace TJ, Kodsi EM, Langston TB, *et al*. Mutation of residues 423 (Met/Ile), 444 (Thr/Met), and 506 (Asn/Ser) confer cholesteryl esterase activity on rat lung carboxylesterase. Ser-506 is required for activation by cAMP-dependent protein kinase. J Biol Chem 2001;276:33165–33174.
226. Liang Y, Medhekar R, Brockman HL, *et al*. Importance of arginines 63 and 423 in modulating the bile salt-dependent and bile salt-independent hydrolytic activities of rat carboxyl ester lipase. J Biol Chem 2000;275:24040–24046.
227. Fleming CD, Bencharit S, Edwards CC, *et al*. Structural insights into drug processing by human carboxylesterase 1: tamoxifen, mevastatin, and inhibition by benzil. J Mol Biol 2005;352:165–177.
228. Morisseau C, Hammock BD. Epoxide hydrolases: mechanisms, inhibitor designs, and biological roles. Annu Rev Pharmacol Toxicol 2005;45:311–333.
229. Pacifici GM, Temellini A, Giuliani L, *et al*. Cytosolic epoxide hydrolase in humans: development and tissue distribution. Arch Toxicol 1988;62:254–257.
230. Coller JK, Fritz P, Zanger UM, *et al*. Distribution of microsomal epoxide hydrolase in humans: an immunohistochemical study in normal tissues, and benign and malignant tumours. Histochem J 2001;33:329–336.

231. Gomez GA, Morisseau C, Hammock BD, *et al*. Structure of human epoxide hydrolase reveals mechanistic inferences on bifunctional catalysis in epoxide and phosphate ester hydrolysis. Biochemistry 2004;43:4716–4723.
232. McKay JA, Weaver RJ, Murray GI, *et al*. Localization of microsomal epoxide hydrolase in normal and neoplastic human kidney. J Histochem Cytochem 1995;43:615–620.
233. Yu Z, Xu F, Huse LM, *et al*. Soluble epoxide hydrolase regulates hydrolysis of vasoactive epoxyeicosatrienoic acids. Circ Res 2000;87:992–998.
234. Baxter SW, Choong DY, Campbell IG. Microsomal epoxide hydrolase polymorphism and susceptibility to ovarian cancer. Cancer Lett 2002;177:75–81.
235. Sinal CJ, Miyata M, Tohkin M, *et al*. Targeted disruption of soluble epoxide hydrolase reveals a role in blood pressure regulation. J Biol Chem 2000;275:40504–40510.
236. Imig JD, Zhao X, Capdevila JH, *et al*. Soluble epoxide hydrolase inhibition lowers arterial blood pressure in angiotensin II hypertension. Hypertension 2002;39:690–694.
237. Jones PD, Wolf NM, Morisseau C, *et al*. Fluorescent substrates for soluble epoxide hydrolase and application to inhibition studies. Anal Biochem 2005;343:66–75.
238. Zeldin DC, Wei S, Falck JR, *et al*. Metabolism of epoxyeicosatrienoic acids by cytosolic epoxide hydrolase: substrate structural determinants of asymmetric catalysis. Arch Biochem Biophys 1995;316:443–451.
239. Argiriadi MA, Morisseau C, Goodrow MH, *et al*. Binding of alkylurea inhibitors to epoxide hydrolase implicates active site tyrosines in substrate activation. J Biol Chem 2000;275:15265–15270.
240. Pinot F, Grant DF, Beetham JK, *et al*. Molecular and biochemical evidence for the involvement of the Asp-333-His-523 pair in the catalytic mechanism of soluble epoxide hydrolase. J Biol Chem 1995;270:7968–7974.
241. Lacourciere GM, Armstrong RN. The catalytic mechanism of microsomal epoxide hydrolase involves an ester intermediate. J Am Chem Soc 1993;115:10466–10467.
242. Morisseau C, Du G, Newman JW, *et al*. Mechanism of mammalian soluble epoxide hydrolase inhibition by chalcone oxide derivatives. Arch Biochem Biophys 1998;356:214–228.
243. Muller F, Arand M, Frank H, *et al*. Visualization of a covalent intermediate between microsomal epoxide hydrolase, but not cholesterol epoxide hydrolase, and their substrates. Eur J Biochem/FEBS 1997;245:490–496.
244. Hyndman D, Bauman DR, Heredia VV, *et al*. The aldo-keto reductase superfamily homepage. Chem Biol Interact 2003;143-144:621–631.
245. Rosemond MJ, Walsh JS. Human carbonyl reduction pathways and a strategy for their study *in vitro* . Drug Metab Rev 2004;36:335–361.
246. Eddington ND, Young D. Biliary excretion of reduced haloperidol glucuronide. Psychopharmacology 1990;100:46–48.
247. Breyer-Pfaff U, Nill K. Stereoselective high-affinity reduction of ketonic nortriptyline metabolites and of ketotifen by aldo-keto reductases from human liver. Adv Exp Med Biol 1999;463:473–480.
248. Eyles DW, Pond SM. Stereospecific reduction of haloperidol in human tissues. Biochem Pharmacol 1992;44:867–871.
249. Wsol V, Szotakova B, Martin HJ, *et al*. Aldo-keto reductases (AKR) from the AKR1C subfamily catalyze the carbonyl reduction of the novel anticancer drug oracin in man. Toxicology 2007;238:111–118.
250. Hermans JJ, Thijssen HH. Stereoselective acetonyl side chain reduction of warfarin and analogs. Partial characterization of two cytosolic carbonyl reductases. Drug Metab Dispos 1992;20:268–274.
251. Chan KK, Lewis RJ, Trager WF. Absolute configurations of the four warfarin alcohols. J Med Chem 1972;15:1265–1270.
252. Jez JM, Flynn TG, Penning TM. A new nomenclature for the aldo-keto reductase superfamily. Biochem Pharmacol 1997;54:639–647.

253. Rosemond MJ, St John-Williams L, Yamaguchi T, *et al*. Enzymology of a carbonyl reduction clearance pathway for the HIV integrase inhibitor, S-1360: role of human liver cytosolic aldo-keto reductases. Chem Biol Interact 2004;147:129–139.
254. Jin Y, Penning TM. Aldo-keto reductases and bioactivation/detoxication. Annu Rev Pharmacol Toxicol 2007;47:263–292.
255. Di Costanzo L, Penning TM, Christianson DW. Aldo-keto reductases in which the conserved catalytic histidine is substituted. Chem Biol Interact 2009;178:127–133.
256. Bohren KM, Grimshaw CE, Gabbay KH. Catalytic effectiveness of human aldose reductase. Critical role of C-terminal domain. J Biol Chem 1992;267:20965–20970.
257. Filling C, Berndt KD, Benach J, *et al*. Critical residues for structure and catalysis in short-chain dehydrogenases/reductases. J Biol Chem 2002;277:25677–25684.
258. Flynn TG, Green NC, Bhatia MB, *et al*. Structure and mechanism of aldehyde reductase. Adv Exp Med Biol 1995;372:193–201.
259. Ma H, Ratnam K, Penning TM. Mutation of nicotinamide pocket residues in rat liver 3 alpha-hydroxysteroid dehydrogenase reveals different modes of cofactor binding. Biochemistry 2000;39:102–109.
260. Askonas LJ, Ricigliano JW, Penning TM. The kinetic mechanism catalysed by homogeneous rat liver 3 alpha-hydroxysteroid dehydrogenase. Evidence for binary and ternary dead-end complexes containing non-steroidal anti-inflammatory drugs. Biochem J 1991;278:835–841.
261. Trauger JW, Jiang A, Stearns BA, *et al*. Kinetics of allopregnanolone formation catalyzed by human 3 alpha-hydroxysteroid dehydrogenase type III (AKR1C2). Biochemistry 2002;41:13451–13459.
262. Li L, Zhang L, Cook PF. Role of the S128, H186, and N187 triad in substrate binding and decarboxylation in the sheep liver 6-phosphogluconate dehydrogenase reaction. Biochemistry 2006;45:12680–12686.
263. Prelog V. Chirality in chemistry. Science (New York) 1976;193:17–24.
264. Musa MM, Ziegelmann-Fjeld KI, Vieille C, *et al*. Asymmetric reduction and oxidation of aromatic ketones and alcohols using W110A secondary alcohol dehydrogenase from thermoanaerobacter ethanolicus. J Org Chem 2007;72:30–34.
265. Benner SA. The stereoselectivity of alcohol dehydrogenases: a stereochemical imperative? Experientia 1982;38:633–636.
266. Miners JO, Smith PA, Sorich MJ, *et al*. Predicting human drug glucuronidation parameters: application of *in vitro* and in silico modeling approaches. Annu Rev Pharmacol Toxicol 2004;44:1–25.
267. Radominska-Pandya A, Ouzzine M, Fournel-Gigleux S, *et al*. Structure of UDP-glucuronosyltransferases in membranes. Methods Enzymol 2005;400:116–147.
268. Li D, Fournel-Gigleux S, Barre L, *et al*. Identification of aspartic acid and histidine residues mediating the reaction mechanism and the substrate specificity of the human UDP-glucuronosyltransferases 1A. J Biol Chem 2007;282:36514–36524.
269. Miley MJ, Zielinska AK, Keenan JE, *et al*. Crystal structure of the cofactor-binding domain of the human phase II drug-metabolism enzyme UDP-glucuronosyltransferase 2B7. J Mol Biol 2007;369:498–511.
270. Johnson LP, Fenselau C. Enzymatic conjugation and hydrolysis of [^{18}O]isoborneol glucuronide. Drug Metab Dispos 1978;6:677–679.
271. Yin H, Bennett G, Jones JP. Mechanistic studies of uridine diphosphate glucuronosyltransferase. Chem Biol Interact 1994;90:47–58.
272. Falany CN, Green MD, Tephly TR. The enzymatic mechanism of glucuronidation catalyzed by two purified rat liver steroid UDP-glucuronosyltransferases. J Biol Chem 1987;262:1218–1222.

273. Koster AS, Noordhoek J. Kinetic properties of the rat intestinal microsomal 1-naphthol:UDP-glucuronosyl transferase. Inhibition by UDP and UDP-N-acetyl glucosamine. Biochim Biophys Acta 1983;761:76–85.
274. Luukkanen L, Taskinen J, Kurkela M, *et al*. Kinetic characterization of the 1A subfamily of recombinant human UDP-glucuronosyltransferases. Drug Metab Dispos 2005; 33:1017–1026.
275. Potrepka RF, Spratt JL. A study on the enzymatic mechanism of guinea-pig hepatic-microsomal bilirubin glucuronyl transferase. Eur J Biochem/FEBS 1972;29: 433–439.
276. Rao ML, Rao GS, Breuer H. Investigations on the kinetic properties of estrone glucuronyltransferase from pig kidney. Biochim Biophys Acta 1976;452:89–100.
277. Sanchez E, Tephly TR. Morphine metabolism. IV. Studies on the mechanism of morphine: uridine diphosphoglucuronyltransferase and its activation by bilirubin. Mol Pharmacol 1975;11:613–620.
278. Vessey DA, Zakim D. Regulation of microsomal enzymes by phospholipids. V. Kinetic studies of hepatic uridine diphosphate-glucuronyltransferase. J Biol Chem 1972;247: 3023–3028.
279. Burchell B. Transformation reactions: glucuronidation. In: Woolf TF, editor. Handbook of drug metabolism. New York: Marcel Dekker, Inc.; 1999. pp. 153–173.
280. Faed EM, Dobbs BR, Lee D. Glucuronidation and elimination of diflunisal in the isolated perfused rat liver: effect of pretreatment with phenobarbitone, clofibric acid and spironolactone. Arch Int Pharmacodyn Ther 1984;272:4–16.
281. McDonagh AF, Palma LA, Lauff JJ, *et al*. Origin of mammalian biliprotein and rearrangement of bilirubin glucuronides *in vivo* in the rat. J Clin Invest 1984;74:763–770.
282. Ruelius HW, Kirkman SK, Young EM, *et al*. Reactions of oxaprozin-1-O-acyl glucuronide in solutions of human plasma and albumin. Adv Exp Med Biol 1986;197:431–441.
283. van Breemen RB, Fenselau C. Acylation of albumin by 1-O-acyl glucuronides. Drug Metab Dispos 1985;13:318–320.
284. Van Breemen RB, Fenselau C, Mogilevsky W, *et al*. Reaction of bilirubin glucuronides with serum albumin. J Chromatogr 1986;383:387–392.
285. Wells DS, Janssen FW, Ruelius HW. Interactions between oxaprozin glucuronide and human serum albumin. Xenobiotica 1987;17:1437–1449.
286. Ding A, Ojingwa JC, McDonagh AF, *et al*. Evidence for covalent binding of acyl glucuronides to serum albumin via an imine mechanism as revealed by tandem mass spectrometry. Proc Natl Acad Sci U S A 1993;90:3797–3801.
287. Hodge JE. The Amadori rearrangement. Adv Carbohydr Chem 1955;10:169–205.
288. Bichlmaier I, Siiskonen A, Finel M, *et al*. Stereochemical sensitivity of the human UDP-glucuronosyltransferases 2B7 and 2B17. J Med Chem 2006;49:1818–1827.
289. Itaaho K, Mackenzie PI, Ikushiro S, *et al*. The configuration of the 17-hydroxy group variably influences the glucuronidation of beta-estradiol and epiestradiol by human UDP-glucuronosyltransferases. Drug Metab Dispos 2008;36:2307–2315.
290. Sten T, Bichlmaier I, Kuuranne T, *et al*. UDP-glucuronosyltransferases (UGTs) 2B7 and UGT2B17 display converse specificity in testosterone and epitestosterone glucuronidation, whereas UGT2A1 conjugates both androgens similarly. Drug Metab Dispos 2009;37:417–423.
291. Timmers CM, Dekker M, Buijman RC, *et al*. Synthesis and inhibitory effect of a trisubstrate transition state analog for UDP-glucuronosyltransferases. Bioorg Med Chem Lett 1997;7:1501–1506.
292. Barre L, Fournel-Gigleux S, Finel M, *et al*. Substrate specificity of the human UDP-glucuronosyltransferase UGT2B4 and UGT2B7. Identification of a critical aromatic amino acid residue at position 33. FEBS J 2007;274:1256–1264.

293. Kubota T, Lewis BC, Elliot DJ, *et al*. Critical roles of residues 36 and 40 in the phenol and tertiary amine aglycone substrate selectivities of UDP-glucuronosyltransferases 1A3 and 1A4. Mol Pharmacol 2007;72:1054–1062.
294. Lewis BC, Mackenzie PI, Elliot DJ, *et al*. Amino terminal domains of human UDP-glucuronosyltransferases (UGT) 2B7 and 2B15 associated with substrate selectivity and autoactivation. Biochem Pharmacol 2007;73:1463–1473.
295. Li Q, Lou X, Peyronneau MA, *et al*. Expression and functional domains of rabbit liver UDP-glucuronosyltransferase 2B16 and 2B13. J Biol Chem 1997;272:3272–3279.
296. Mackenzie PI. Expression of chimeric cDNAs in cell culture defines a region of UDP glucuronosyltransferase involved in substrate selection. J Biol Chem 1990;265:3432–3435.
297. Mackenzie PI, Bock KW, Burchell B, *et al*. Nomenclature update for the mammalian UDP glycosyltransferase (UGT) gene superfamily. Pharmacogenet Genomics 2005;15:677–685.
298. Martineau I, Tchernof A, Belanger A. Amino acid residue ILE211 is essential for the enzymatic activity of human UDP-glucuronosyltransferase 1A10 (UGT1A10). Drug Metab Dispos 2004;32:455–459.
299. Ritter JK, Chen F, Sheen YY, *et al*. Two human liver cDNAs encode UDP-glucuronosyltransferases with 2 log differences in activity toward parallel substrates including hyodeoxycholic acid and certain estrogen derivatives. Biochemistry 1992; 31:3409–3414.
300. Ritter JK, Chen F, Sheen YY, *et al*. A novel complex locus UGT1 encodes human bilirubin, phenol, and other UDP-glucuronosyltransferase isozymes with identical carboxyl termini. J Biol Chem 1992;267:3257–3261.
301. Senay C, Jedlitschky G, Terrier N, *et al*. The importance of cysteine 126 in the human liver UDP-glucuronosyltransferase UGT1A6. Biochim Biophys Acta 2002;1597: 90–96.
302. Xiong Y, Bernardi D, Bratton S, *et al*. Phenylalanine 90 and 93 are localized within the phenol binding site of human UDP-glucuronosyltransferase 1A10 as determined by photoaffinity labeling, mass spectrometry, and site-directed mutagenesis. Biochemistry 2006;45:2322–2332.
303. Kerdpin O, Mackenzie PI, Bowalgaha K, *et al*. Influence of N-terminal domain histidine and proline residues on the substrate selectivities of human UDP-glucuronosyltransferase 1A1, 1A6, 1A9, 2B7, and 2B10. Drug Metab Dispos 2009;37:1948–1955.
304. Bone R, Agard DA. Mutational remodeling of enzyme specificity. Methods Enzymol 1991;202:643–671.
305. Sorich MJ, McKinnon RA, Miners JO, *et al*. The importance of local chemical structure for chemical metabolism by human uridine 5′-diphosphate-glucuronosyltransferase. J Chem Inform Model 2006;46:2692–2697.
306. Kim KH. Quantitative structure-activity relationships of the metabolism of drugs by uridine diphosphate glucuronosyltransferase. J Pharm Sci 1991;80:966–970.
307. Ebner T, Burchell B. Substrate specificities of two stably expressed human liver UDP-glucuronosyltransferases of the UGT1 gene family. Drug Metab Dispos 1993;21:50–55.
308. Turgeon D, Carrier JS, Chouinard S, *et al*. Glucuronidation activity of the UGT2B17 enzyme toward xenobiotics. Drug Metab Dispos 2003;31:670–676.
309. Mannervik B, Alin P, Guthenberg C, *et al*. Identification of three classes of cytosolic glutathione transferase common to several mammalian species: correlation between structural data and enzymatic properties. Proc Natl Acad Sci U S A 1985;82:7202–7206.
310. Lyttle MH, Hocker MD, Hui HC, *et al*. Isozyme-specific glutathione-S-transferase inhibitors: design and synthesis. J Med Chem 1994;37:189–194.
311. Reinemer P, Dirr HW, Ladenstein R, *et al*. The three-dimensional structure of class pi glutathione S-transferase in complex with glutathione sulfonate at 2.3 A resolution. EMBO J 1991;10:1997–2005.
312. Armstrong RN. Structure, catalytic mechanism, and evolution of the glutathione transferases. Chem Res Toxicol 1997;10:2–18.

313. Graminski GF, Kubo Y, Armstrong RN. Spectroscopic and kinetic evidence for the thiolate anion of glutathione at the active site of glutathione S-transferase. Biochemistry 1989;28:3562–3568.
314. Jung G, Breitmaier E, Voelter W. Dissociation equilibrium of glutathione. A Fourier transform-13 C-NMR spectroscopic study of pH-dependence and of charge densities. Eur J Biochem/FEBS 1972;24:438–445.
315. Reuben DME, Bruice TC. Reaction of thiol anions with benzene oxide and malachite green. J Am Chem Soc 1976;98:114–121.
316. Takayama H, Watanabe A, Hosokawa M, *et al*. Synthesis of a new class of camptothecin derivatives, the long-chain fatty acid esters of 10-hydroxycamptothecin, as a potent prodrug candidate, and their *in vitro* metabolic conversion by carboxylesterases. Bioorg Med Chem Lett 1998;8:415–418.
317. Clark AG, Sinclair M. The Meisenheimer complex of glutathione and trinitrobenzene. A potent inhibitor of the glutathione S-transferase from Galleria mellonella. Biochem Pharmacol 1988;37:259–263.
318. Chen WJ, Graminski GF, Armstrong RN. Dissection of the catalytic mechanism of isozyme 4-4 of glutathione S-transferase with alternative substrates. Biochemistry 1988; 27:647–654.
319. Lyon RP, Hill JJ, Atkins WM. Novel class of bivalent glutathione S-transferase inhibitors. Biochemistry 2003;42:10418–10428.
320. Keese MA, Bose M, Mulsch A, *et al*. Dinitrosyl-dithiol-iron complexes, nitric oxide (NO) carriers *in vivo*, as potent inhibitors of human glutathione reductase and glutathione-S-transferase. Biochem Pharmacol 1997;54:1307–1313.
321. Caccuri AM, Ascenzi P, Antonini G, *et al*. Structural flexibility modulates the activity of human glutathione transferase P1-1. Influence of a poor co-substrate on dynamics and kinetics of human glutathione transferase. J Biol Chem 1996;271:16193–16198.
322. Ricci G, Caccuri AM, Lo Bello M, *et al*. Structural flexibility modulates the activity of human glutathione transferase P1-1. Role of helix 2 flexibility in the catalytic mechanism. J Biol Chem 1996;271:16187–16192.
323. Federici L, Lo Sterzo C, Pezzola S, *et al*. Structural basis for the binding of the anticancer compound 6-(7-nitro-2,1,3-benzoxadiazol-4-ylthio)hexanol to human glutathione s-transferases. Cancer Res 2009;69:8025–8034.
324. Patskovsky YV, Patskovska LN, Listowsky I. Functions of His107 in the catalytic mechanism of human glutathione S-transferase hGSTM1a-1a. Biochemistry 1999;38:1193–1202.
325. Federici L, Masulli M, Gianni S, *et al*. A conserved hydrogen-bond network stabilizes the structure of Beta class glutathione S-transferases. Biochem Biophys Res Commun 2009;382:525–529.
326. Wongsantichon J, Robinson RC, Ketterman AJ. Structural contributions of delta class Glutathione transferase active site residues to catalysis. Biochem J 2010.
327. Chou HC, Lang NP, Kadlubar FF. Metabolic activation of the N-hydroxy derivative of the carcinogen 4-aminobiphenyl by human tissue sulfotransferases. Carcinogenesis 1995;16:413–417.
328. Chou HC, Lang NP, Kadlubar FF. Metabolic activation of N-hydroxy arylamines and N-hydroxy heterocyclic amines by human sulfotransferase(s). Cancer Res 1995;55:525–529.
329. Chou HC, Ozawa S, Fu PP, *et al*. Metabolic activation of methyl-hydroxylated derivatives of 7,12-dimethylbenz[a]anthracene by human liver dehydroepiandrosterone-steroid sulfotransferase. Carcinogenesis 1998;19:1071–1076.
330. Gamage N, Barnett A, Hempel N, *et al*. Human sulfotransferases and their role in chemical metabolism. Toxicol Sci 2006;90:5–22.
331. Nagata K, Yamazoe Y. Pharmacogenetics of sulfotransferase. Annu Rev Pharmacol Toxicol 2000;40:159–176.

332. Klaassen CD, Boles JW. Sulfation and sulfotransferases 5: the importance of 3′-phosphoadenosine 5′-phosphosulfate (PAPS) in the regulation of sulfation. FASEB J 1997;11:404–418.
333. Kakuta Y, Petrotchenko EV, Pedersen LC, *et al*. The sulfuryl transfer mechanism. Crystal structure of a vanadate complex of estrogen sulfotransferase and mutational analysis. J Biol Chem 1998;273:27325–27330.
334. Pedersen LC, Petrotchenko E, Shevtsov S, *et al*. Crystal structure of the human estrogen sulfotransferase-PAPS complex: evidence for catalytic role of Ser137 in the sulfuryl transfer reaction. J Biol Chem 2002;277:17928–17932.
335. Kakuta Y, Pedersen LG, Carter CW, *et al*. Crystal structure of estrogen sulphotransferase. Nat Struct Biol 1997;4:904–908.
336. Chapman E, Best MD, Hanson SR, *et al*. Sulfotransferases: structure, mechanism, biological activity, inhibition, and synthetic utility. Angew Chem Int Ed 2004;43:3526–3548.
337. Duffel MW, Jakoby WB. On the mechanism of aryl sulfotransferase. J Biol Chem 1981;256:11123–11127.
338. Zhang H, Varlamova O, Vargas FM, *et al*. Sulfuryl transfer: the catalytic mechanism of human estrogen sulfotransferase. J Biol Chem 1998;273:10888–10892.
339. Tyapochkin E, Cook PF, Chen G. Isotope exchange at equilibrium indicates a steady state ordered kinetic mechanism for human sulfotransferase. Biochemistry 2008; 47:11894–11899.
340. Varin L, Ibrahim RK. Novel flavonol 3-sulfotransferase. Purification, kinetic properties, and partial amino acid sequence. J Biol Chem 1992;267:1858–1863.
341. Whittemore RM, Pearce LB, Roth JA. Purification and kinetic characterization of a phenol-sulfating form of phenol sulfotransferase from human brain. Arch Biochem Biophys 1986;249:464–471.
342. Pi N, Yu Y, Mougous JD, *et al*. Observation of a hybrid random ping-pong mechanism of catalysis for NodST: a mass spectrometry approach. Protein Sci 2004;13:903–912.
343. Walle T, Walle UK, Shwed JA, *et al*. Human phenol sulfotransferases: chiral substrates and expression in Hep G2 cells. Chem Biol Interact 1994;92:47–55.
344. Banoglu E, Duffel MW. Importance of peri-interactions on the stereospecificity of rat hydroxysteroid sulfotransferase STa with 1-arylethanols. Chem Res Toxicol 1999; 12:278–285.
345. Campo VL, Bernardes LS, Carvalho I. Stereoselectivity in drug metabolism: molecular mechanisms and analytical methods. Curr Drug Metab 2009;10:188–205.
346. Hartman AP, Wilson AA, Wilson HM, *et al*. Enantioselective sulfation of beta 2-receptor agonists by the human intestine and the recombinant M-form phenolsulfotransferase. Chirality 1998;10:800–803.
347. Walle T, Walle UK. Stereoselective sulfate conjugation of 4-hydroxypropranolol and terbutaline by the human liver phenolsulfotransferases. Drug Metab Dispos 1992;20:333–336.
348. Walle T, Walle UK, Thornburg KR, *et al*. Stereoselective sulfation of albuterol in humans. Biosynthesis of the sulfate conjugate by HEP G2 cells. Drug Metab Dispos 1993;21:76–80.
349. Banoglu E, Duffel MW. Studies on the interactions of chiral secondary alcohols with rat hydroxysteroid sulfotransferase STa. Drug Metab Dispos 1997;25:1304–1310.
350. Campbell NR, Van Loon JA, Sundaram RS, *et al*. Human and rat liver phenol sulfotransferase: structure-activity relationships for phenolic substrates. Mol Pharmacol 1987;32:813–819.
351. Duffel MW. Molecular specificity of aryl sulfotransferase IV (tyrosine-ester sulfotransferase) for xenobiotic substrates and inhibitors. Chem Biol Interact 1994;92:3–14.
352. Duffel MW, Marshal AD, McPhie P, *et al*. Enzymatic aspects of the phenol (aryl) sulfotransferases. Drug Metab Rev 2001;33:369–395.

353. Chen G, Banoglu E, Duffel MW. Influence of substrate structure on the catalytic efficiency of hydroxysteroid sulfotransferase STa in the sulfation of alcohols. Chem Res Toxicol 1996;9:67–74.
354. Brix LA, Barnett AC, Duggleby RG, *et al*. Analysis of the substrate specificity of human sulfotransferases SULT1A1 and SULT1A3: site-directed mutagenesis and kinetic studies. Biochemistry 1999;38:10474–10479.
355. Riddle B, Jencks WP. Acetyl-coenzyme A: arylamine N-acetyltransferase. Role of the acetyl-enzyme intermediate and the effects of substituents on the rate. J Biol Chem 1971;246:3250–3258.
356. Minchin RF, Hanna PE, Dupret JM, *et al*. Arylamine N-acetyltransferase I. Int J Biochem Cell Biol 2007;39:1999–2005.
357. Windmill KF, Gaedigk A, Hall PM, *et al*. Localization of N-acetyltransferases NAT1 and NAT2 in human tissues. Toxicol Sci 2000;54:19–29.
358. Minchin RF. Acetylation of p-aminobenzoylglutamate, a folic acid catabolite, by recombinant human arylamine N-acetyltransferase and U937 cells. Biochem J 1995; 307:1–3.
359. Wang H, Vath GM, Gleason KJ, *et al*. Probing the mechanism of hamster arylamine N-acetyltransferase 2 acetylation by active site modification, site-directed mutagenesis, and pre-steady state and steady state kinetic studies. Biochemistry 2004;43:8234–8246.
360. Wang H, Liu L, Hanna PE, *et al*. Catalytic mechanism of hamster arylamine N-acetyltransferase 2. Biochemistry 2005;44:11295–11306.
361. Wu H, Dombrovsky L, Tempel W, *et al*. Structural basis of substrate-binding specificity of human arylamine N-acetyltransferases. J Biol Chem 2007;282:30189–30197.
362. Minchin RF, Kadlubar FF, Ilett KF. Role of acetylation in colorectal cancer. Mutat Res 1993;290:35–42.
363. Dupret JM, Rodrigues-Lima F. Structure and regulation of the drug-metabolizing enzymes arylamine N-acetyltransferases. Curr Med Chem 2005;12:311–318.
364. Sim E, Walters K, Boukouvala S. Arylamine N-acetyltransferases: from structure to function. Drug Metab Rev 2008;40:479–510.
365. Kawamura A, Graham J, Mushtaq A, *et al*. Eukaryotic arylamine N-acetyltransferase. Investigation of substrate specificity by high-throughput screening. Biochem Pharmacol 2005;69:347–359.
366. Goodfellow GH, Dupret JM, Grant DM. Identification of amino acids imparting acceptor substrate selectivity to human arylamine acetyltransferases NAT1 and NAT2. Biochem J 2000;348:159–166.
367. Knights KM, Drogemuller CJ. Xenobiotic-CoA ligases: kinetic and molecular characterization. Curr Drug Metab 2000;1:49–66.
368. Hutt AJ, Caldwell J. Amino acid conjugation. In: Mulder GJ, editor. Conjugation reactions in drug metabolism: an integrated approach. New York: Taylor {&} Francis; 1990. pp. 274–305.
369. Amigo L, McElroy MC, Morales MN, *et al*. Subcellular distribution and characteristics of ciprofibroyl-CoA synthetase in rat liver. Its possible identity with long-chain acyl-CoA synthetase. Biochem J 1992;284:283–287.
370. Bronfman M, Amigo L, Morales MN. Activation of hypolipidaemic drugs to acyl-coenzyme A thioesters. Biochem J 1986;239:781–784.
371. Bronfman M, Morales MN, Amigo L, *et al*. Hypolipidaemic drugs are activated to acyl-CoA esters in isolated rat hepatocytes. Detection of drug activation by human liver homogenates and by human platelets. Biochem J 1992;284:289–295.
372. Chen CS, Chen T, Shieh WR. Metabolic stereoisomeric inversion of 2-arylpropionic acids. On the mechanism of ibuprofen epimerization in rats. Biochim Biophys Acta 1990; 1033:1–6.

373. Grillo MP, Wait JC, Tadano Lohr M, *et al*. Stereoselective flunoxaprofen-S-acyl-glutathione thioester formation mediated by acyl-CoA formation in rat hepatocytes. Drug Metab Dispos 2010;38:133–142.
374. Gulick AM, Lu X, Dunaway-Mariano D. Crystal structure of 4-chlorobenzoate:CoA ligase/synthetase in the unliganded and aryl substrate-bound states. Biochemistry 2004;43:8670–8679.
375. Hao H, Wang G, Sun J. Enantioselective pharmacokinetics of ibuprofen and involved mechanisms. Drug Metab Rev 2005;37:215–234.
376. Iwakawa S, Spahn H, Benet LZ, *et al*. Stereoselective disposition of carprofen, flunoxaprofen, and naproxen in rats. Drug Metab Dispos 1991;19:853–857.
377. Tracy TS, Wirthwein DP, Hall SD. Metabolic inversion of (R)-ibuprofen. Formation of ibuprofenyl-coenzyme A. Drug Metab Dispos 1993;21:114–120.
378. Wu R, Cao J, Lu X, *et al*. Mechanism of 4-chlorobenzoate:coenzyme a ligase catalysis. Biochemistry 2008;47:8026–8039.
379. Berg P. Acyl adenylates; an enzymatic mechanism of acetate activation. J Biol Chem 1956;222:991–1013.
380. Jencks WP, Lipmann F. Studies on the initial step of fatty acid activation. J Biol Chem 1957;225:207–223.
381. Kochan G, Pilka ES, von Delft F, *et al*. Structural snapshots for the conformation-dependent catalysis by human medium-chain acyl-coenzyme A synthetase ACSM2A. J Mol Biol 2009;388:997–1008.
382. Hisanaga Y, Ago H, Nakagawa N, *et al*. Structural basis of the substrate-specific two-step catalysis of long chain fatty acyl-CoA synthetase dimer. J Biol Chem 2004; 279:31717–31726.
383. Horswill AR, Escalante-Semerena JC. Characterization of the propionyl-CoA synthetase (PrpE) enzyme of Salmonella enterica: residue Lys592 is required for propionyl-AMP synthesis. Biochemistry 2002;41:2379–2387.
384. Li C, Olurinde MO, Hodges LM, *et al*. Covalent binding of 2-phenylpropionyl-S-acyl-CoA thioester to tissue proteins *in vitro*. Drug Metab Dispos 2003;31:727–730.
385. Nakamura Y, Yamaguchi T, Takahashi S, *et al*. Optical isomerization mechanism of R(-)hydratropic acid derivatives. J Pharmacobiodyn 1981; 4.
386. Reichel C, Brugger R, Bang H, *et al*. Molecular cloning and expression of a 2-arylpropionyl-coenzyme A epimerase: a key enzyme in the inversion metabolism of ibuprofen. Mol Pharmacol 1997;51:576–582.
387. Waku K. Origins and fates of fatty acyl-CoA esters. Biochim Biophys Acta 1992;1124: 101–111.
388. Hansch C, Lien EJ, Helmer F. Structure–activity correlations in the metabolism of drugs. Arch Biochem Biophys 1968;128:319–330.
389. Kasuya F, Igarashi K, Fukui M. Inhibition of a medium chain acyl-CoA synthetase involved in glycine conjugation by carboxylic acids. Biochem Pharmacol 1996;52:1643–1646.
390. Koetsier MJ, Jekel PA, van den Berg MA, *et al*. Characterization of a phenylacetate-CoA ligase from Penicillium chrysogenum. Biochem J 2009;417:467–476.
391. Kasuya F, Yamaoka Y, Igarashi K, *et al*. Molecular specificity of a medium chain acyl-CoA synthetase for substrates and inhibitors: conformational analysis. Biochem Pharmacol 1998;55:1769–1775.
392. Daly AK. Pharmacogenetics. In; Woolf TF, editor. Handbook of drug metabolism. New York: Marcel Dekker, Inc.; 1999. pp. 188–189.
393. Georgieva P, Wu Q, McLeish MJ, *et al*. The reaction mechanism of phenylethanolamine N-methyltransferase: a density functional theory study. Biochim Biophys Acta 2009;1794: 1831–1837.

394. Weinshilboum RM, Otterness DM, Szumlanski CL. Methylation pharmacogenetics: catechol O-methyltransferase, thiopurine methyltransferase, and histamine N-methyltransferase. Annu Rev Pharmacol Toxicol 1999;39:19–52.
395. Axelrod J. Purification and properties of phenylethanolamine-N-methyl transferase. J Biol Chem 1962;237:1657–1660.
396. Guldberg HC, Marsden CA. Catechol-O-methyl transferase: pharmacological aspects and physiological role. Pharmacol Rev 1975;27:135–206.
397. Kirshner N, Goodall M. The formation of adrenaline from noradrenaline. Biochim Biophys Acta 1957;24:658–659.
398. Mannisto PT, Kaakkola S. Catechol-O-methyltransferase (COMT): biochemistry, molecular biology, pharmacology, and clinical efficacy of the new selective COMT inhibitors. Pharmacol Rev 1999;51:593–628.
399. Mannisto PT, Ulmanen I, Lundstrom K, *et al*. Characteristics of catechol O-methyltransferase (COMT) and properties of selective COMT inhibitors. Progress in drug research. Fortschr Arzneimittelforsch 1992;39:291–350.
400. Remy CN. Metabolism of thiopyrimidines and thiopurines. S-Methylation with S-adenosylmethionine transmethylase and catabolism in mammalian tissues. J Biol Chem 1963;238:1078–1084.
401. Weinshilboum R. Thiopurine pharmacogenetics: clinical and molecular studies of thiopurine methyltransferase. Drug Metab Dispos 2001;29:601–605.
402. Woodson LC, Ames MM, Selassie CD, *et al*. Thiopurine methyltransferase. Aromatic thiol substrates and inhibition by benzoic acid derivatives. Mol Pharmacol 1983;24:471–478.
403. Drummer OH, Jarrott B, Louis WJ. Demonstration of a S-methyl metabolite of captopril in patients undergoing chronic captopril therapy. Clin Exp Pharmacol Physiol 1982;7:81–86.
404. Perrett D, Sneddon W, Stephens AD. Studies on D-penicillamine metabolism in cystinuria and rheumatoid arthritis: isolation of S-methyl-D-penicillamine. Biochem Pharmacol 1976;25:259–264.
405. Lok R, Coward JK. Steric constraints in intramolecular reactions at sp3 carbon implications for methylase mechanisms. Bioorg Chem 1976;5:169–175.
406. Woodard RW, Tsai MD, Floss HG, *et al*. Stereochemical course of the transmethylation catalyzed by catechol O-methyltransferase. J Biol Chem 1980;255:9124–9127.
407. Lotta T, Vidgren J, Tilgmann C, *et al*. Kinetics of human soluble and membrane-bound catechol O-methyltransferase: a revised mechanism and description of the thermolabile variant of the enzyme. Biochemistry 1995;34:4202–4210.
408. Vidgren J, Svensson LA, Liljas A. Crystal structure of catechol O-methyltransferase. Nature 1994;368:354–358.
409. Vidgren J, Ovaska M. Structural aspects in the inhibitor design of catechol O-methyltransferase. In: Veerapandian P, editor. Structure-based drug design. New York: Marcel Dekker, Inc.; 1997. pp. 343–363.
410. Rivett AJ, Roth JA. Kinetic studies on the O-methylation of dopamine by human brain membrane-bound catechol O-methyltransferase. Biochemistry 1982;21:1740–1742.
411. Tunnicliff G, Ngo TT. Kinetics of rat brain soluble catechol-O-methyltransferase and its inhibition by substrate analogues. Int J Biochem 1983;15:733–738.
412. Hegazi MF, Borchardt RT, Showen RL. a-Deuterium and carbon-13 isotope effects for methyl transfer catalyzed by catechol-O-methyltransferase. SN2-like transition state. J Am Chem Soc 1979;101:4359–4365.
413. Hegazi MF, Borchard RT, Schowen RL. Letter: SN2-like transition state for methyl transfer catalyzed by catechol-O-methyl-transferase. J Am Chem Soc 1976;98:3048–3049.
414. Peng Y, Feng Q, Wilk D, *et al*. Structural basis of substrate recognition in thiopurine s-methyltransferase. Biochemistry 2008;47:6216–6225.
415. Blaschke E, Hertting G. Enzymic methylation of L-ascorbic acid by catechol O-methyltransferase. Biochem Pharmacol 1971;20:1363–1370.

416. Bowers-Komro DM, McCormick DB, King GA, *et al*. Confirmation of 2-O-methyl ascorbic acid as the product from the enzymatic methylation of L-ascorbic acid by catechol-O-methyltransferase. Int J Vitam Nutr Res 1982;52:186–193.
417. Backstrom R, Honkanen E, Pippuri A, *et al*. Synthesis of some novel potent and selective catechol O-methyltransferase inhibitors. J Med Chem 1989;32:841–846.
418. Borgulya J, Bruderer H, Bernauer K, *et al*. Catechol-O-methyltransferase-inhibitors pyrocatechol derivatives: synthesis and structure-activity studies. Helv Chim Acta 1989;72:952–968.
419. Palma PN, Bonifacio MJ, Loureiro AI, *et al*. Molecular modeling and metabolic studies of the interaction of catechol-O-methyltransferase and a new nitrocatechol inhibitor. Drug Metab Dispos 2003;31:250–258.
420. Keith RA, Otterness DM, Kerremans AL, *et al*. S-Methylation of D- and L-penicillamine by human erythrocyte membrane thiol methyltransferase. Drug Metab Dispos 1985;13:669–676.
421. Glauser TA, Kerremans AL, Weinshilboum RM. Human hepatic microsomal thiol methyltransferase. Assay conditions, biochemical properties, and correlation studies. Drug Metab Dispos 1992;20:247–255.
422. Krynetski EY, Evans WE. Pharmacogenetics as a molecular basis for individualized drug therapy: the thiopurine S-methyltransferase paradigm. Pharm Res 1999;16:342–349.
423. Ames MM, Selassie CD, Woodson LC, *et al*. Thiopurine methyltransferase: structure-activity relationships for benzoic acid inhibitors and thiophenol substrates. J Med Chem 1986;29:354–358.
424. Raxworthy MJ, Youde IR, Gulliver PA. Catechol-O-methyltransferase: substrate-specificity and stereoselectivity for beta-adrenoceptor agents. Xenobiotica 1986;16:47–52.